OCS STUDY
MMS 85-0025

GULF OF MEXICO CIRCULATION MODELING STUDY

Annual Progress Report

Year I

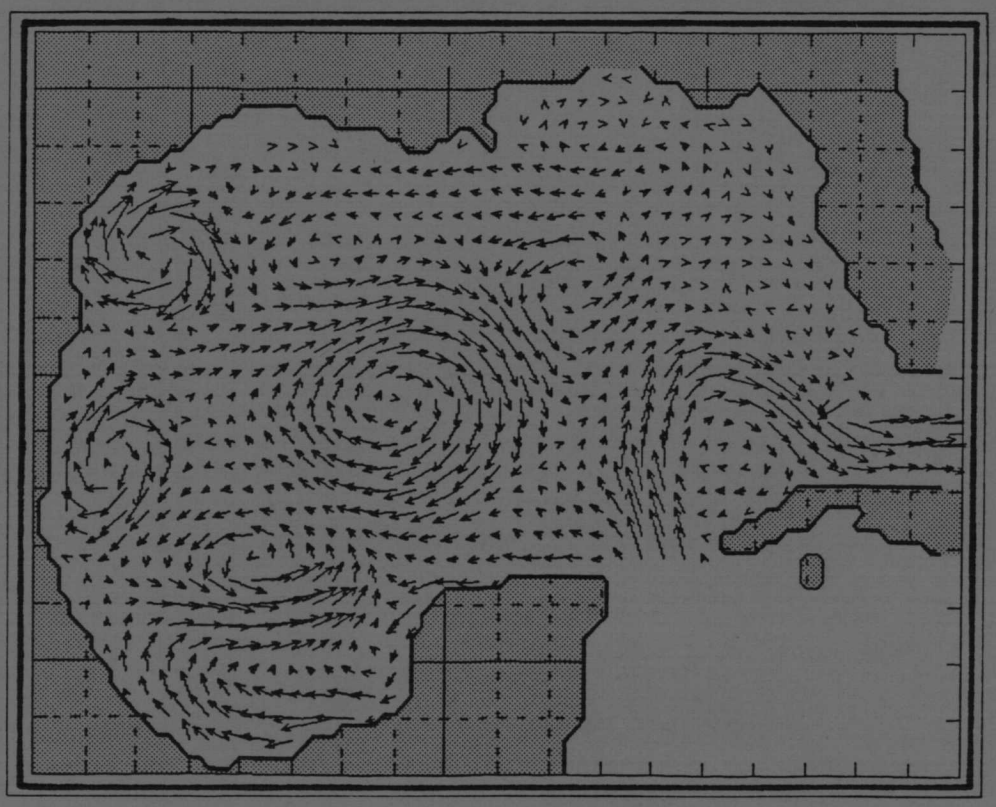

U.S. DEPARTMENT OF THE INTERIOR/MINERALS MANAGEMENT SERVICE

OCS STUDY
MMS 85-0025

GULF OF MEXICO
CIRCULATION MODELING STUDY

ANNUAL PROGRESS REPORT

YEAR I

United States Department of the Interior

Minerals Management Service

Prepared under Contract 14-12-0001-30073

Alan J. Wallcraft, Ph.D

JAYCOR

November 1984

Prepared by the
Environmental Studies Section
Minerals Management Service
Gulf of Mexico OCS Regional Office
Metairie, LA

DISCLAIMER

This report has been reviewed by the Minerals Management Service and approved for publication. Approval does not signify that the contents necessarily reflect the views and policies of the Bureau, nor does mention of trade names or commercial products constitute endorsement or recommendation for use.

Request Copies From:

United States Department of the Interior
Minerals Management Service
Gulf of Mexico OCS Regional Office
P.O. Box 7944
Metairie, Louisiana 70010

Attention: Public Information Unit
Telephone (504)838-0519

TABLE OF CONTENTS

I.	INTRODUCTION	1
II.	EXPERIMENT 09	3
III.	EXPERIMENT 34	6
IV.	EXPERIMENT 40	8
V.	EXPERIMENT 60	12
VI.	EXPERIMENT 68	18
VII.	FIGURES	24
VIII.	REFERENCES	102

I. INTRODUCTION

This final report gives details of the first year of a four year numerical ocean circulation modeling program for the Gulf of Mexico. The aim of the program is to progressively upgrade, in modest increments, an existing numerical ocean circulation model of the Gulf so that the final model has a horizontal resolution of about 10 km and vertical resolution approaching 1 to 10 m in the mixed layer, 10 m at the thermocline and 100 m in the deep water. Throughout the four year period, the validity of the upgraded model will be continuously tested, and velocity field time series delivered periodically based on the most realistic simulation of Gulf circulation available.

Experiments in the first year were with the existing NORDA/JAYCOR two layer hydrodynamic primitive equation ocean circulation model of the Gulf on a 0.2 degree grid. They concentrated on correctly specifying the coastline and bottom topography for maximum realism in circulation simulation, and on how best to include wind forcing. Details of selected experiments are presented in this report.

Experiment 9 represents the best (compared to our incomplete knowledge of the real Gulf) simulation available at the beginning of the project. It is forced by flow through the Yucatan Straits only (no wind forcing), and exhibits many of the flow features observed in the Gulf. Simulated surface currents sampled every ten days for three Loop Current eddy cycles (1140 days) were delivered to MMS at the start of the contract period as an 'early simulation run'. Experiment 34 is similar to Experiment 9, but with

the addition of seasonal wind forcing. The basic circulation patterns show far more variability in this case. Experiment 40 has no wind forcing and its total inflow transport is identical to that in Experiment 9, but the distribution of transport between the model's two layers has been changed (upper layer transport reduced). It exhibits Loop Current eddies that are nearer to the size observed in the Gulf (Experiment 9 has rather large eddies). The increased lower layer flow helps prevent intrusion onto shelf areas, and its sea surface variability is remarkably similar to that obtained from satellite altimeter crossovers for the Gulf. Experiment 60 is identical to Experiment 40 except that the horizontal eddy viscosity has been reduced. Some of the flow features seen in Experiment 9 were less obvious in Experiment 40, but the latter's lower velocities allowed the reduction in eddy viscosity and Experiment 60 exhibits these features plus some new circulation patterns. Experiment 68 is identical to Experiment 40 with the addition of wind forcing from the Navy Corrected Geostrophic Wind data set for the Gulf. This wind set has wind stresses every 12 hours from 1967 to 1982. The addition of winds increases the velocities encountered, and attempts to add this wind forcing to Experiment 60 were not successful. Simulated surface currents sampled every three days for more than 10 years were delivered to MMS from Experiment 68, as representing the best simulation available from the first year effort.

II. EXPERIMENT 9

Since the ocean model contained many innovative features it was discussed in detail in Hurlburt and Thompson (1980). In particular Section 2 (pp 1613-1614) gives the model equations and Appendix B (pp 1647-1650) describes the numerical design of the model. Since that time the capability to handle general basin geometry has been added but this does not affect the description in any major way. Wind forcing is treated identically to interfacial and bottom stress terms, i.e., wind stress appears directly as an additive term in the momentum equation [see p 1614 of Hurlburt and Thompson (1980)].

In terms of 'realism' Experiment 9 was the most successful Gulf of Mexico numerical simulation prior to the start of this project. The model was driven from rest to statistical equilibrium solely by a steady inflow through the Yucatan Straits which was compensated by outflow through the Florida Straits. The model parameters were:

- upper/lower layer inflow transport = 26/4 Sv,
- horizontal eddy viscosity, A = 300 m^2/sec,
- Coriolis parameter at the southern boundary f = 5 x 10^{-5} sec^{-1},
- gravitational acceleration, g = 9.8 m/sec^2,
- reduced gravity, g' = .03(H1+H2)/H2 m/sec^2,
- reference layer thicknesses, H1 = 200m and H2 = 3400m,
- minimum depth of bottom topography = 500m, grid spacing, 25 by 25 Km,

- o beta, $df/dy = 2 \times 10^{-11}\ m^{-1}\ sec^{-1}$,
- o wind stress = 0,
- o interfacial stress = 0,
- o coefficient of quadratic bottom stress = .002; and
- o time step = 1 hour.

Figure 1 compares 'instantaneous' upper ocean flow patterns just before an eddy is shed by the Loop Current (a) from the numerical model and (b) from observations by Leipper (1970). The ability of the model to simulate observed features is clearly demonstrated by this comparison, which is remarkable given the simplicity of the model forcing. However some discrepancies remain, for example the eddy has not penetrated as far into the Gulf and is more intense than that shown in the observations. Waves can be seen moving around the wall of the Loop Current in both the model and the observations, but in the model they are at the limit of resolution and therefore unrealistically large. Moreover in the Gulf the waves are more pronounced on the eastern wall of the Loop and can form strong cold intrusions that may contribute to the eddy shedding process (Vukovitch and Maul, 1984). This is an example of a feature that would benefit greatly from 10km model grid resolution. As shed eddies propagate westward (Figure 2a) the model spontaneously develops a counter rotating vortex pair (Figure 2b), a structure repeatedly observed in the Western Gulf (Figure 3). The roles of the wind and the Loop Current eddies in the formation of this structure have been a matter of some controversy (Merrell and Morrison, 1981). Although wind forcing was not present in this simulation a major role for winds has not yet been ruled out. After spin up the

experiment sheds an eddy once every 390 days and the eddy shedding cycles are very similar.

III. EXPERIMENT 34

Experiment 34 is similar to Experiment 9, but with the addition of wind forcing based on a seasonal climatology from ship observations (Elliot, 1979). Linear interpolation in time was used between the seasonal fields to produce the wind stress at each time step. The model parameters were:

- upper/lower layer inflow transport = 26/4 Sv,
- horizontal ddy viscosity, A = 300 m^2/sec,
- Coriolis parameter at the southern boundary f = 4.5 x 10^{-5} sec^{-1},
- gravitational acceleration, g = 9.8 m/sec^2,
- reduced gravity, g' = .03(H1+H2)/H2 m/sec^2,
- reference layer thicknesses, H1 = 200 m and H2 = 3300 m,
- minimum depth of bottom topography = 500m,
- grid spacing, 20 by 22 Km (0.2 by 0.2 degrees),
- beta, df/dy = 2 x 10^{-11} m^{-1} sec^{-1},
- wind stress from seasonal climatology based on ship observations,
- interfacial stress = 0,
- coefficient of quadratic bottom stress = .002; and
- time step = 1.5 hours.

Seasonal climatological winds obviously cannot represent most of the wind variability, and Experiment 31 which was driven solely by these winds attains a steady yearly cycle (JAYCOR, 1983). Even so the addition of wind forcing increases the variability of the Loop Current

system, including the eddy shedding period and eddy path. For example Figure 4 compares 360 model days from Experiments 28 and 34 (which are identical except that Experiment 28 has no wind forcing). From these snapshots, taken every 90 days, there is little difference between the two experiments. But if Experiment 34 is sampled every 20 days, as in Figure 5, it is apparent that eddies were shed in the space of about one year. Figure 5 also shows that the circulation pattern in the western Gulf can change very rapidly at times. Figure 6 shows the mean interface deviation and its variability for experiments with wind forcing only, port forcing only and with wind plus port forcing. This demonstrates that even in the mean the interaction of wind and port forcing is not linear, i.e., the mean of the dual forcing experiment is not the sum of the other two means. The variability is increased in the dual forcing case, particularly in the central and western Gulf.

Figures 4, 5 and 6 also clearly demonstrate that ocean circulation climatologies are inappropriate for use in oil spill risk analysis in the Gulf of Mexico. Figures 4 and 5 show the highly dynamic nature of flow in the Gulf, and that there is no obvious averaging period (since the dominant Loop Current eddy shedding cycle can take anywhere from 6 to 18 months). Figure 6 shows that variability is as strong as the mean signal, and that the mean is quite different from circulation at any given point in time.

IV. EXPERIMENT 40

Experiment 9 exhibits many of the circulation features found in the Gulf, but discrepancies remain. Some problems, such as the correct simulation of the waves on the wall of the Loop Current, can only be solved by upgrades to the model proposed for years 2, 3 and 4 of this project. Others, such as the correct simulation of circulation on shelf areas, cannot be completely solved without a breakthrough in model design which is outside the original scope of the project. However the major aim of the first year effort was to investigate just how realistic the simulation could be made without major changes to the model.

Loop Current intrusion onto the continental shelf was identified as a major problem area. This is caused by the fact that the model's bottom topography is confined to the lower layer, so the minimum topography depth is taken to be 500 m and there is a flat shelf in the model between the 500 m isobath and the coast (Figure 7). Note that intrusion of strong Loop Current related flows onto the continental slope/shelf does occur in the Gulf, so the problem is how to control such intrusions in the model and how to have confidence in the results given the apparent deficiencies in model formulation.

Coastal areas are so important for oil spill risk analysis that the use of a layered circulation model might be carefully examined. But the Loop Current and its associated eddies dominate the overall Gulf circulation, and have a major impact on shelf circulation in both the eastern and western Gulf. Given the state of the art in supercomputers

it is simply not practical to produce a circulation model of the Gulf that has 10 Km (or even 25 Km) horizontal grid resolution Gulf-wide to simulate the Loop Current system, and high vertical resolution to give improved simulations over the shelf. Therefore the choice was between a layered model such as the one used here (possibly coupled to local shelf models), or a level model not significantly better Gulf-wide than the existing geostrophic climatology. In year four of the project, the layered model will be coupled to a one dimensional mixed layer model with high vertical resolution. This will improve simulation accuracy over shelf areas, but will not solve the intersection problem. Further details on the question of model design can be found in the original proposal (JAYCOR, 1983).

Several ad hoc methods were tried to control the flow over the shelf areas. For example the Yucatan coastline was extended to cover most of the Campeche Bank in an attempt to prevent early westward bending of the Loop Current, and interfacial friction was applied over shelf areas only to try to control intrusion. But none of these attempts were very successful, and the best solution came from simulations addressing the fact that the Loop Current eddies in Experiment 9 are large and have high maximum currents (they are at the very edge of the acceptable range of eddy sizes).

Eddy radius is dependent on the upper layer velocity at the core of the Loop Current (Hurlburt and Thompson, 1980). It can be controlled by three parameters, (a) upper layer rest thickness, (b) the density contrast between layers (i.e., g'), and (c) inflow transport and its distribution between layers. Upper layer thickness and g' were

carefully chosen in the original experiments to give the best representation possible of the Gulf in a two layer hydrodynamic model. Data on the actual inflow transport through the Yucatan Straits is not plentiful, but the figure of 30 Sv for the total average transport is consistent with what data is available. Data on the distribution of that transport in the vertical is almost non-existent, indeed even the direction of deep flow is not entirely certain. Therefore the original distribution of 26 Sv in the upper layer and 4 Sv in the lower layer was somewhat arbitrary, and the upper layer transport can be lowered to produce smaller eddies. Exactly what range of eddy sizes is realistic is hard to quantify, but there is one source of Gulf wide data that can be used as a guide. Maps of sea surface variability for the Gulf have been produced from all hydrographic, STD and XBT data (Maul and Herman, 1984), and from satellite altimeter cross-overs (Marsh, et al., 1984). The 20 Sv upper and 10 Sv lower layer distribution of inflow transport in Experiment 40 gives rise to a variability map very similar to that obtained from the satellite (Figure 8), these maps agree more closely with each other than with the map from hydrographic data (Figure 9). Based on the agreement of variability maps, the mean sea surface from Experiment 40 may well be the best mean available for the Gulf (Figure 10). The model parameters were:

- upper/lower layer inflow transport = 20/10 Sv,
- horizontal eddy viscosity, A = 300 m^2/sec,
- Coriolis parameter at the southern boundary f = 4.5 x 10^{-5} sec^{-1},
- gravitational acceleration, g = 9.8 m/sec^2,

- reduced gravity, $g' = .03(H1+H2)/H2$ m/sec^2,
- reference layer thicknesses, H1 = 200 m and H2 = 3300 m,
- minimum depth of bottom topography = 500 m,
- grid spacing, 20 by 22 Km (0.2 by 0.2 degrees),
- beta, $df/dy = 2 \times 10^{-11}$ m^{-1} sec^{-1},
- wind stress = 0,
- interfacial stress = 0,
- coefficient of quadratic bottom stress = .003; and
- time step = 1.5 hours.

As a side effect of increased flow in the lower layer intrusion onto the Florida Shelf has been reduced, as can be seen from a comparison of free surface snapshots from Experiments 28 (with 26/4 transport distribution) and 40 (Figure 11). This is because lower layer flow tends to follow the bottom topography contours (or more exactly f/H contours), and the increased deep transport allowed the upper layer flow to feel the continental slope more strongly.

V. EXPERIMENT 60

Horizontal eddy viscosity is used in the model to parameterize sub-grid scale processes. As a general rule eddy viscosity should be chosen as low as possible in high resolution models, although if it is too low circulation features can be produced that are not adequately resolved by the model grid. These features will not necessarily be simulated accurately. For example, the waves moving around the Loop Current eddy in Experiment 9 fall into this category. There is no substitute for high horizontal resolution.

Experiment 40 does not exhibit the smaller scale features, such as the meanders on the wall of the Loop Current and the counter-rotating vortex pair as dramatically as earlier experiments. However since this experiment has lower maximum speeds the horizontal eddy viscosity can be lowered. Experiment 60 therefore is identical to Experiment 40 except that the eddy viscosity is 100 rather than 300 m^2/sec. The full model parameters were:

- upper/lower layer inflow transport = 20/10 Sv,
- horizontal eddy viscosity, A = 100 m^2/sec,
- Coriolis parameter at the southern boundary f = 4.5×10^{-5} sec^{-1},
- gravitational acceleration, g = 9.8 m/sec^2,
- reduced gravity, g' = .03(H1+H2)/H2 m/sec^2,
- reference layer thicknesses, H1 = 200 m and H2 = 3300 m,
- minimum depth of bottom topography = 500 m,

- o grid spacing, 20 by 22 Km (0.2 by 0.2 degrees),
- o beta, df/dy = 2×10^{-11} m^{-1} sec^{-1},
- o wind stress = 0,
- o interfacial stress = 0,
- o coefficient of quadratic bottom stress = .003; and
- o time step = 1.5 hours.

Figures 12 to 19 show upper layer velocities from Experiment 60 covering 300 days at irregular intervals. Figures 12, 13 and 14 are 40 days apart and show a Loop Current eddy moving into the western Gulf. In Figure 12 there is a pair of eddies in the northeast Gulf. In Figure 13 there are six or more small eddies in the northeastern Gulf that have been spun off the main Loop Current eddy, this may be the feature observed as a meandering current in Brookes and Legeckis (1984). Forty days later the currents in this area have again changed and most of the flow is to the east (Figure 14). Figure 15 shows the situation one hundred days later. The flow patterns in the entire western half of the Gulf are extremely complex as the Loop Current eddy dissipates on the coast of Mexico at about 24N. Note also the current along the continental slope off Florida. Ninety days later an eddy is about to break off from the Loop Current, Figures 16 to 19 are ten days apart. Cyclonic rings are moving around the wall of the Loop, and one appears to pass right through the space between the Loop and the shed eddy (Figure 19). During this time the eddy is intruding significantly onto the Campeche Bank.

On 19 November 1980, the NOAA Buoy Office (NDBO) deployed three experimental TzD drifting buoys, at approximately 24.5N and 92W, in an eddy that had just been shed by

the Loop Current (Kirwan et al., 1984). All three drifters stayed in the eddy for at least five months as it propagated westward to the Mexican coast, see Figure 20. The buoys were undrogued but had 200 m thermistor cables, which clearly coupled the drifters to the deeper circulation. Figure 21 shows simulated drifter tracks for 160 days from Experiment 60. They start earlier in the eddy cycle than the NBDO buoy tracks. The simulated drifter moves in response to the upper layer velocity from the ocean model, which represents the mean velocity above the thermocline. Along the drifter tracks the upper layer thickness is between 250 and 350 m. The simulated drifter position is calculated every 45 minutes based on the velocities at the four previous positions using a Adams-Bashforth prediction method. Velocities are linearly interpolated in space and time between the archived model velocity fields that are available once every ten model days. Interpolation in time is not an ideal way to calculate velocities since the eddy moves west about 30 Km in ten days. The slight elongation of the eddy's east-west axis this causes is acceptable, but it also filters out any short time scale velocity fluctuations. One advantage of simulated drifters is that the ocean model data also gives a view of the entire Gulf, Figures 22 and 23 show snapshots of the model free surface deviation every 30 days from the simulated deployment date (model day 1680) until model day 2010.

The simulated drifters are in good general agreement with the actual drifter data. Both follow approximately the same path into the southwest Gulf. Experience with the model suggest that this is the preferred eddy trajectory although they can also track due west to arrive at the coast

further north. The observed average rotation period is between 14 and 17 days, with a westward translation speed of 5 to 10 cm/sec and velocity component speeds of on the order of 50 cm/sec (Kirwan et al., 1984). The simulated eddy has a rotation period of 15 to 16 days, a westward translation speed of 3 to 6 cm/sec and velocity component speeds of on the order of 50 cm/sec. The lower model eddy translation speeds may be due to the absence of wind forcing, or to the model's idealized vertical structure. The addition of a third layer and thermodynamics to the model in year three of this project will improve the vertical density structure, and may lead to different translation speeds.

The simulated drifters exhibit very regular loops and appear to remain at approximately the same relative position within the eddy for long periods. The actual drifters on the other hand are much more variable, with paths indicative of changes of the drifter location relative to the ring center. These changes are probably primarily due to windage effects on the drifters, and might be minimized by adding a drogue at the end of the thermistor line (i.e., at 200 m) on future buoys. In principle windage could be accounted for in drifter simulations; model experiments with wind forcing automatically account for layer averaged Ekman effects, but allowing for winds acting directly on the buoy would require knowledge of the the relative effectiveness of such forcing.

Figure 24 follows the path of simulated drifter number 3 for 300 days. Remarkably it is still tracking the eddy after all this time, even though the eddy has almost totally dissipated by model day 1980 (see Figure 23). Drifter 1599 tracked the eddy remnants until mid-June 1981,

but drifters 1598 and 1600 left the eddy in mid-April and early-May respectively. The model eddy probably dissipated too slowly, because its interaction with the continental shelf cannot be modeled accurately. But equally it is not necessarily the case that the actual eddy had entirely disappeared by mid-June 1981, it is possible that wind effects caused drifter 1599 to leave the eddy at that time. In any case the model accurately simulates the northward motion of the eddy once it reaches the coast of Mexico. However the paths of 1598 and 1600 once they leave the eddy suggest that the remnant of a previous Loop Current eddy that persists off the Texas coast in the model simulation throughout this time period was not present in the summer of 1981. Similar features occur in almost every model simulation, even in simulations with wind forcing only, where it is a wind induced gyre rather than a Loop Current eddy. Their presence is explainable by the northward migration of anti-cyclonic rings along the coast until they reach Texas, where the continental slope turns east and they can go no further. But in the Gulf the rings probably dissipate more quickly against the continental shelf than they do in the model, since the latter cannot include topography shallower than 500 m.

Figure 25 contains time series of velocity for drifters 1598, 1599 and 1600. The strong high frequency contribution is unusual and is largely due to the 30 hour basin tidal resonance and possibly inertial oscillations, along with diurnal and semidiurnal tides and a 7-hour free gravity mode (Kirwan et al., 1984). Figure 26 shows time series of velocity for simulated drifters 3 and 4. These show no high frequency components, as is to be expected

given that the simulation only has access to new model velocity fields once every ten days. High frequency components might appear in simulated drifters that were calculated "on the fly" within the ocean model, since new velocity fields would then be available every 90 minutes. The low frequency velocity components of the actual buoys agree well with the simulated drifters. Both show periodicity associated with the eddy circulation and velocities of about 50 cm/sec. The simulated time series are far more regular, as is expected from the comparison of drifter tracks.

VI. EXPERIMENT 68

Simulations forced by winds based on a seasonal climatology from ship observations have already been described. Such wind fields are not ideal for driving ocean models since they contain very little of the total wind variability and mean wind strengths are in general far weaker than instantaneous winds. Recognizing this deficiency NORDA funded JAYCOR to produce a wind set for the Gulf based on the Navy's twelve hourly surface pressure analysis, which is available from 1967 to 1982 (Rhodes et al., 1984). The geostrophic winds, corrected geostrophic winds, and wind stresses (all on a one degree grid covering the Gulf) every 12 hours from 1967 to 1982 are on magnetic tape. These will be made available through the MMS Gulf of Mexico regional office.

Figure 27 shows the wind stress and wind stress curl from this data set for 0000 and 1200 GMT on 14 January and 0000 GMT on 15 January 1976. There is large temporal variability of the wind field during this period, as general easterly flow gives way to strong northerly flow after a frontal passage in just a 24 hour period. The wind stress curl field also shows the rapid change, from a relatively weak field to a very strong field with strong horizontal gradients. Figure 28 shows similar plots for 14 and 15 July 1976. Even in the summer, when flow is generally weaker, very significant differences can be seen in a short time period. These strong variations and very rapid changes in the wind field indicate why the modeling of Gulf circulation requires wind data on short temporal scales.

Figures 29 to 32 show the seasonal climatologies averaged over the period 1967-1982. The wind stress and wind stress curls are much stronger in the winter season than the summer season as would be expected. There are persistent areas of positive curl over the Yucatan and negative curl in the southwest Gulf that are present for all seasons, but were not seen in any previous study of Gulf wind stresses. Although not present at all time periods (Figures 27 and 28), these are also the dominant features of the instantaneous curl fields.

There have been no published accounts of driving an ocean circulation model for long time periods with winds sampled as frequently as those available in this wind set. Previously a monthly climatology would have been considered an exceptionally good data set for such an application. One of the initial goals of this first year effort was to determine how best to use this data set to drive the ocean model. The model simulates the layer averaged circulation above and below the thermocline, and so only includes the longer term effects of winds on ocean currents. But it is clearly preferable for the ocean model to integrate the effect of short term variability on these currents, rather than for the winds to be averaged before input to the model. Before testing began it was expected that inertial oscillations and gravity waves generated by the highly variable forcing would make using the 12 hourly winds directly impractical. So the plan was to test the model with increasingly long wind averages until these problems became manageable. In all cases the wind stresses are linearly interpolated in time between inputs, so the wind forcing is slightly different at each time step.

Experiment 68 is identical to Experiment 40 except for the addition of wind forcing after the port forced circulation has fully spun up. Wind input is every 12 hours, at first 1967 winds were used repeatedly to spin up the wind driven flow and then winds from 1967 to 1977 were applied in sequence. The expected difficulties with frequent wind input did not arise, although attempts to add these winds to Experiment 60 (with lower eddy viscosity) were unsuccessful. The model parameters were:

- o upper/lower layer inflow transport = 20/10 Sv,
- o horizontal eddy viscosity, A = 300 m^2/sec,
- o Coriolis parameter at the southern boundary f = 4.5 x 10^{-5} sec^{-1},
- o gravitational acceleration, g = 9.8 m/sec^2,
- o reduced gravity, g' = .03(H1+H2)/H2 m/sec^2,
- o reference layer thicknesses, H1 = 200 m and H2 = 3300 m,
- o minimum depth of bottom topography = 500 m,
- o grid spacing, 20 by 22 Km (0.2 by 0.2 degrees),
- o beta, df/dy = 2 x 10^{-11} m^{-1} sec^{-1},
- o wind stress from 12 hourly Navy Corrected Geostrophic Wind set,
- o interfacial stress = 0,
- o coefficient of quadratic bottom stress = .003; and
- o time step = 1.5 hours.

Figures 33 to 39 show upper layer currents (i.e., vertically averaged currents above the thermocline) every 60 days for 360 days. Vectors are only drawn at every second point (i.e., every 0.4 degrees) to improve readability.

Figure 34 shows the furthest northward penetration of the Loop Current ever attained by the ocean model, this configuration is often seen in the Gulf. After the eddy breaks off the Loop Current intrudes onto the Florida Shelf and some of the flow splits off to the north for a brief time (Figures 35 and 36). Similar intrusions have been observed in the Gulf, but the models inadequate representation of shelf topography make it likely that the simulated currents in shallow areas (say less than 100 m) are too high. A persistent anti-cyclonic gyre in the north west Gulf has been a feature of almost all Gulf simulations performed to date. The addition of wind forcing in Experiment 68 has increased its average size and its effect on incoming Loop Current eddies (Figures 37, 38 and 39). The presence of a gyre in this position is explainable by the northward migration of anti-cyclonic eddies along the coast of Mexico until the continental slope bends eastward and they can go no further. However in the Gulf the gyre probably dissipates relatively rapidly against the shallow shelf area. The ocean model cannot include a shallow shelf, but it may be possible for it to parameterize the effect of such a region on strong currents. Ad hoc patches to the model of this kind can only be justified if (a) there is clearly a problem with the existing model simulation and (b) there is sufficient observational data available to verify that the patch is indeed "correcting" the simulation towards more realistic flow patterns. Modifying the simulation towards the general perception of what the circulation should be, without supporting data, is dangerous. Our understanding of Gulf circulation has changed radically in the last ten years, and given the sparsity of the existing observational data base

it is likely to continue changing. In the case of the gyre in the northwest Gulf condition (a) probably can be satisfied, but obtaining the data to satisfy condition (b) will be difficult. MMS's planned observational program in the western Gulf will be of assistance in this area. Finally it should be noted that problems of this kind can sometimes be solved by less drastic measures. For example the Loop Current intrusions onto the Florida Shelf were eventually reduced by re-evaluating the inflow transport distribution. Similarly the north western gyre was least obvious in Experiment 60 which has the lowest eddy viscosity. It is possible therefore that next years simulations with a 10 km grid and correspondingly lower eddy viscosity will resolve this question.

Simulated surface currents from Experiment 68 have been delivered to MMS as representing the best simulation data available to date. They consist of velocity component (u and v) fields on a 0.2 degree rectangular grid covering the Gulf area, sampled every three days for 3780 model days (10.3 years). Velocity plots taken once every 30 days (i.e. plots of every tenth set of fields) for the entire ten year period were also delivered. Figures 33 to 39 represent a very small subset of these plots, note that a current vector is only drawn at every second point (i.e., on a 0.4 degree grid) to improve readability.

The velocities represent mean currents above the thermocline and are therefore essentially independent of local winds. To a good approximation they can be treated as geostrophic surface currents. The Oil Spill Trajectory Analysis (OSTA) model can therefore include the simulated surface currents in exactly the same way as the previous

climatological geostrophic surface currents. Except that now new current data is available more frequently, and the OSTA model can include variation in surface currents (over a ten year period) as well as variation in wind driving. However the use of ten years of surface currents, rather than climatology (which is effectively one year of data), means that the OSTA model will require more computer resources to complete its statistical analysis of risk.

FIGURES 1-39

FIGURE 1: (a) Instantaneous view of the interface deviation in a two-layer simulation of the Gulf of Mexico driven from rest to statistical equilibrium solely by inflow through the Yucatan Straits (Experiment 9). The contor interval is 25 m, with solid contours representing downward deviations. (b) Depth of the 22 degree isothermal surface, 4-18 August 1966 (Alaminos cruise 66-A-11), from Leipper (1970). The contour interval is 25 m.

a)

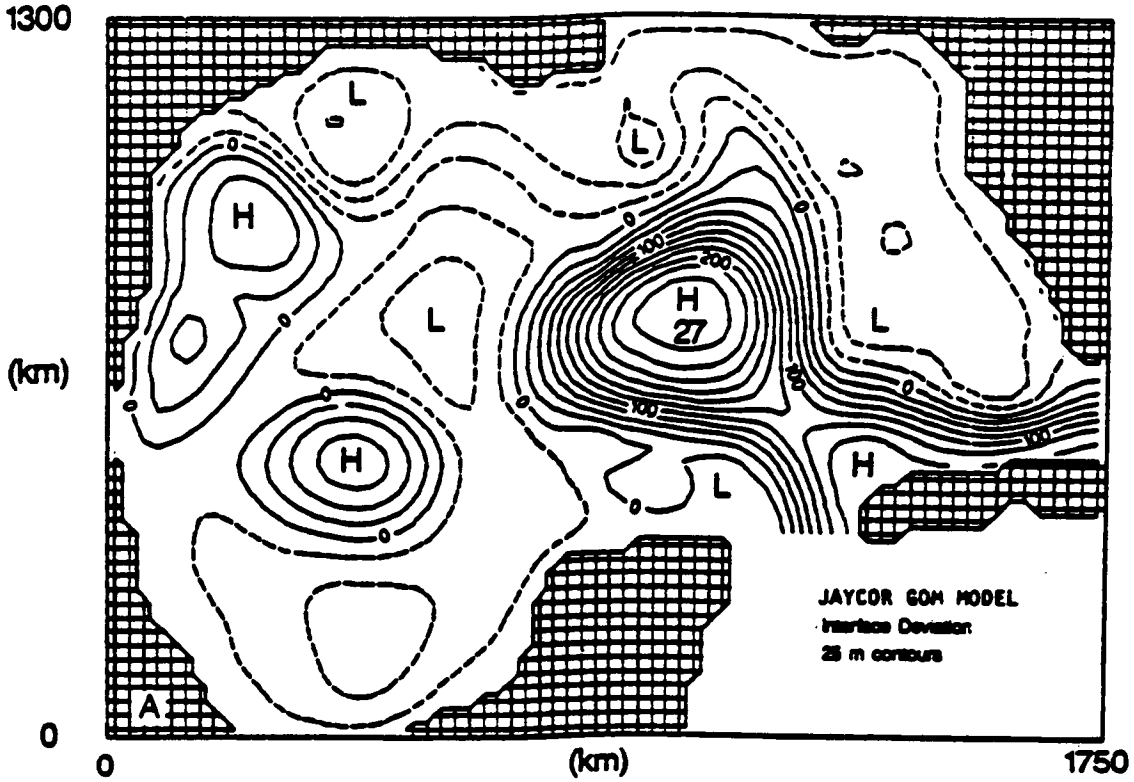
1300
(km)
0
0
(km)
1750
H
L
H
27
JAYCOR GOM MODEL
Interface Deviation
25 m contours
A

b)

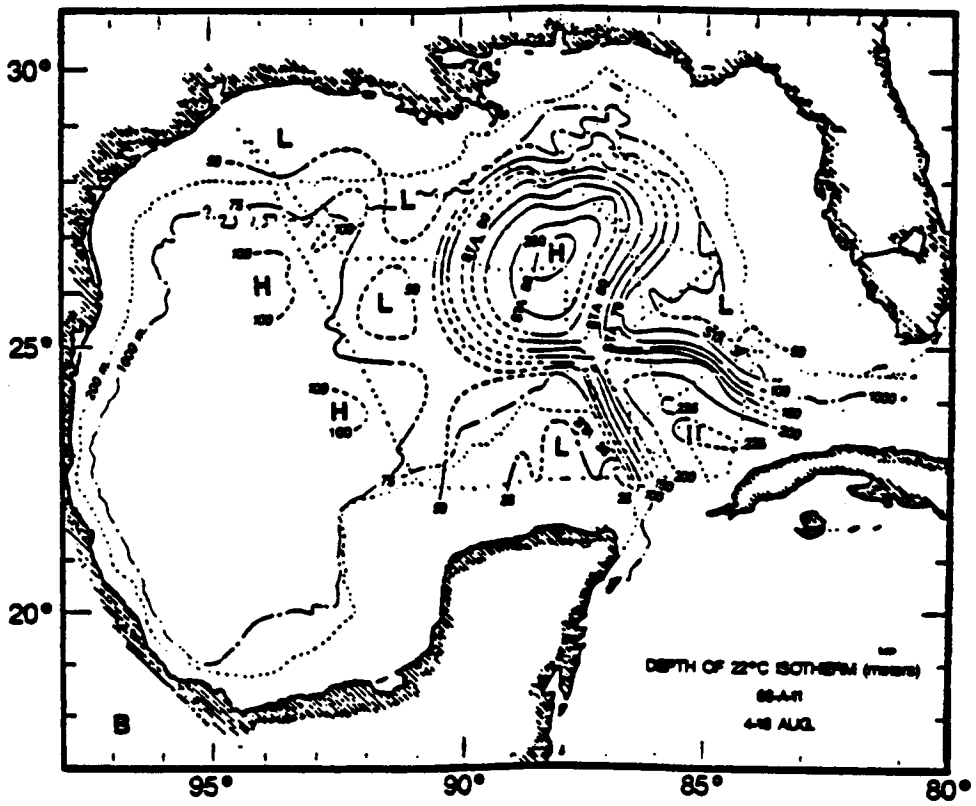
30°
25°
20°
95°
90°
85°
80°
H
L
B

FIGURE 2: (a) Interface deviation from the Gulf of Mexico simulation at model day 1970 after an eddy has separated from the Loop Current and propagated westward. (b) Ninety days later the major anti-cyclonic eddy at day 1970 has developed into a counter-rotating vortex pair in the western Gulf. The cyclonic vortex is to the north and the anti-cyclonic to the south.

(a)

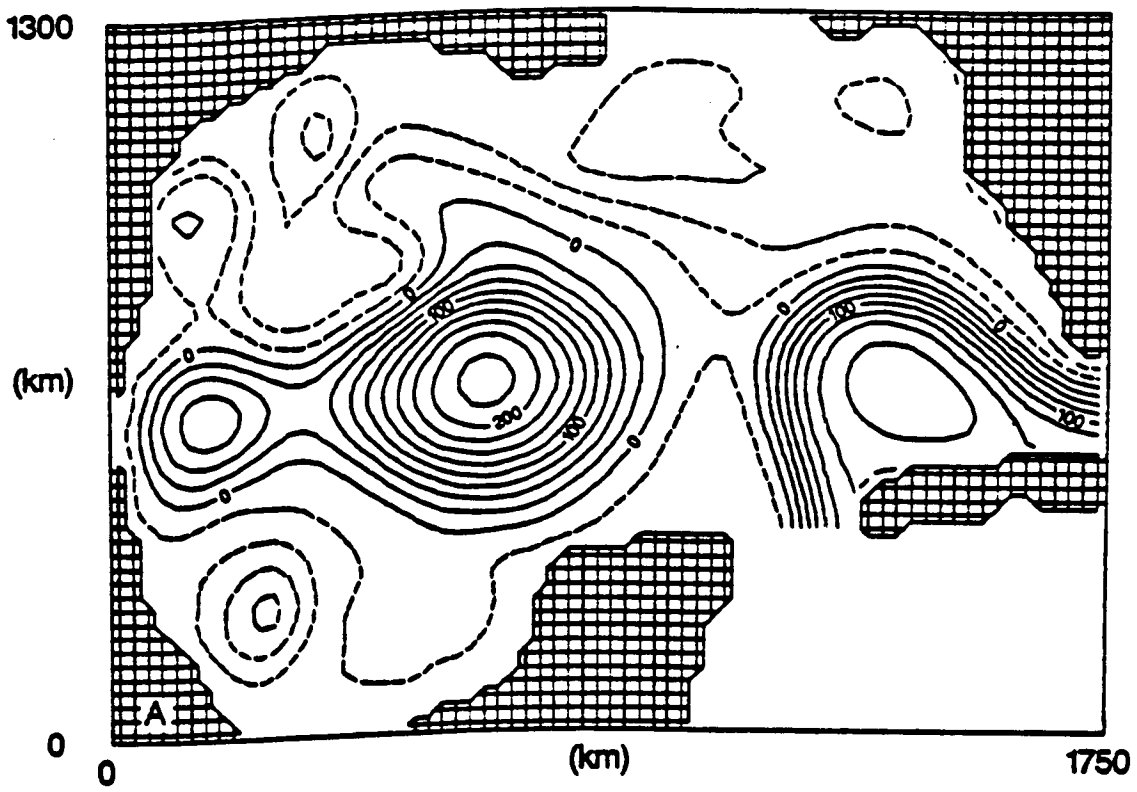

(b)

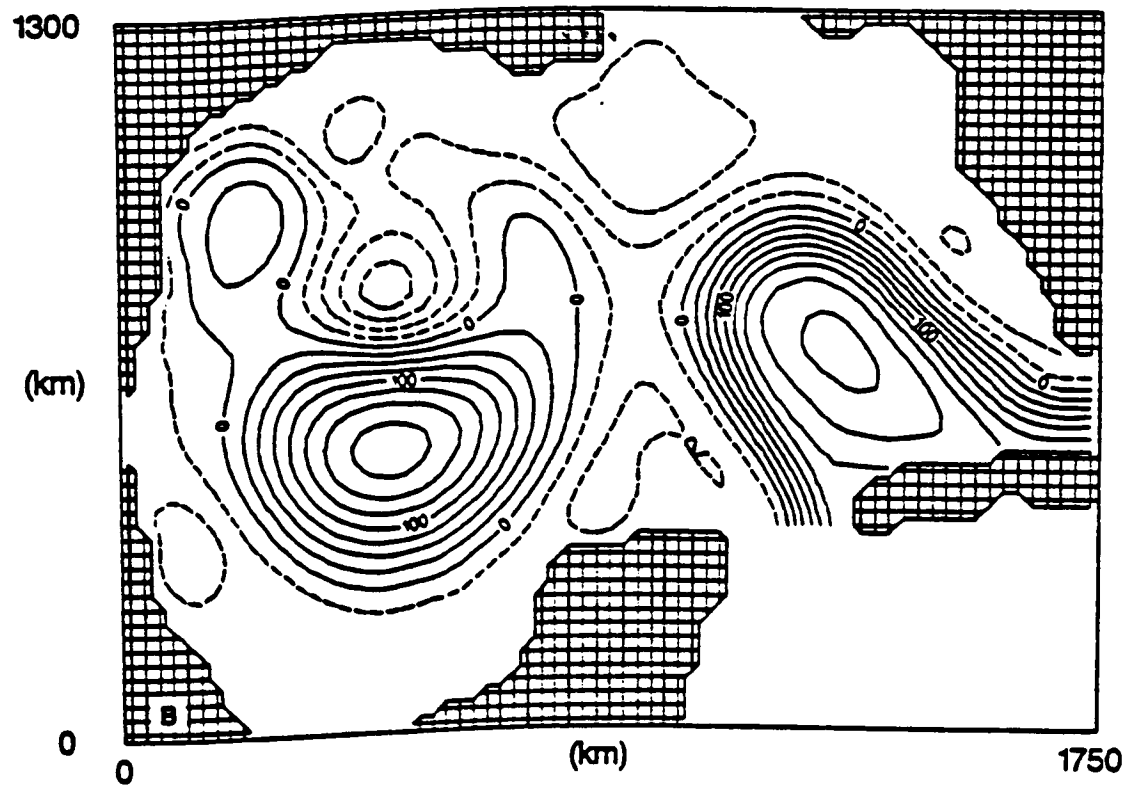

FIGURE 3: Counter-rotating vortex pair in the western Gulf of Mexico as shown by the depth of the 15 degree isotherm (in meters), observed in April 1978. The cyclonic vortex is to the north and the anti-cyclonic to the south (from Merrell and Morrison, 1981).

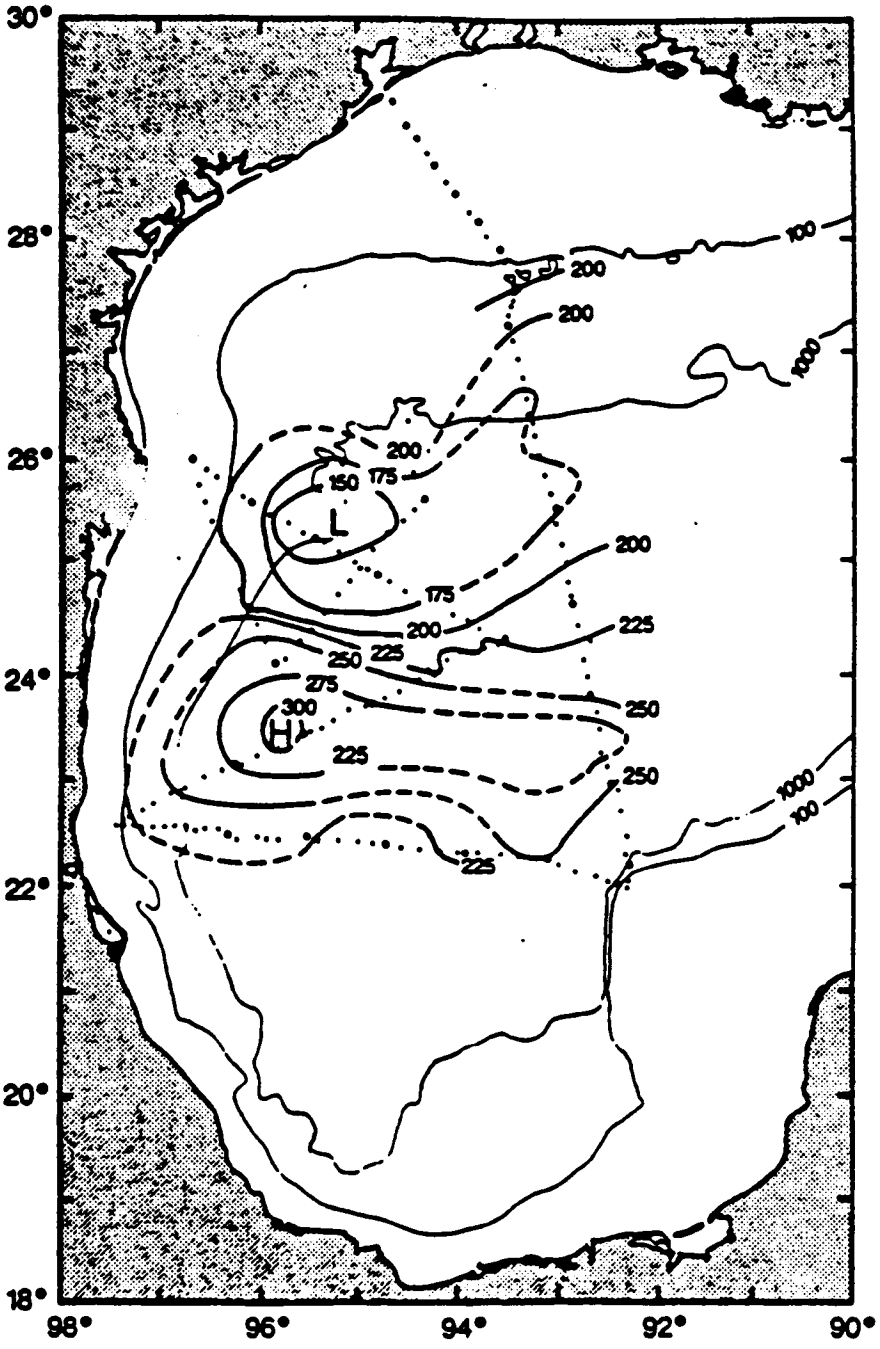
30°
28°
26°
24°
22°
20°
18°
98°
96°
94°
92°
90°
100
200
200
1000
200
150
175
L
200
175
200
225
250
225
275
300
H
250
225
250
1000
100
225

FIGURE 4: Instantaneous view of the interface deviation every 90 days, from day 90 of model year 9 to day 0 of model year 10, for Experiment 28 (left) and Experiment 34 (right). Experiment 34 is identical to 28 except for the addition of wind forcing. The contour interval is 25 m.

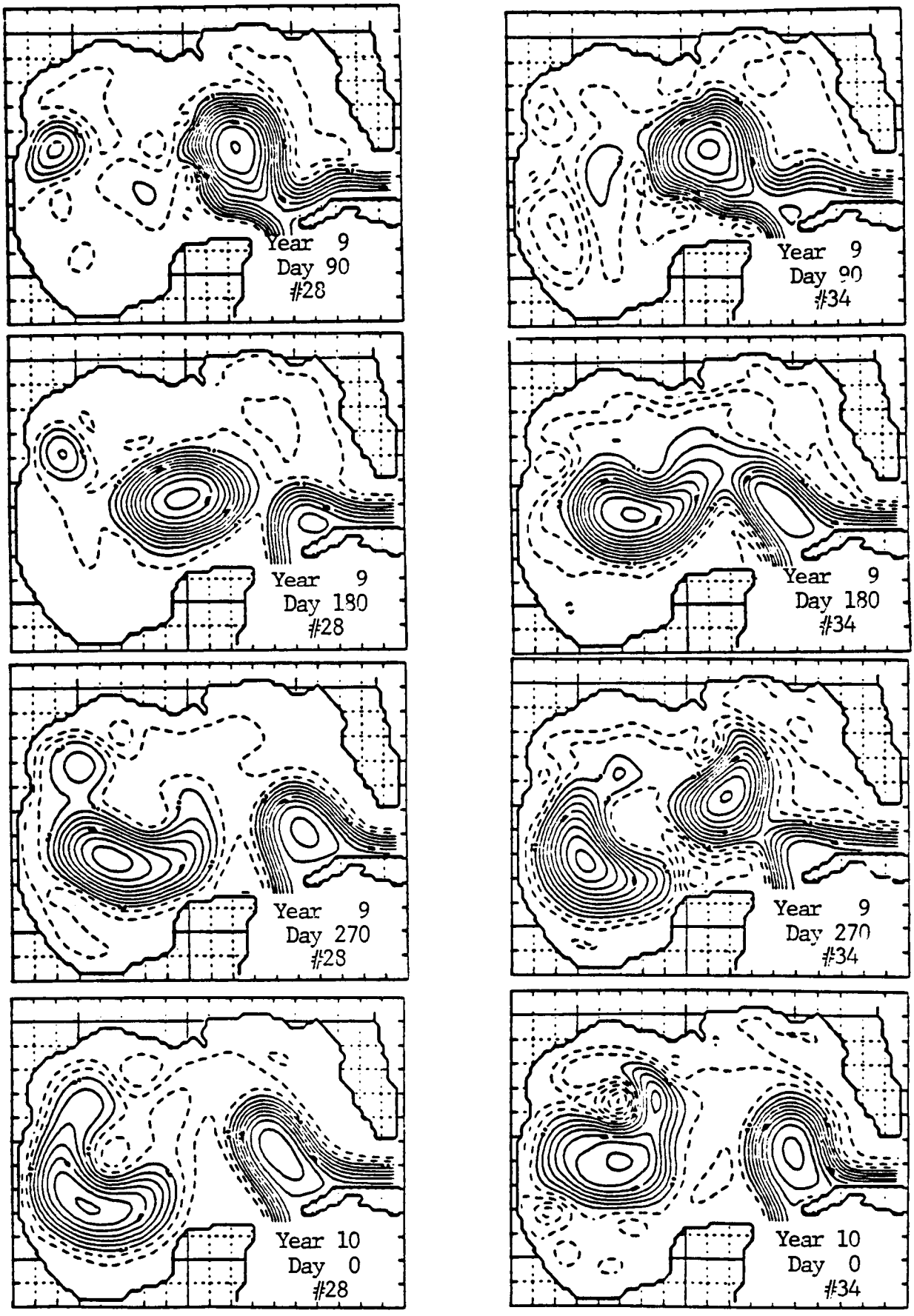
Year 9
Day 90
#28
Year 9
Day 90
#34
Year 9
Day 180
#28
Year 9
Day 180
#34
Year 9
Day 270
#28
Year 9
Day 270
#34
Year 10
Day 0
#28
Year 10
Day 0
#34

FIGURE 5: Instantaneous view of the interface deviation every 20 days, from day 260 of model year 9 to day 0 of model year 10, for Experiment 34.

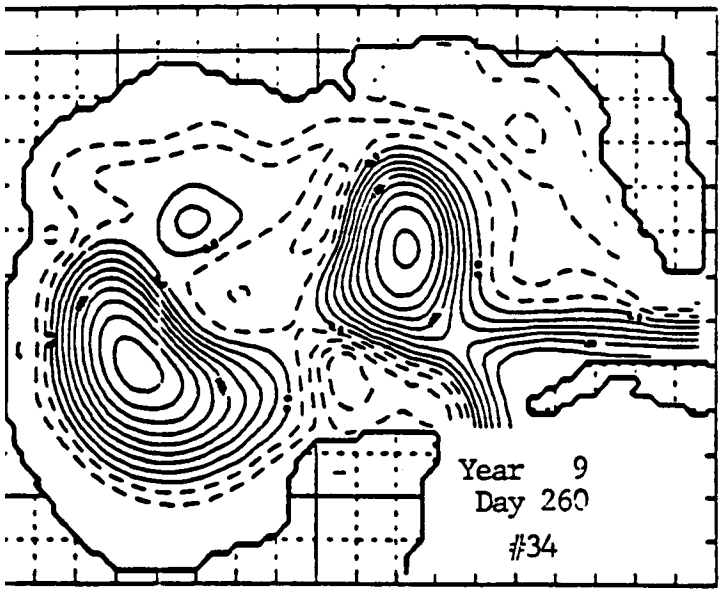
Year 9
Day 260
#34

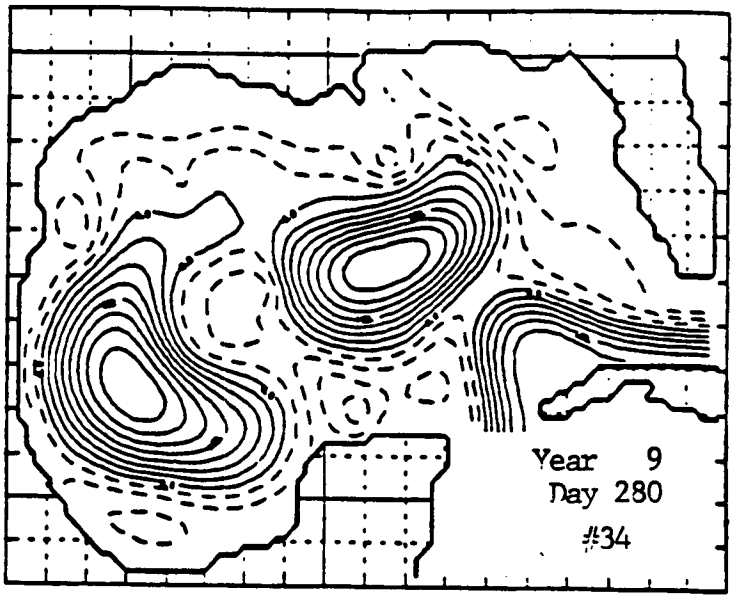
Year 9
Day 280
#34

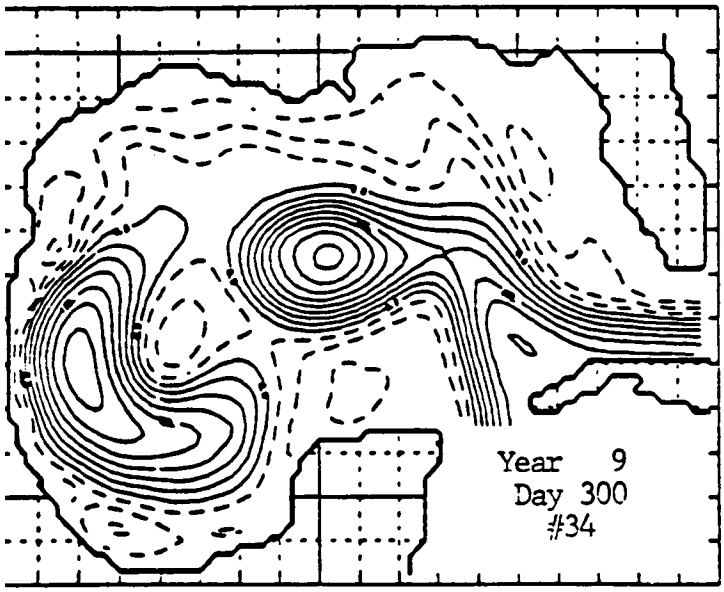
Year 9
Day 300
#34

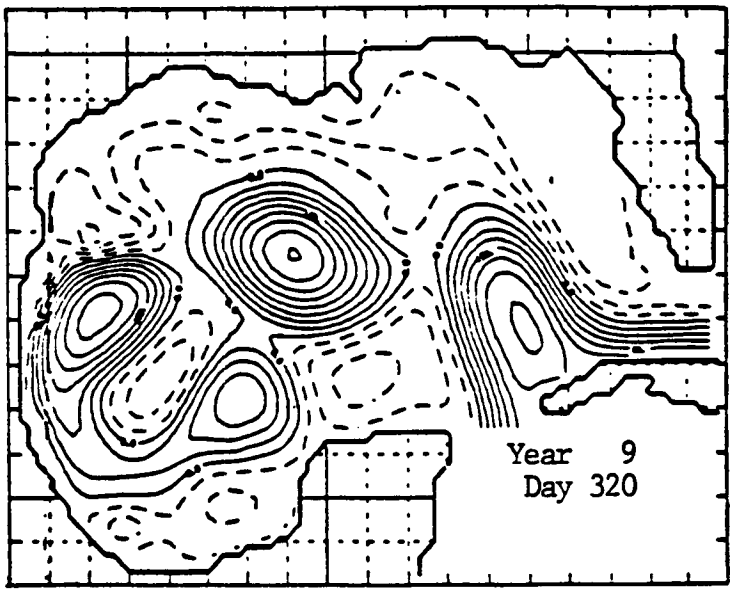
Year 9
Day 320

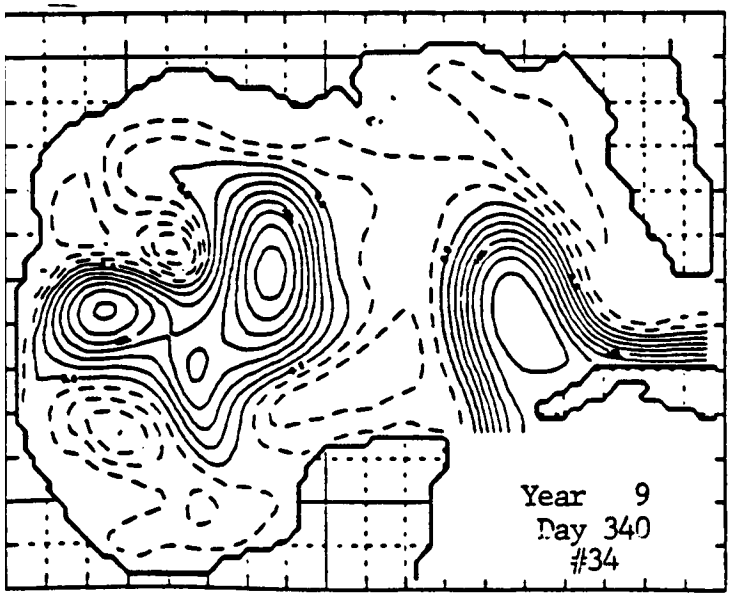
Year 9
Day 340
#34

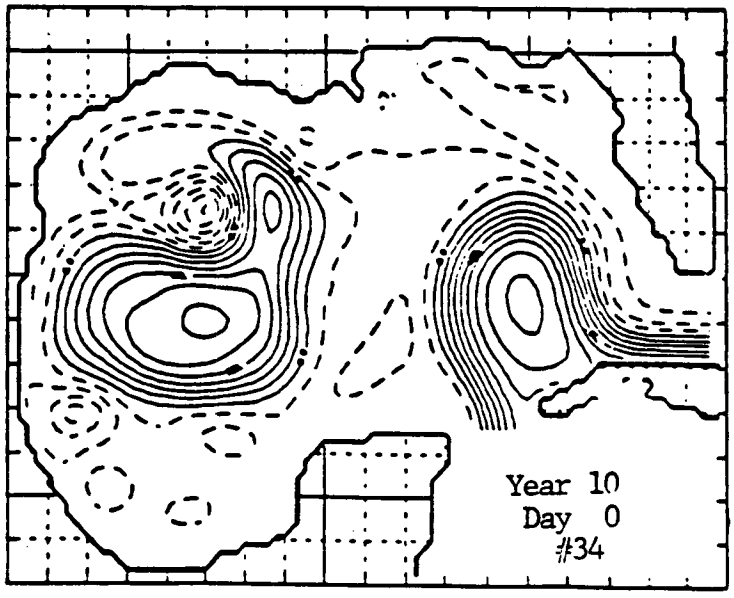
Year 10
Day 0
#34

FIGURE 6: Interface deviation mean and variability, for the Gulf of Mexico from ocean model. (a) Experiment 31, wind forcing only; (b) Experiment 28, port forcing only; (c) Experiment 34 wind plus port forcing. The contour interval is 12.5 m.

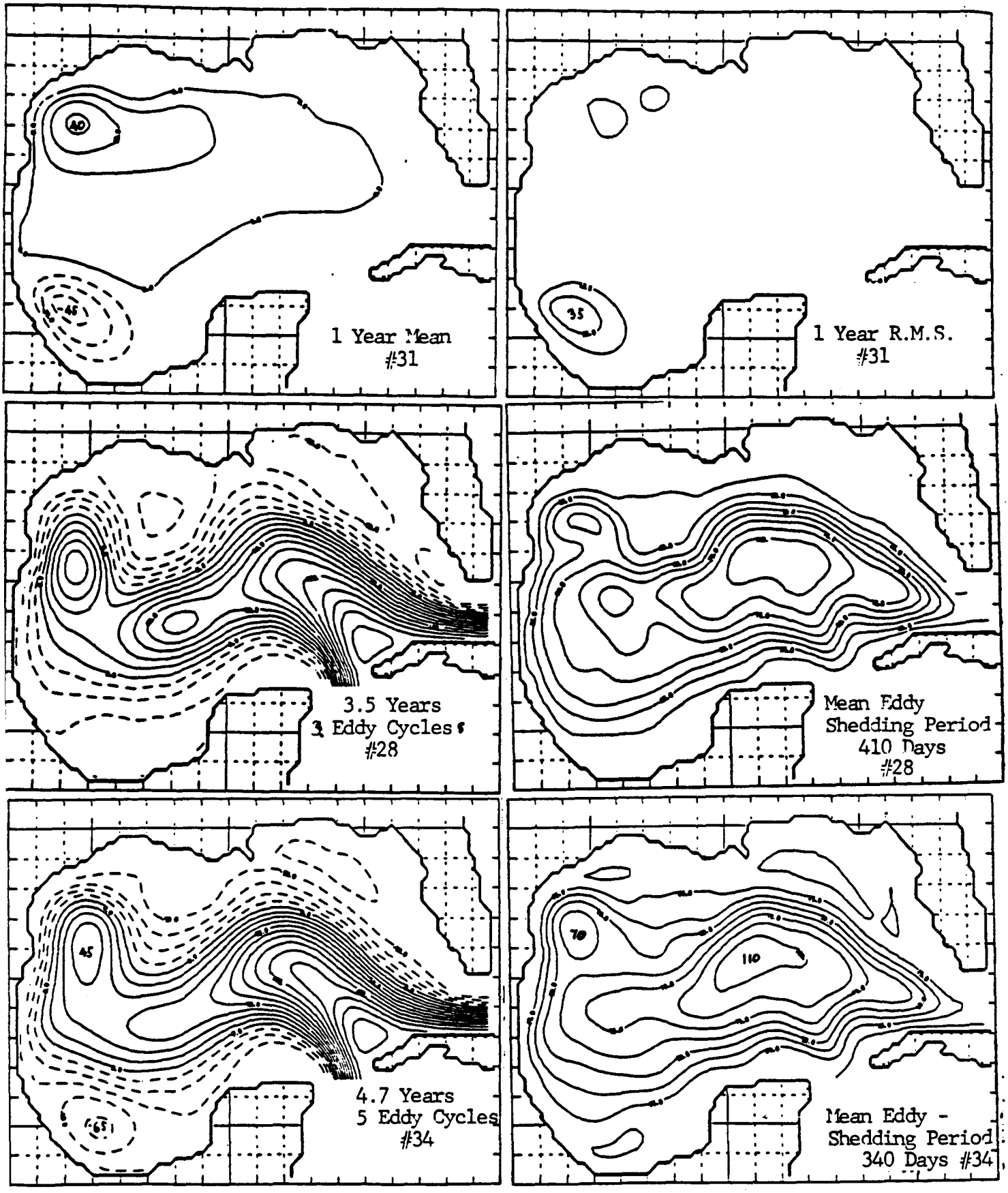
40
45
1 Year Mean
#31
35
1 Year R.M.S.
#31
3.5 Years
3 Eddy Cycles
#28
Mean Eddy
Shedding Period
410 Days
#28
45
65
4.7 Years
5 Eddy Cycles
#34
70
110
Mean Eddy -
Shedding Period
340 Days #34

FIGURE 7: Bottom topography and coastline geometry for Gulf of Mexico model on 0.2 degree grid. The contour interval is 250 m and the shallowest depth is 500 m. The section of the Caribbean shown is treated as land by the model, the position of the inflow port is marked by the termination of contour lines in the Yucatan Strait.

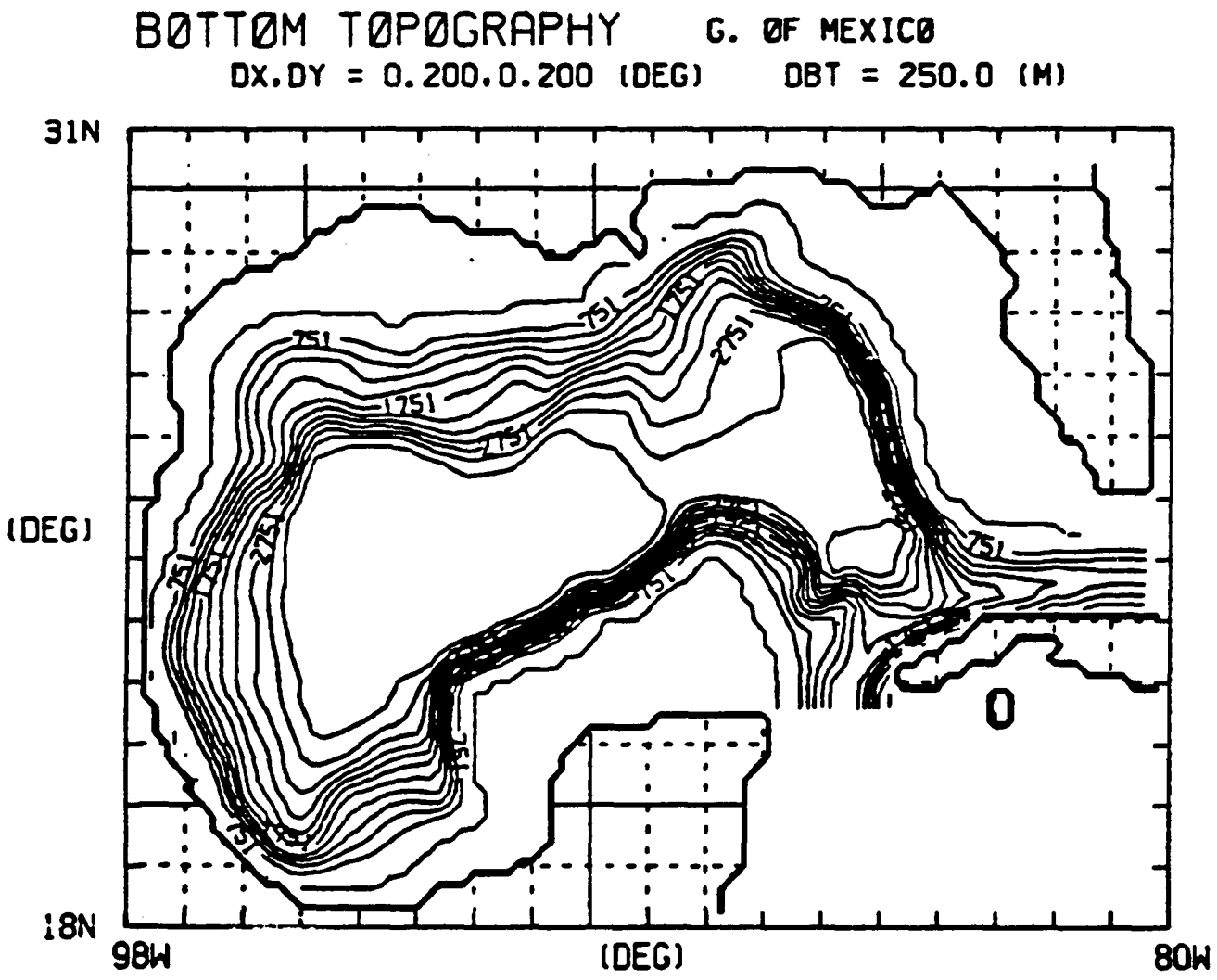
BØTTØM TØPØGRAPHY G. ØF MEXICØ
DX.DY = 0.200.0.200 (DEG) DBT = 250.0 (M)
31N
(DEG)
18N
98W
(DEG)
80W
0

FIGURE 8: Sea surface height variability for the Gulf of Mexico. (a) Based on about 16,000 GEOS-3 and SEASAT cross overs, spanning nearly four years (from Marsh, Cheney and McCarthy, 1984). (b) Based on an ocean model simulation with port forcing only (Experiment 40), measured over three eddy cycles at statistical equilibrium with the free surface sampled every ten days for a total of over 300,000 "observations".

SEA SURFACE VARIABILITY FROM GEOS-3 AND SEASAT CROSS OVERS (CM)

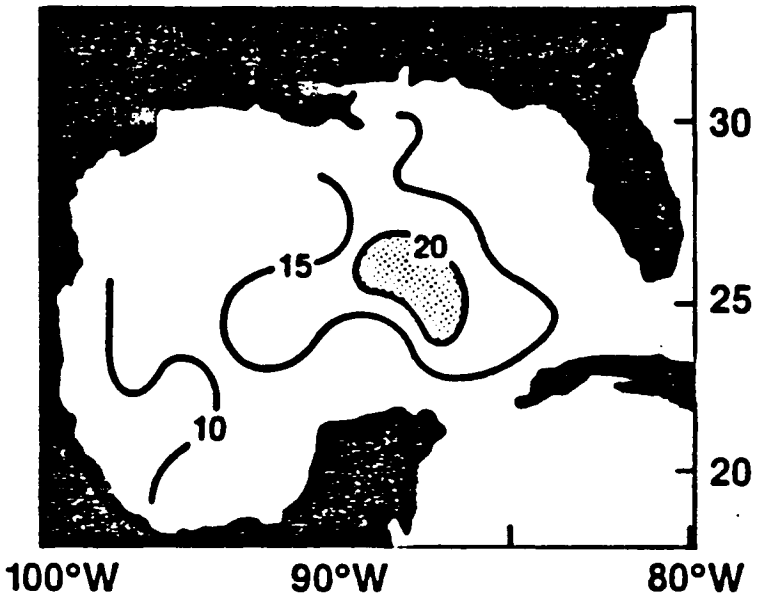

SEA SURFACE VARIABILITY (CM) FROM NORDA MODEL

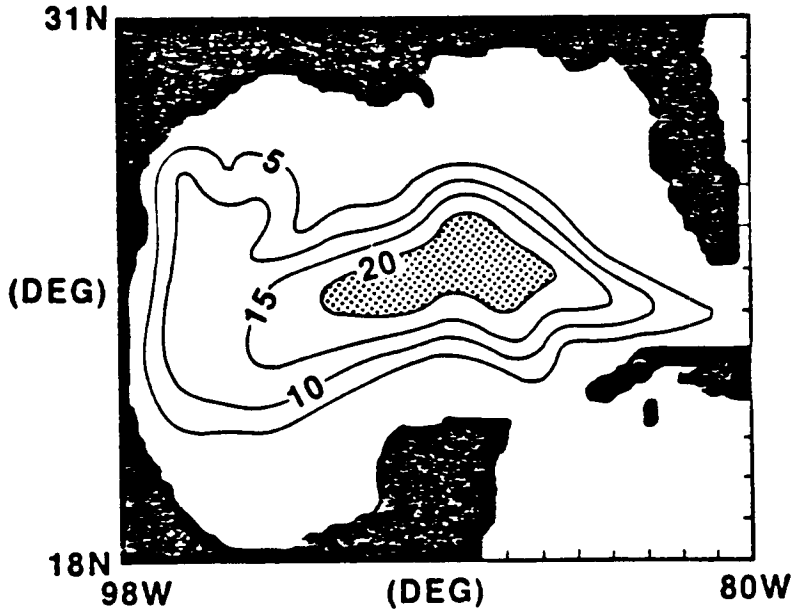

FIGURE 9: Sea surface height (a) variability and (b) mean, for the Gulf of Mexico. Based on all available hydrographic, STD and XBT data at over 16,000 stations, with substantial filtering (from Maul and Herman, 1984).

STANDARD DEVIATION OF MEAN DYNAMIC TOPOGRAPHY

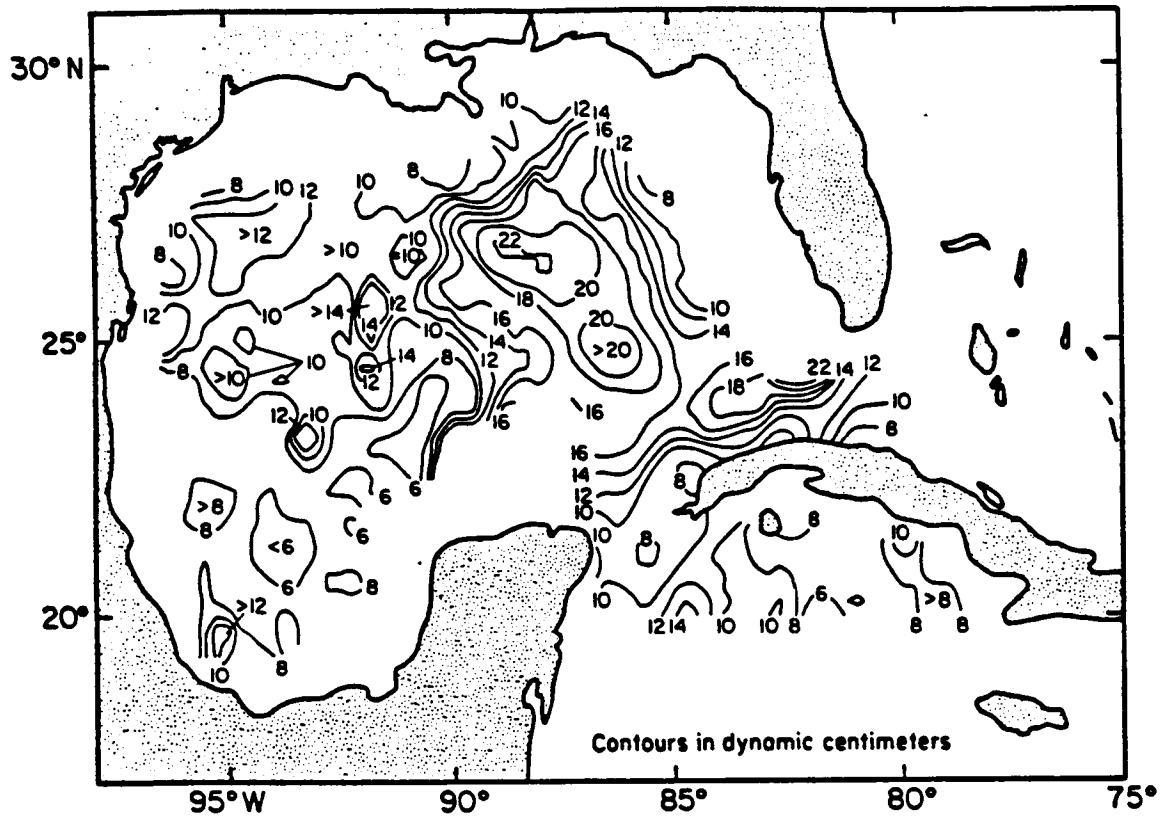

MEAN DYNAMIC TOPOGRAPHY AT 25 km RESOLUTION

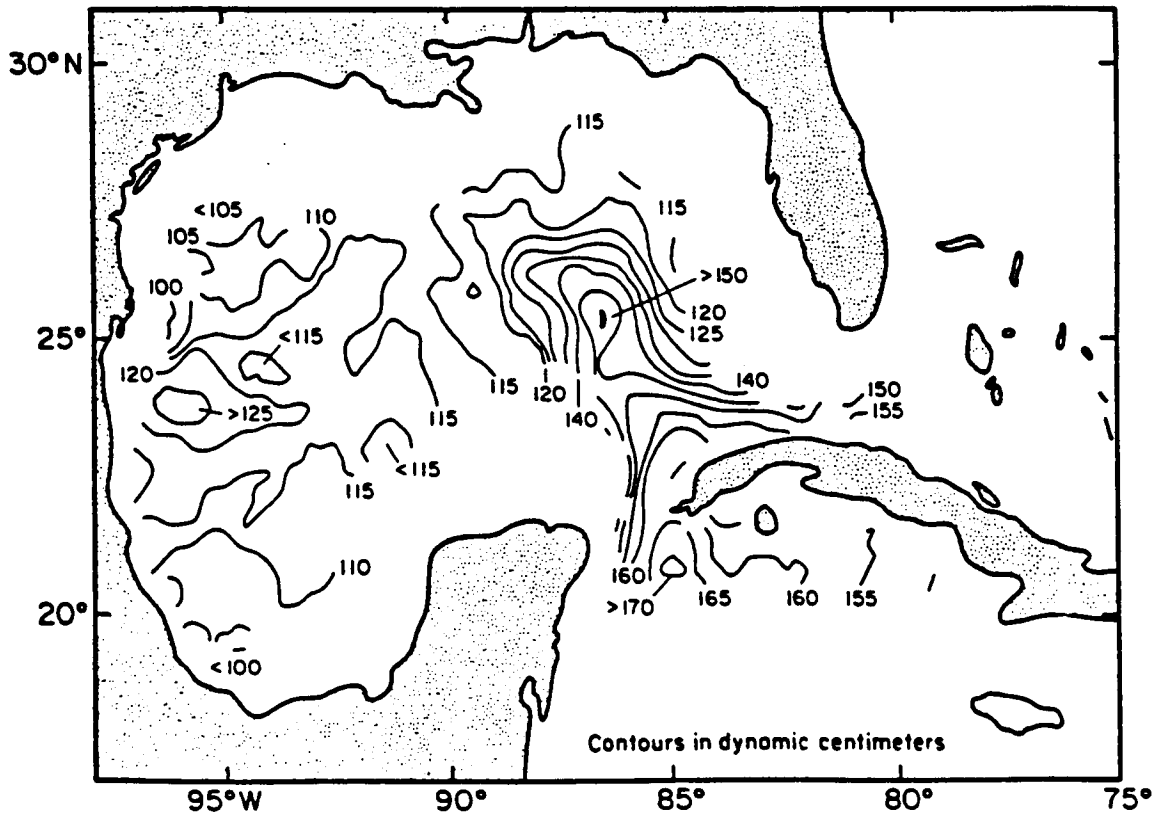

FIGURE 10: Mean sea surface height for the Gulf of Mexico. Based on an ocean model simulation with port forcing only (Experiment 40), measured over three eddy cycles at statistical equilibrium. The contour interval is 5 cm.

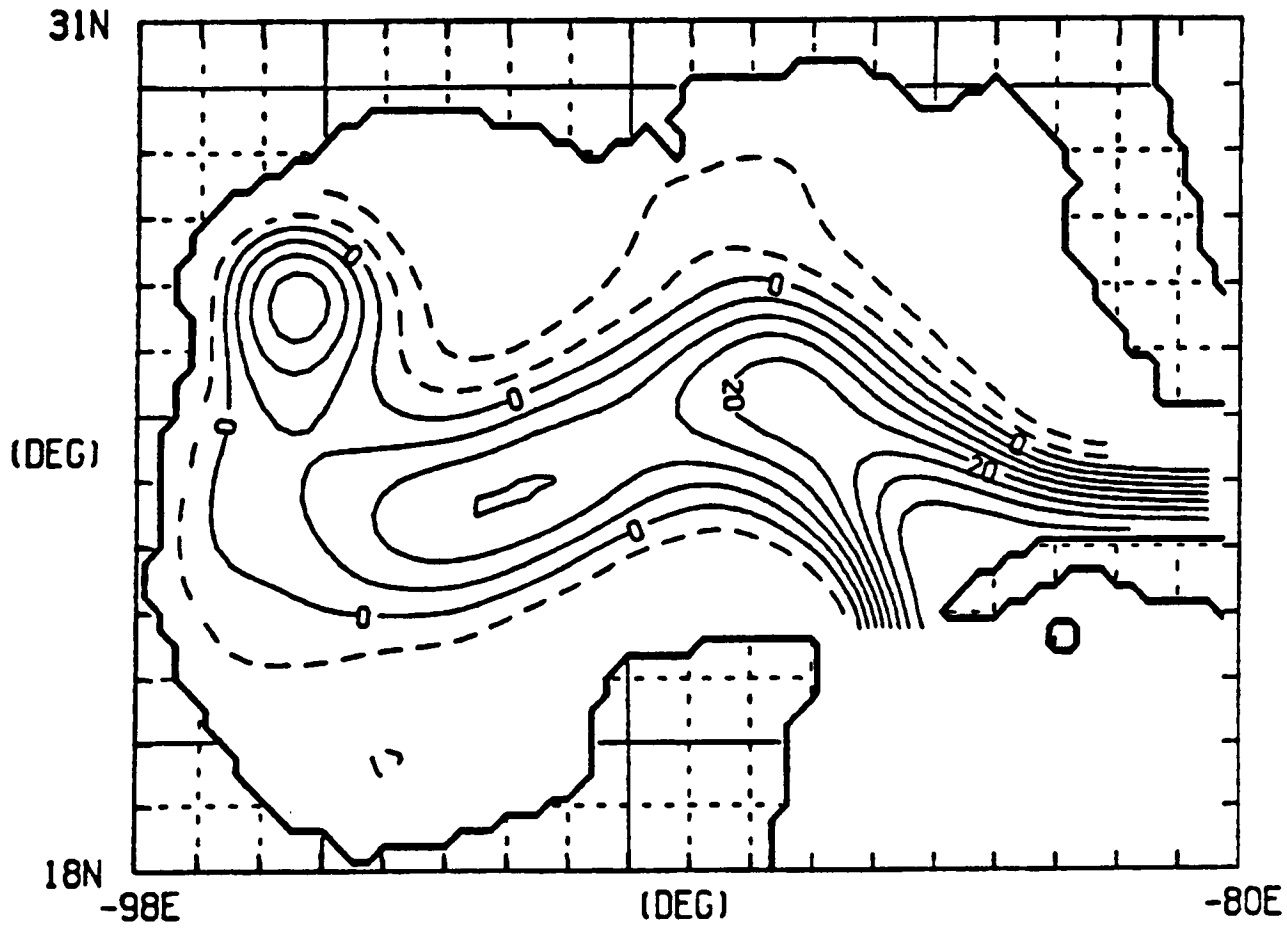
MEAN FREE SUR. DEV. G. ØF MEXICØ 0. 40
DX.DY = 0.2 0.2 (DEG) DBT = 5.0(CM)
31N
(DEG)
18N
-98E
(DEG)
-80E
0
20

FIGURE 11: Instantaneous view of the free surface deviation (a) from Experiment 28 (with 26 upper and 4 Sv lower layer inflow transport), and (b) Experiment 40 (with 20 upper and 10 Sv lower layer inflow transport). In similar phase of eddy cycle, Experiment 40 shows less intrusion of the Loop Current onto the Florida Shelf. The contour interval is 10 cm.

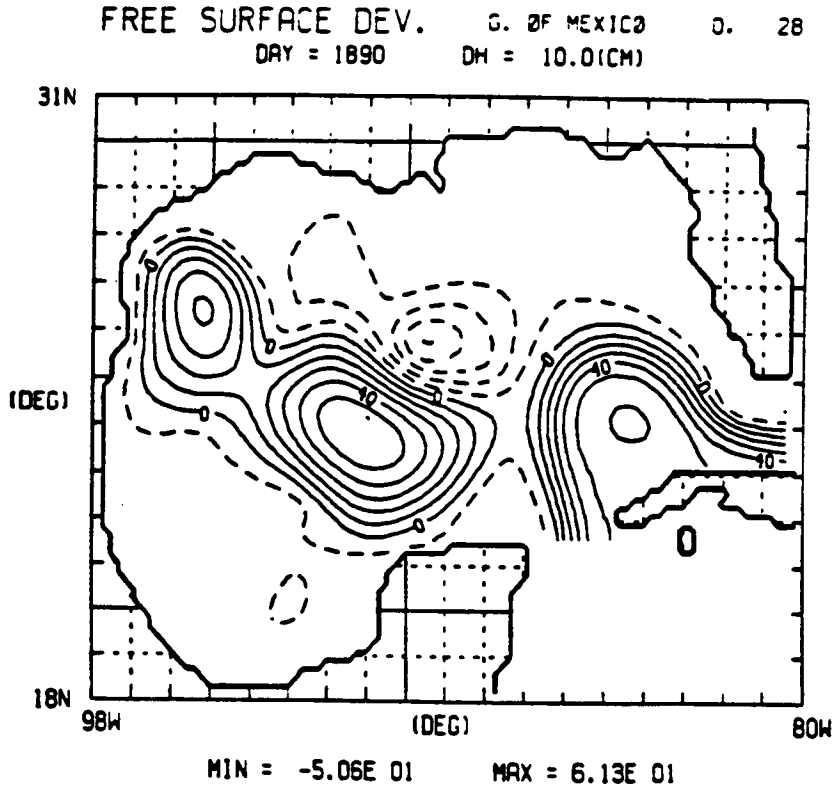
FREE SURFACE DEV. G. ØF MEXICØ D. 28
DAY = 1890 DH = 10.0(CM)
31N
(DEG)
18N
98W
(DEG)
80W
MIN = -5.06E 01 MAX = 6.13E 01

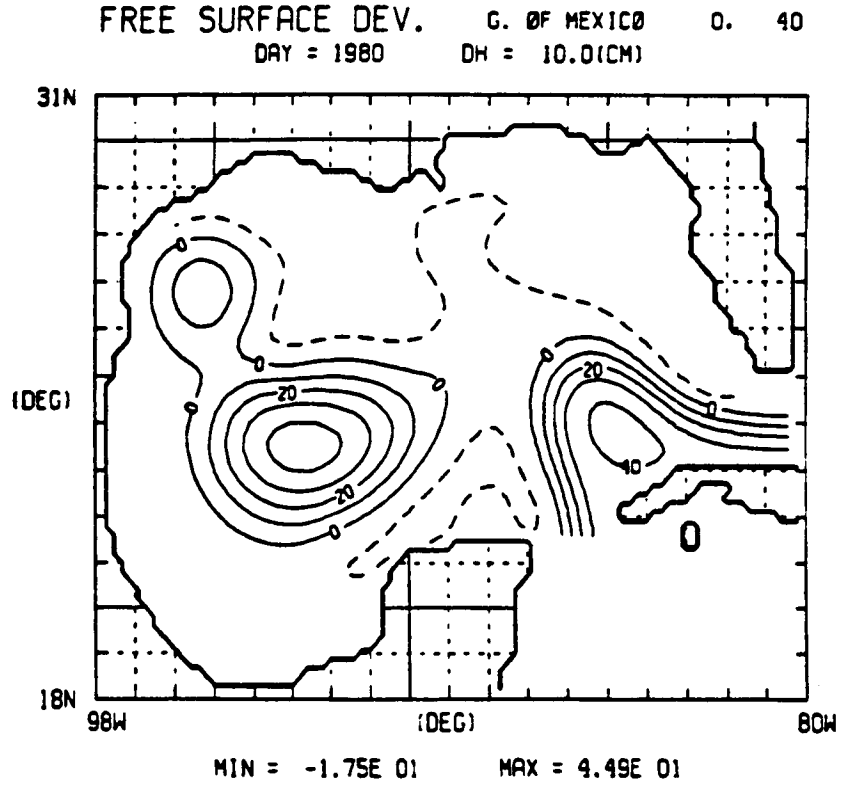
FREE SURFACE DEV. G. ØF MEXICØ D. 40
DAY = 1980 DH = 10.0(CM)
31N
(DEG)
18N
98W
(DEG)
80W
MIN = -1.75E 01 MAX = 4.49E 01

FIGURE 12: Instantaneous view of upper layer averaged velocities from Experiment 60 on model day 2130, velocities above 50 cm/sec are not shown.

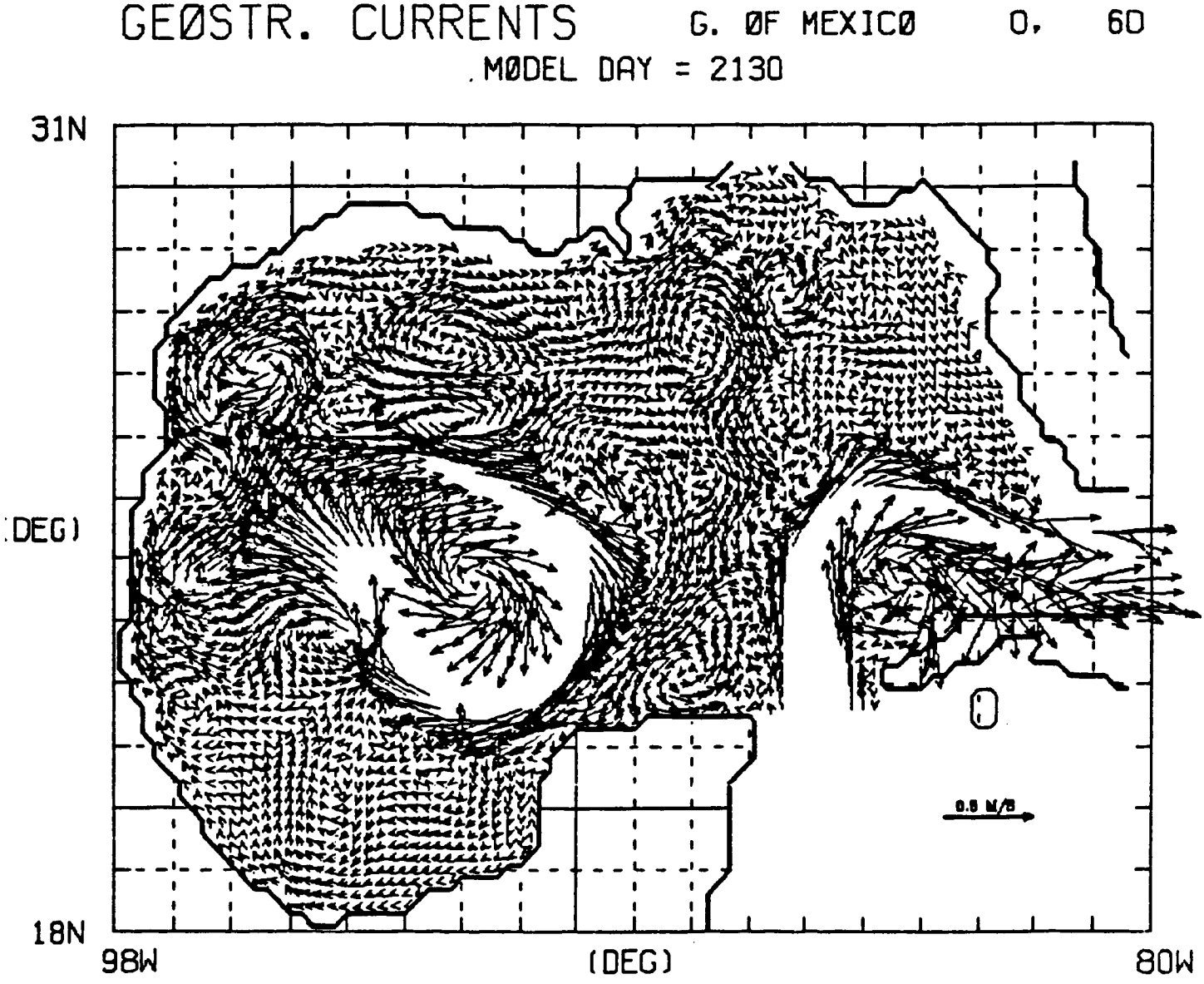
GEØSTR. CURRENTS G. ØF MEXICØ O. 6D
MØDEL DAY = 2130
31N
(DEG)
18N
98W
(DEG)
80W
0.5 M/S
VECTØRS UP TØ 0.50 M/S PLØTTED (MAX = 0.90 M/S)

FIGURE 13: Instantaneous view of upper layer averaged velocities from Experiment 60 on model day 2170, velocities above 50 cm/sec are not shown.

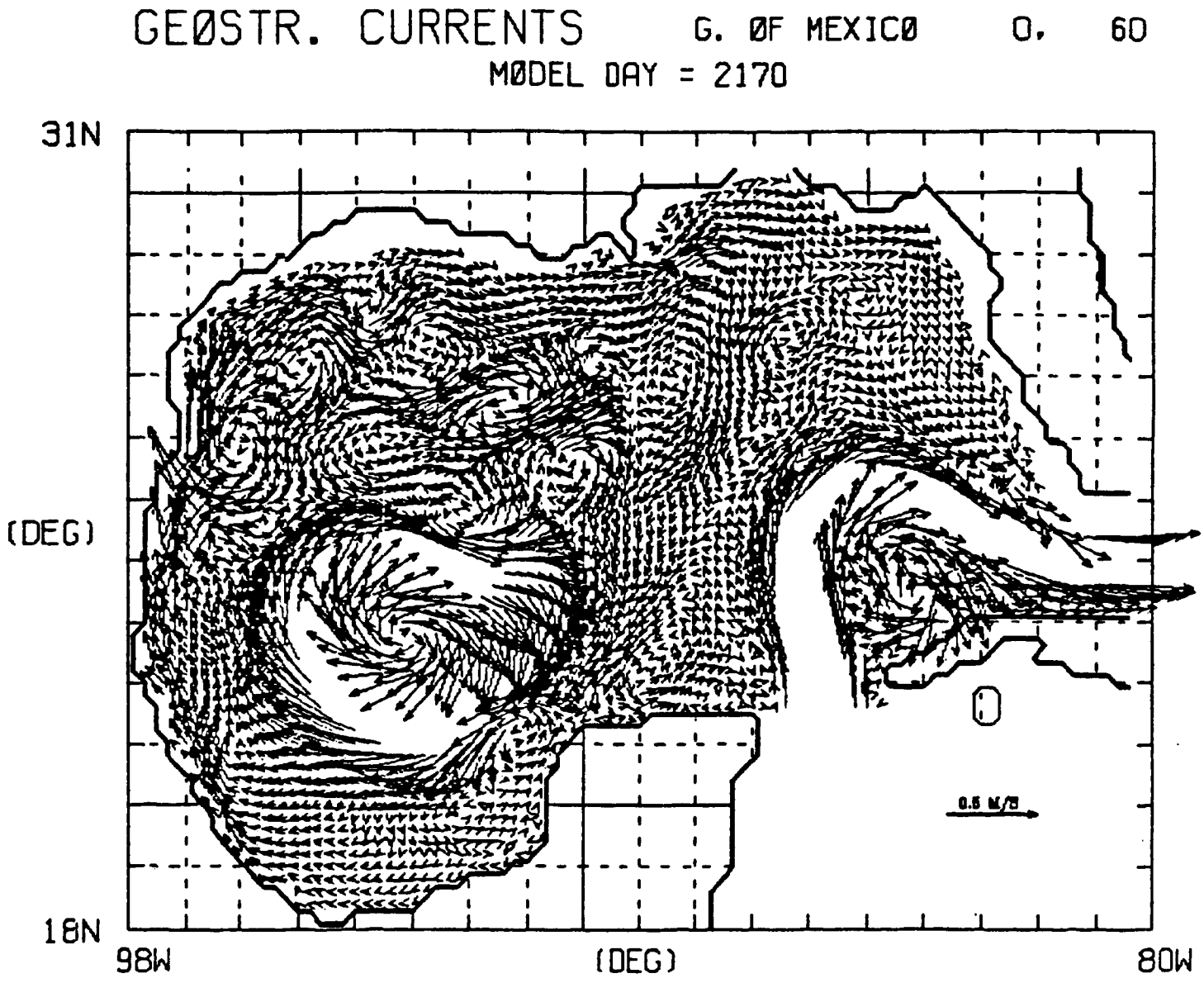
GEØSTR. CURRENTS G. ØF MEXICØ O. 60
MØDEL DAY = 2170
31N
(DEG)
18N
98W
(DEG)
80W
0.5 M/S
VECTØRS UP TØ 0.50 M/S PLØTTED (MAX = 0.91 M/S)

FIGURE 14: Instantaneous view of upper layer averaged velocities from Experiment 60 on model day 2210, velocities above 50 cm/sec are not shown.

GEØSTR. CURRENTS G. ØF MEXICØ O. 60

MØDEL DAY = 2210

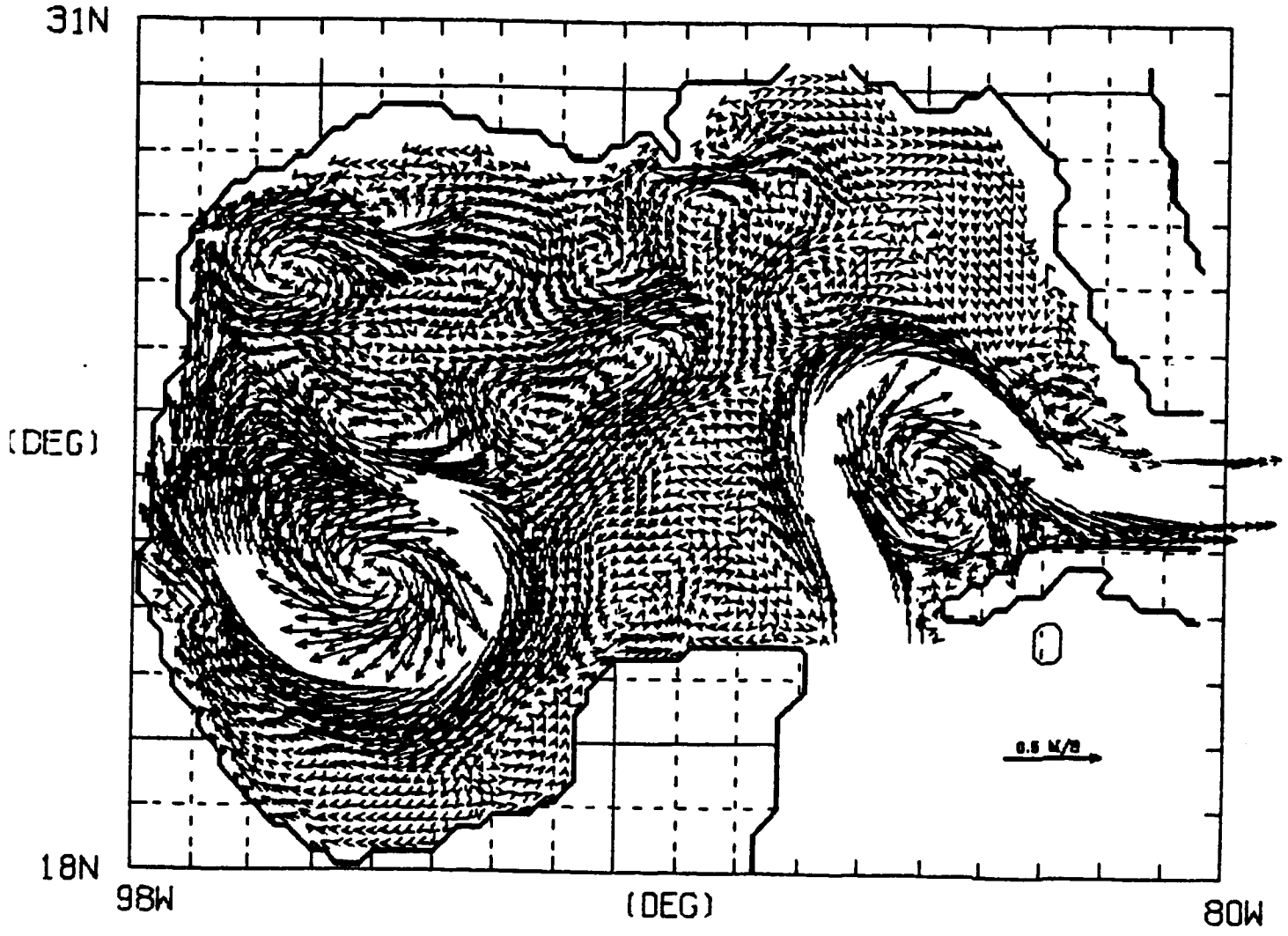

VECTØRS UP TØ 0.50 M/S PLØTTED (MAX = 0.88 M/S)

FIGURE 15: Instantaneous view of upper layer averaged velocities from Experiment 60 on model day 2320, velocities above 50 cm/sec are not shown.

GEØSTR. CURRENTS G. ØF MEXICØ 0. 60

MØDEL DAY = 2320

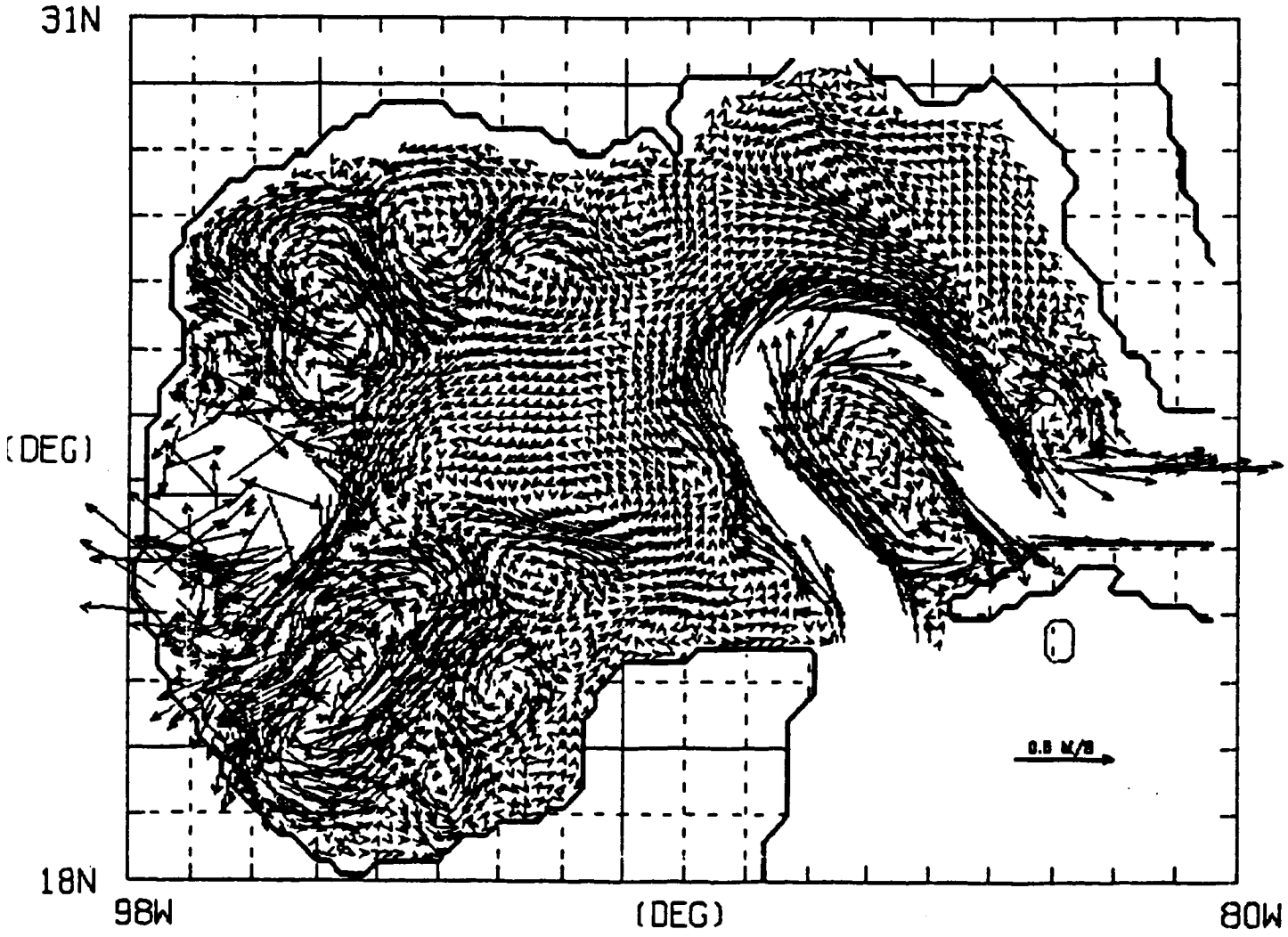

VECTØRS UP TØ 0.50 M/S PLØTTED (MAX = 1.23 M/S)

FIGURE 16: Instantaneous view of upper layer averaged velocities from Experiment 60 on model day 2410, velocities above 50 cm/sec are not shown.

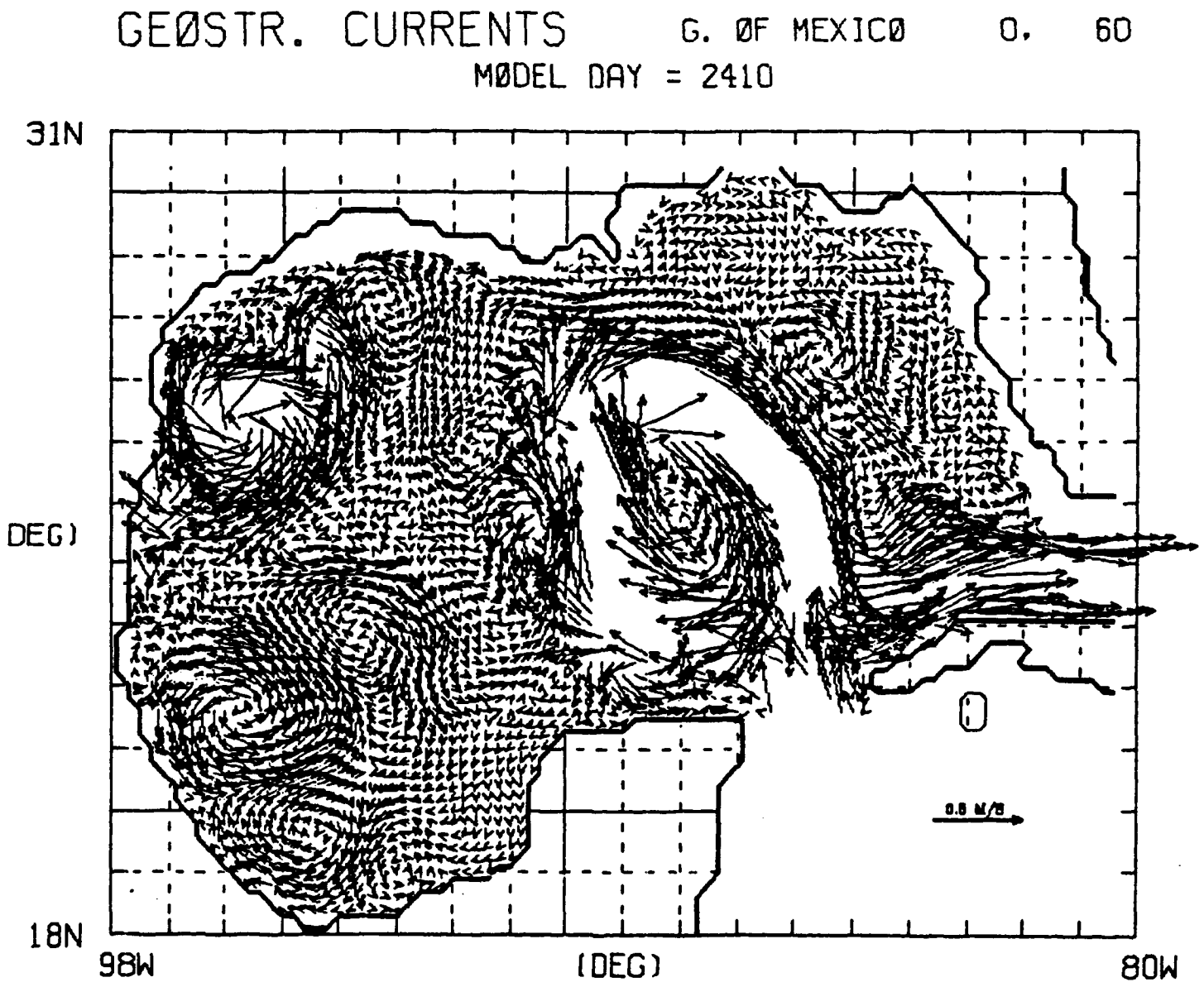
GEØSTR. CURRENTS G. ØF MEXICØ 0. 60
MØDEL DAY = 2410
31N
DEG)
18N
98W
(DEG)
80W
0.5 M/S
VECTØRS UP TØ 0.50 M/S PLØTTED (MAX = 1.06 M/S)

FIGURE 17: Instantaneous view of upper layer averaged velocities from Experiment 60 on model day 2420, velocities above 50 cm/sec are not shown.

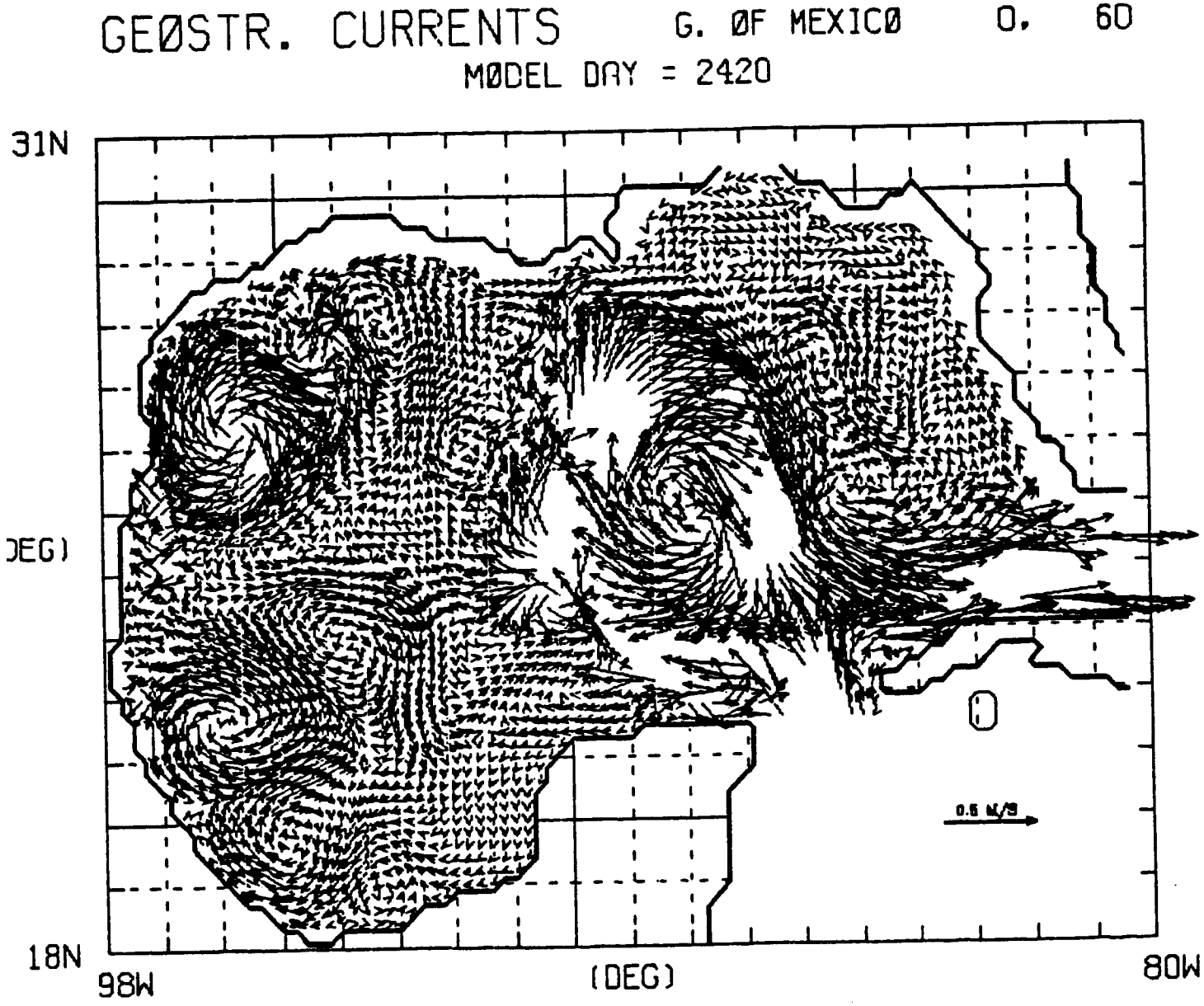
GEØSTR. CURRENTS G. ØF MEXICØ O. 60
MØDEL DAY = 2420
31N
DEG)
18N
98W
(DEG)
80W
0.5 M/S
VECTØRS UP TØ 0.50 M/S PLØTTED (MAX = 1.09 M/S)

FIGURE 18: Instantaneous view of upper layer averaged velocities from Experiment 60 on model day 2430, velocities above 50 cm/sec are not shown.

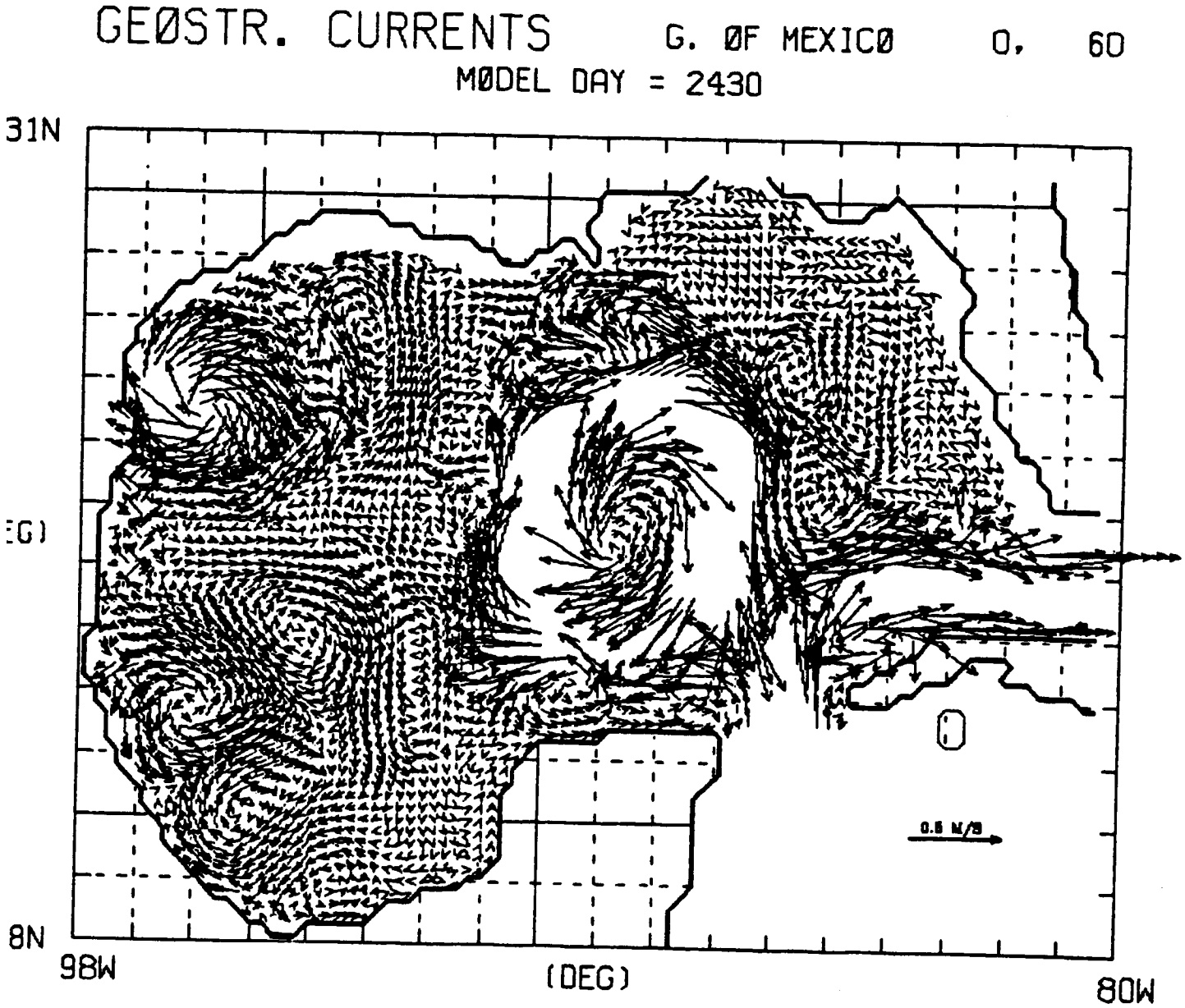
GEØSTR. CURRENTS
G. ØF MEXICØ
0. 60
MØDEL DAY = 2430
31N
8N
98W
(DEG)
80W
0.5 M/S
VECTØRS UP TØ 0.50 M/S PLØTTED (MAX = 0.99 M/S)

FIGURE 19: Instantaneous view of upper layer averaged velocities from Experiment 60 on model day 2440, velocities above 50 cm/sec are not shown.

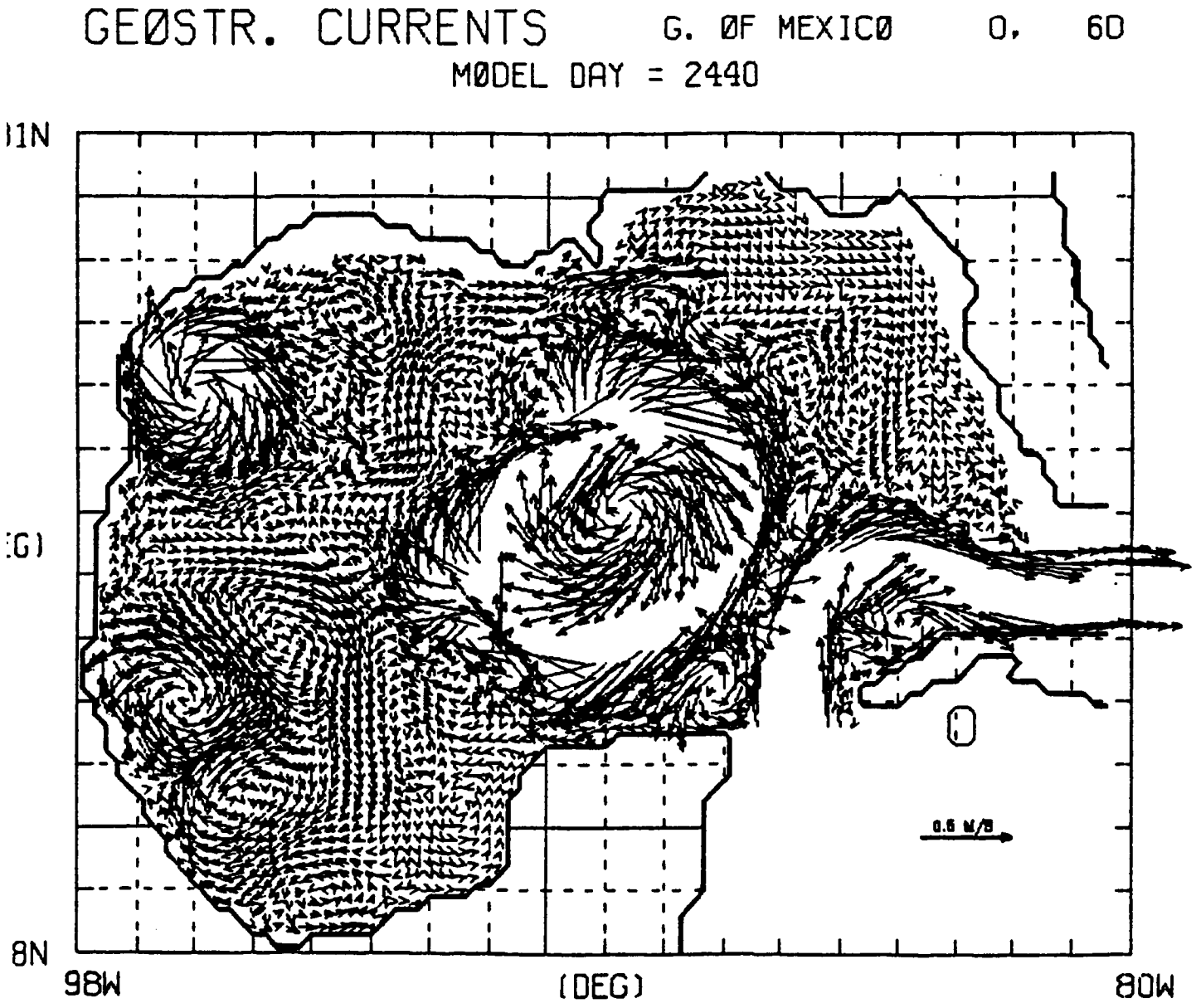
GEØSTR. CURRENTS
G. ØF MEXICØ
O. 6D
MØDEL DAY = 2440
)1N
:G)
8N
98W
(DEG)
8ØW
0.5 M/S
VECTØRS UP TØ 0.50 M/S PLØTTED (MAX = 1.01 M/S)

FIGURE 20: Paths of NDBO drifters (a) 1598, (b) 1599, and (c) 1600 from November 20, 1980, through May 11, 1981. The numbers 0 through 6 give the positions on November 20, December 20, January 20, February 20, March 20, April 20, May 11, respectively (from Kirwan et al., 1984).

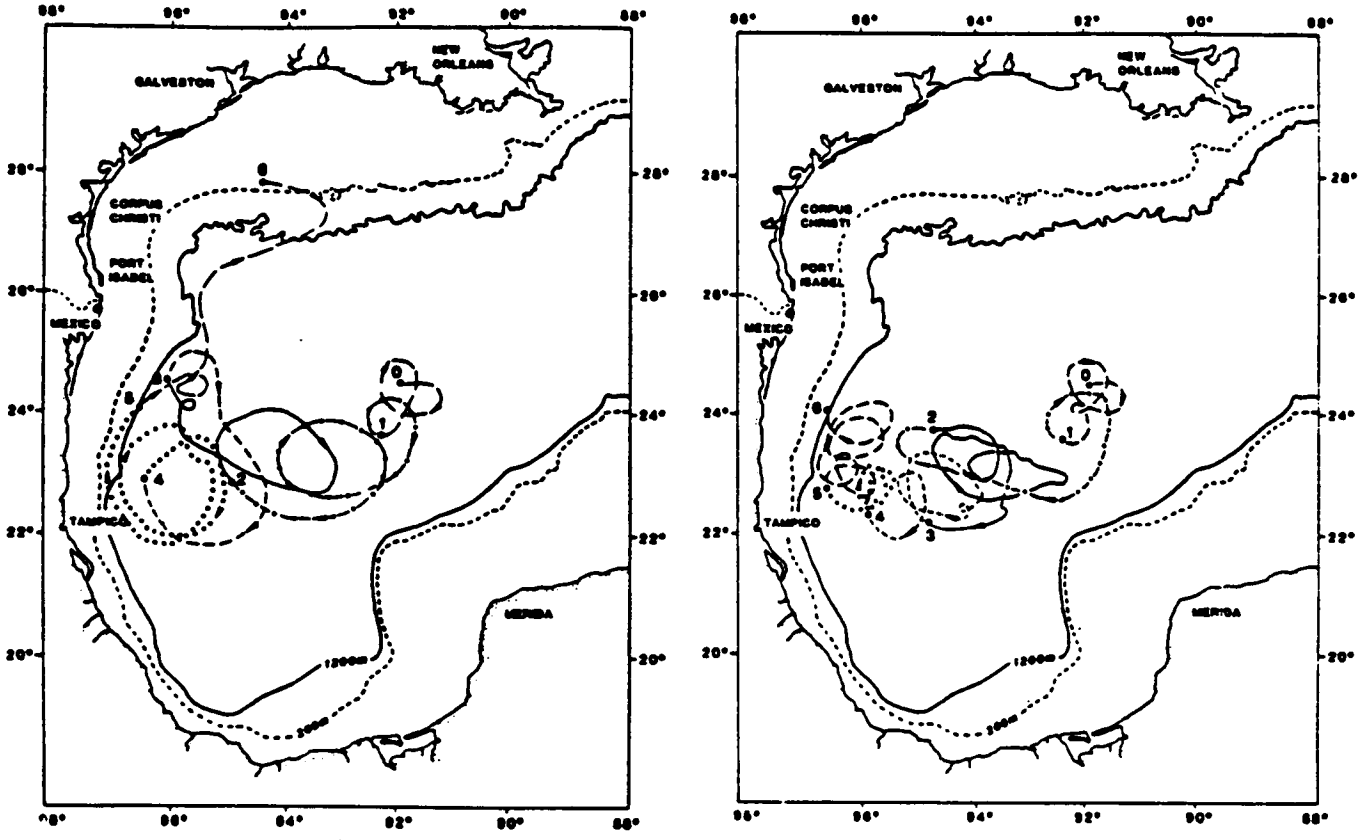
GALVESTON
NEW ORLEANS
CORPUS CHRISTI
PORT ISABEL
MEXICO
TAMPICO
MERIDA
a
b

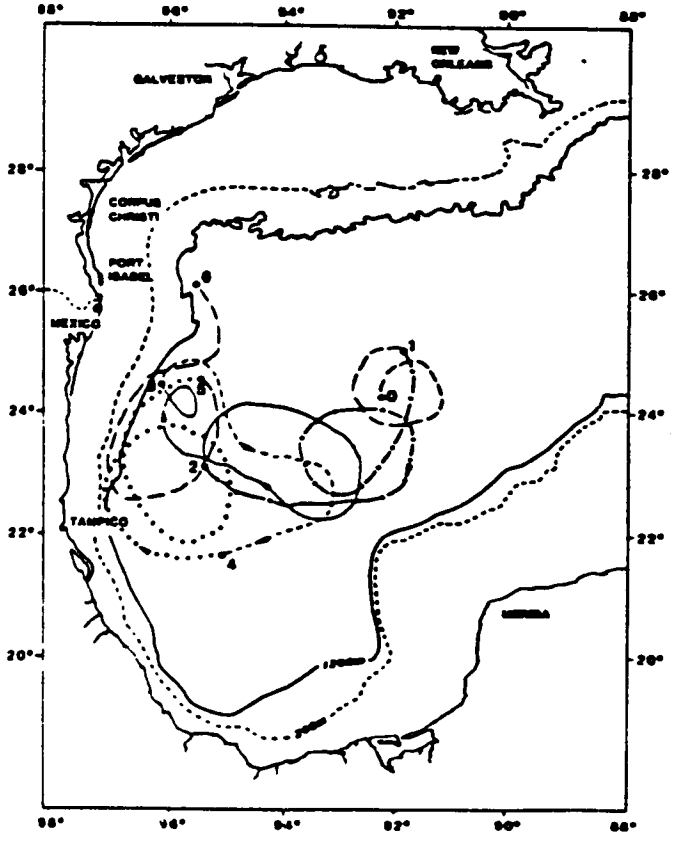
GALVESTON
NEW ORLEANS
CORPUS CHRISTI
PORT ISABEL
MEXICO
TAMPICO
c

FIGURE 21: Paths of simulated drifters (a) 3, and (b) 4 from model day 1680 to model day 1840 of Gulf model Experiment 60 (which is forced solely by inflow through the Yucatan Straits). The tracks start earlier in the eddy cycle than those in Figure 20. The simulated drifter moves in response to the upper layer velocity from the ocean model, which represents the mean velocity above the thermocline. Along the drifter tracks the upper layer thickness is between 250 and 350 m. The track is drawn as a solid line for 20 days, then dashed for 20 days, and so on. There is a dot every 5 days.

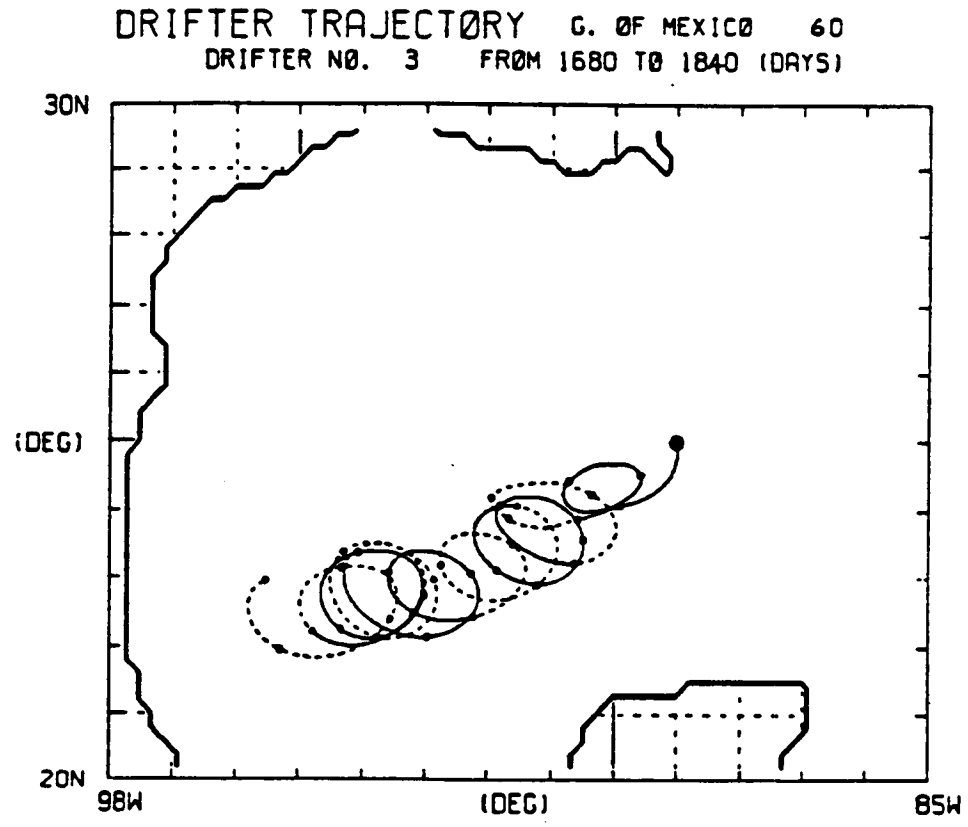
DRIFTER TRAJECTØRY G. ØF MEXICØ 60
DRIFTER NØ. 3 FRØM 1680 TØ 1840 (DAYS)
30N
(DEG)
20N
98W
(DEG)
85W

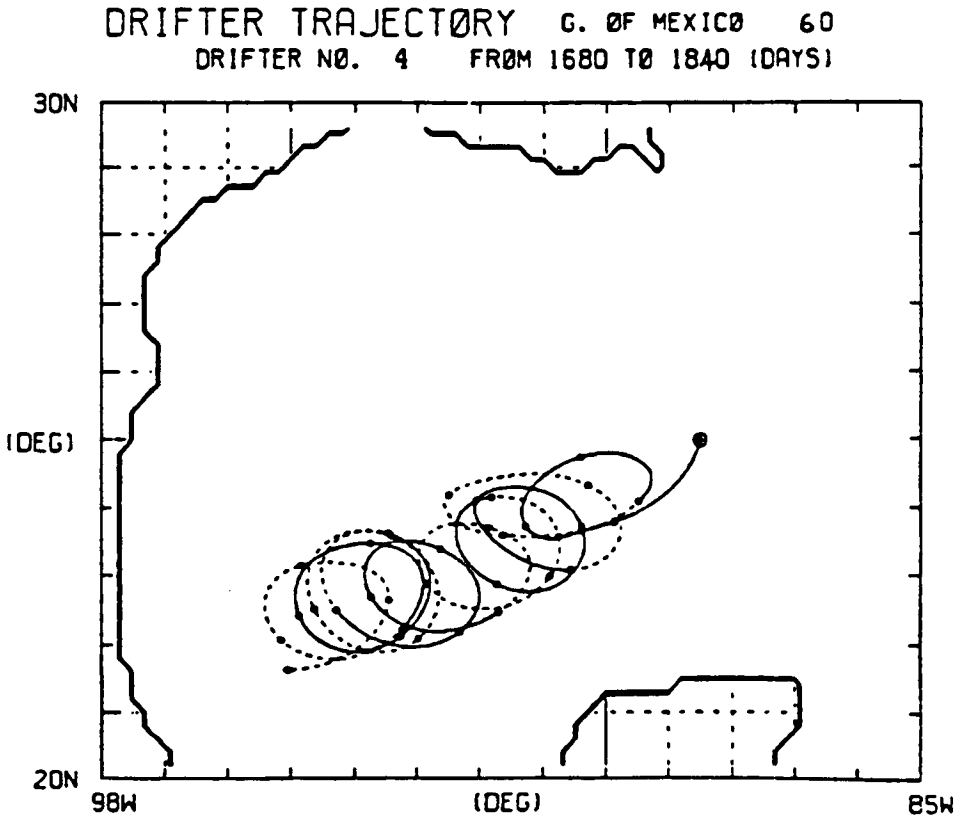
DRIFTER TRAJECTØRY G. ØF MEXICØ 60
DRIFTER NØ. 4 FRØM 1680 TØ 1840 (DAYS)
30N
(DEG)
20N
98W
(DEG)
85W

FIGURE 22: Instantaneous view of the free surface deviation every 30 days, from model day 1680 to model day 1830, for model Experiment number 60. The contour interval is 10 cm, and solid contours represent upward deviations with respect to the sea surface height at rest.

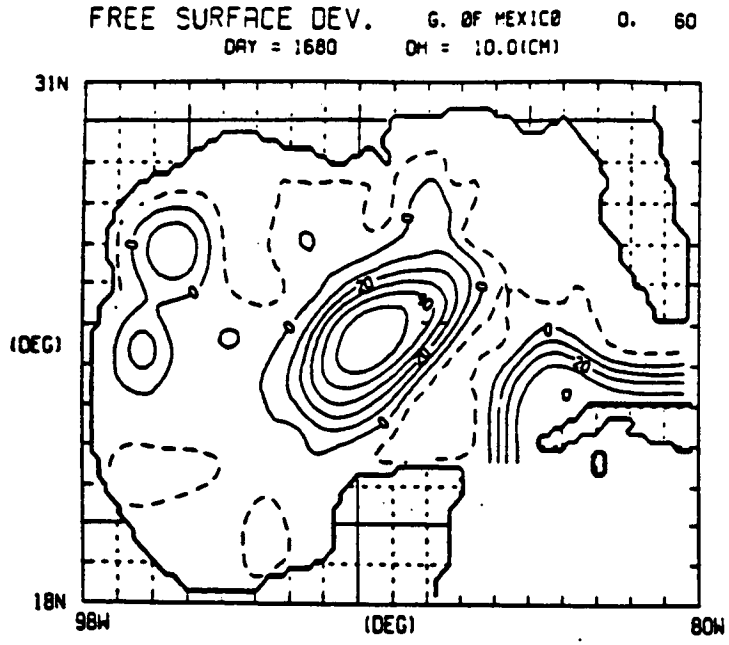
FREE SURFACE DEV. G. OF MEXICO 0. 60
DAY = 1680 DH = 10.0(CM)
31N
(DEG)
18N
98W
(DEG)
80W
0

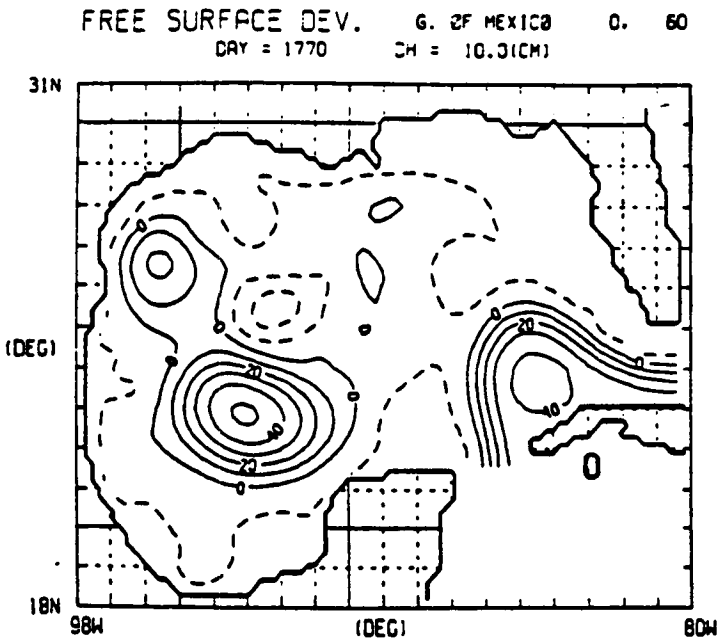
FREE SURFACE DEV. G. OF MEXICO 0. 60
DAY = 1770 DH = 10.0(CM)
31N
(DEG)
18N
98W
(DEG)
80W
0

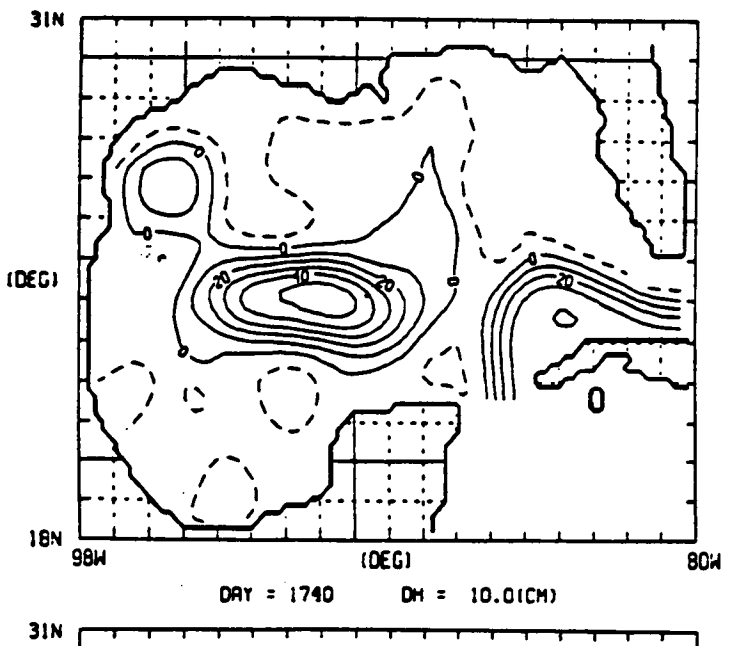
DAY = 1710 DH = 10.0(CM)
31N
(DEG)
18N
98W
(DEG)
80W
0

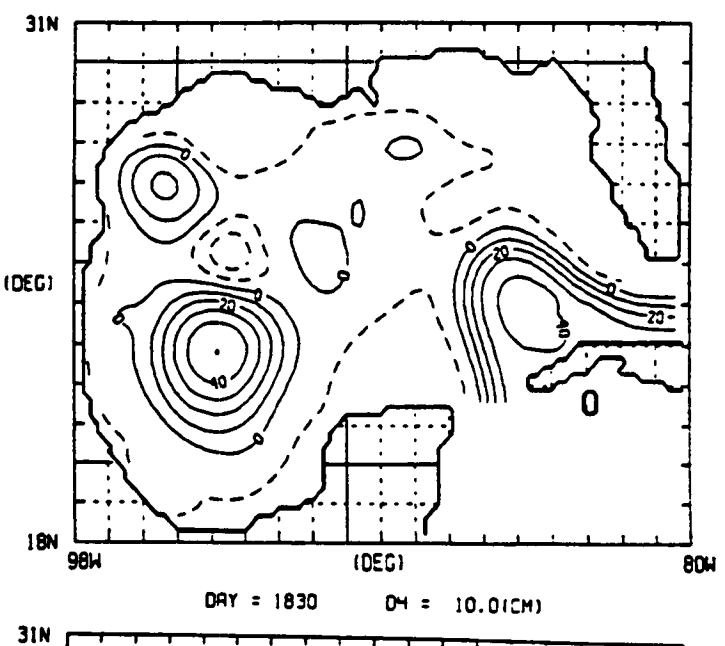
DAY = 1800 DH = 10.0(CM)
31N
(DEG)
18N
98W
(DEG)
80W
0

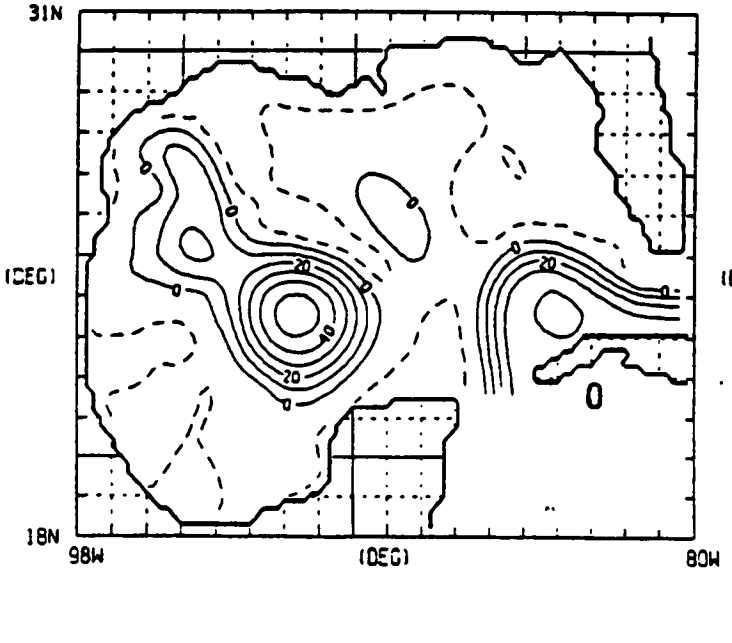
DAY = 1740 DH = 10.0(CM)
31N
(DEG)
18N
98W
(DEG)
80W
0

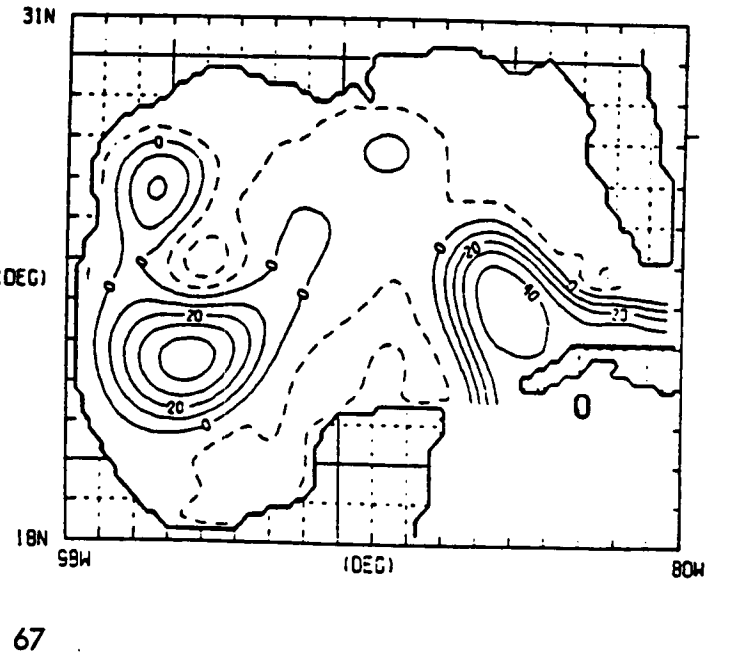
DAY = 1830 DH = 10.0(CM)
31N
(DEG)
18N
98W
(DEG)
80W
0

FIGURE 23: Instantaneous view of the free surface deviation every 30 days, from model day 1860 to model day 2010 (Experiment 60).

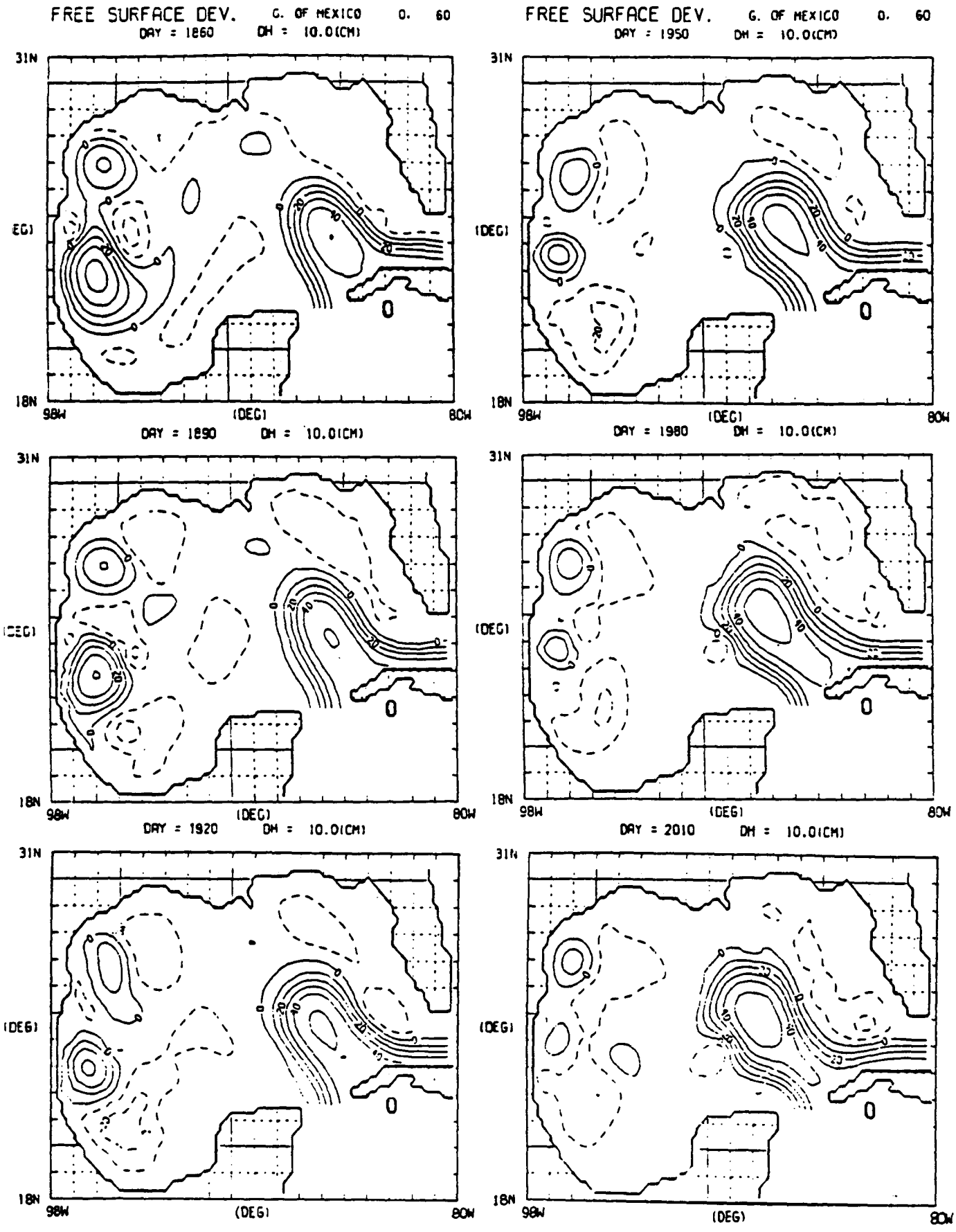
FREE SURFACE DEV. G. OF MEXICO 0. 60
DAY = 1860 DH = 10.0(CM)
FREE SURFACE DEV. G. OF MEXICO 0. 60
DAY = 1950 DH = 10.0(CM)
DAY = 1890 DH = 10.0(CM)
DAY = 1980 DH = 10.0(CM)
DAY = 1920 DH = 10.0(CM)
DAY = 2010 DH = 10.0(CM)
31N
18N
98W
80W
(DEG)
0

FIGURE 24: Path of simulated drifter number 3 from model day 1680 to model day 1980 (Experiment 60).

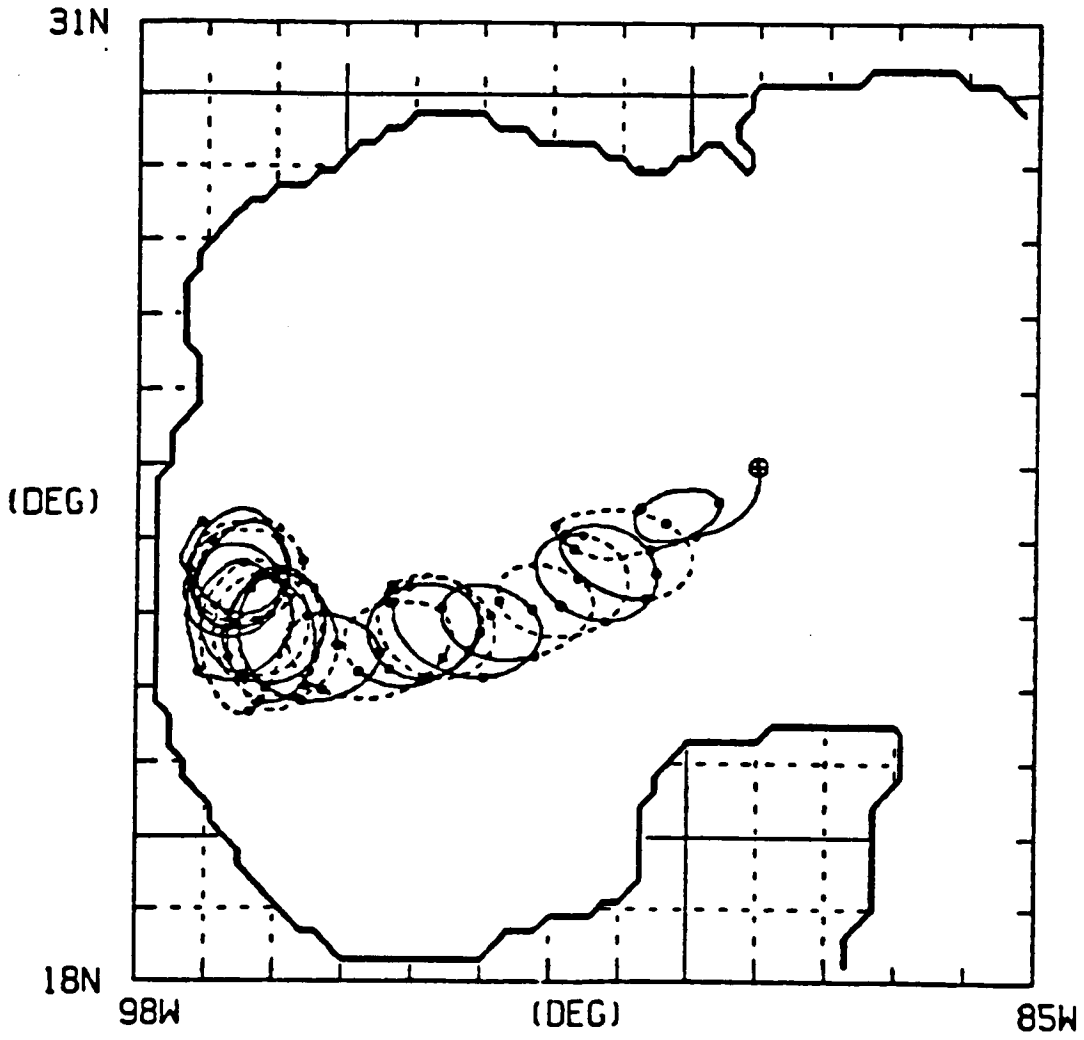
DRIFTER TRAJECTØRY G. ØF MEXICØ 60
DRIFTER NØ. 3 FRØM 1680 TØ 1980 (DAYS)
31N
(DEG)
18N
98W
(DEG)
85W

FIGURE 25: Time series of velocity for drifters (a) 1598, (b) 1599, and (c) 1600. From Kirwan et al., (1984).

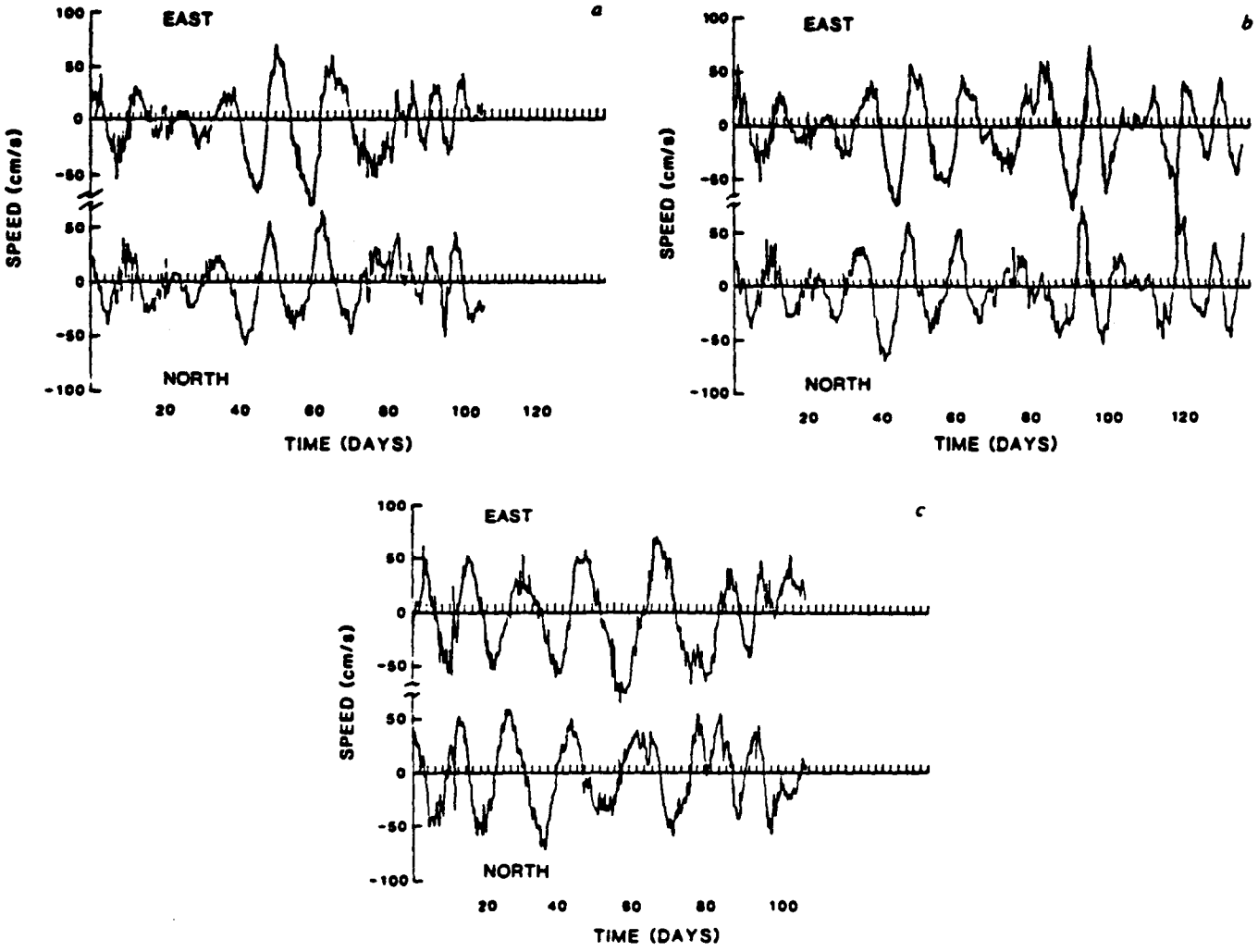
a
EAST
NORTH
SPEED (cm/s)
100
50
0
-50
-100
20
40
60
80
100
120
TIME (DAYS)
b
EAST
NORTH
SPEED (cm/s)
TIME (DAYS)
c
EAST
NORTH
SPEED (cm/s)
TIME (DAYS)

FIGURE 26: Time series of velocity for simulated drifters (a) 3 and (b) 4 from model day 1680 to model day 1880 (Experiment 60).

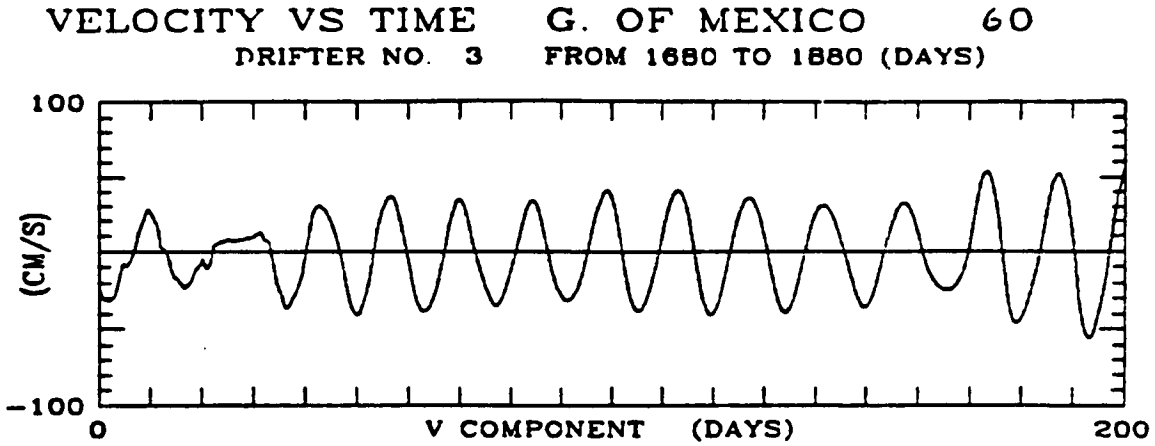
VELOCITY VS TIME G. OF MEXICO 60
DRIFTER NO. 3 FROM 1680 TO 1880 (DAYS)
100
(CM/S)
-100
0
V COMPONENT (DAYS)
200

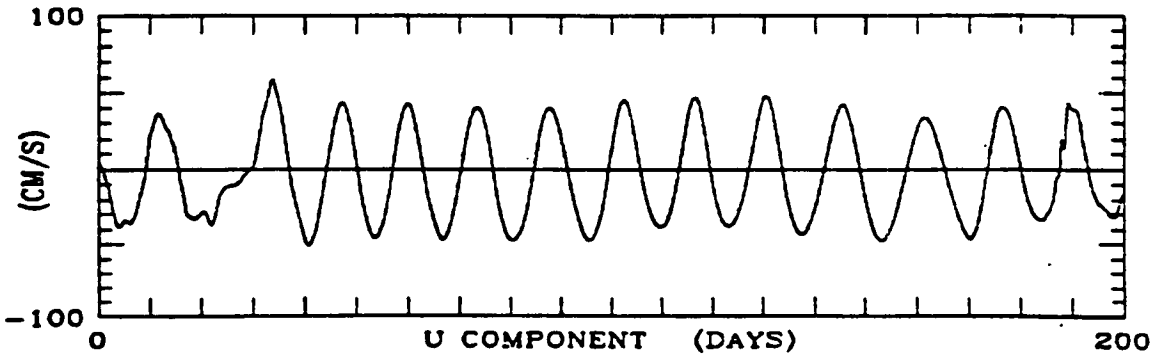
100
(CM/S)
-100
0
U COMPONENT (DAYS)
200

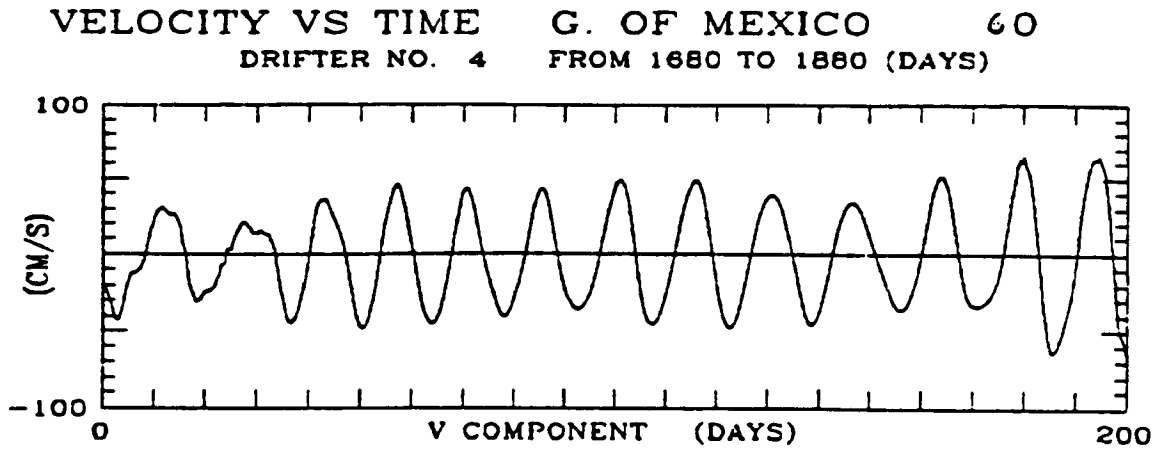
VELOCITY VS TIME G. OF MEXICO 60
DRIFTER NO. 4 FROM 1680 TO 1880 (DAYS)
100
(CM/S)
-100
0
V COMPONENT (DAYS)
200

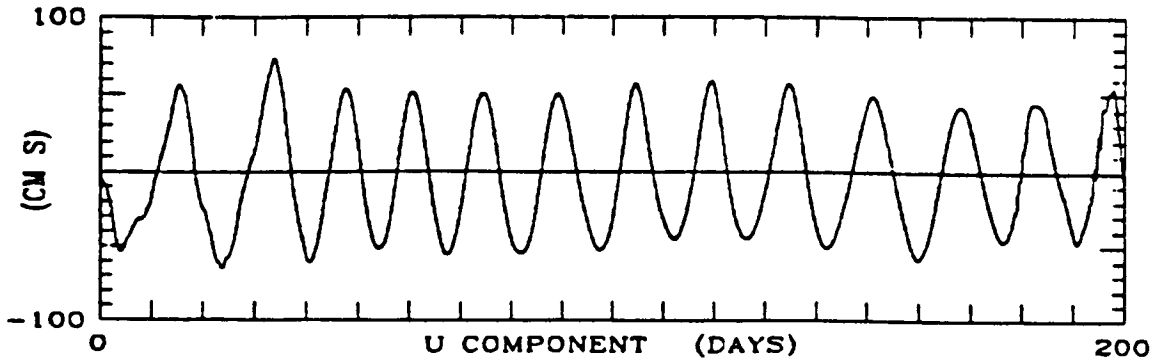
100
(CM S)
-100
0
U COMPONENT (DAYS)
200

FIGURE 27: Instantaneous wind stress and wind stress curl from the Navy Corrected Geostrophic Wind data set, for 0000 and 1200 GMT on 14 January and 0000 GMT on 15 January 1976.

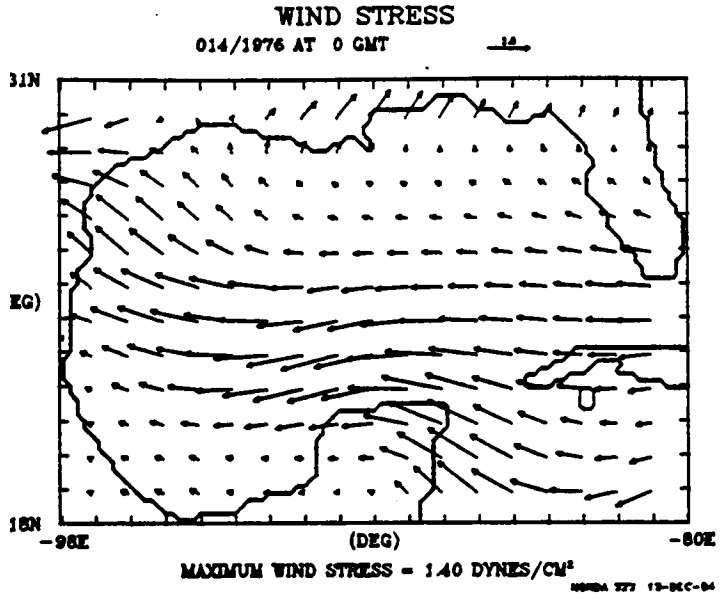
WIND STRESS
014/1976 AT 0 GMT
31N
EG)
18N
-98E
(DEG)
-80E
MAXIMUM WIND STRESS = 1.40 DYNES/CM²

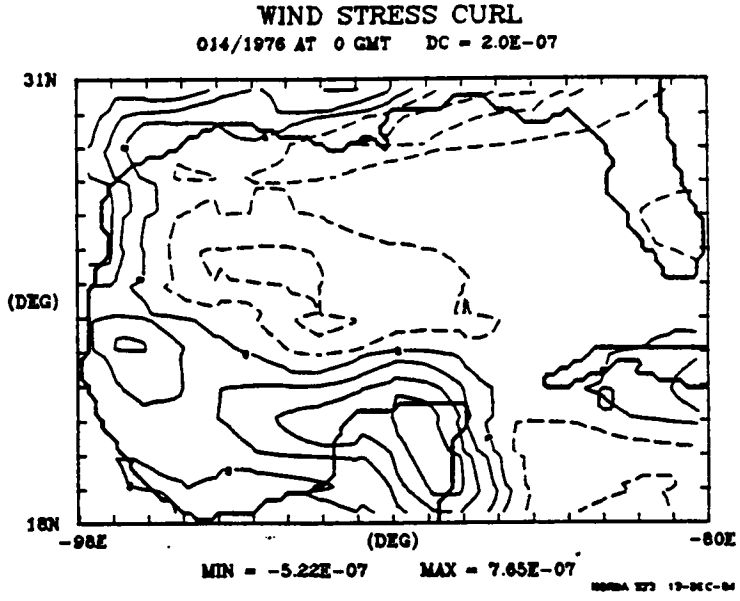
WIND STRESS CURL
014/1976 AT 0 GMT DC = 2.0E-07
31N
(DEG)
18N
-98E
(DEG)
-80E
MIN = -5.22E-07 MAX = 7.65E-07

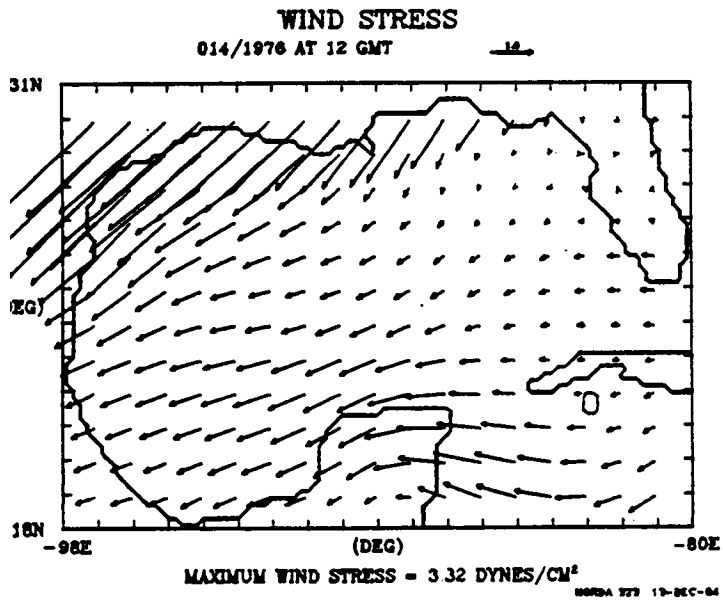
WIND STRESS
014/1976 AT 12 GMT
31N
EG)
18N
-98E
(DEG)
-80E
MAXIMUM WIND STRESS = 3.32 DYNES/CM²

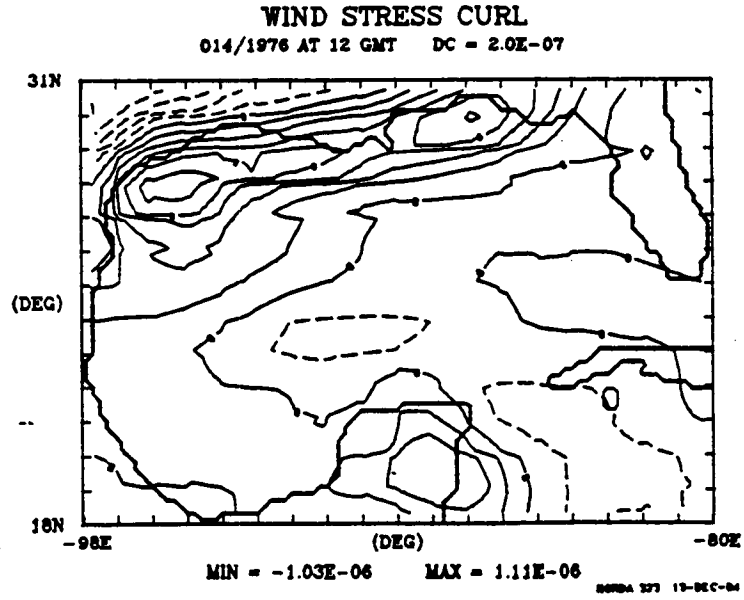
WIND STRESS CURL
014/1976 AT 12 GMT DC = 2.0E-07
31N
(DEG)
18N
-98E
(DEG)
-80E
MIN = -1.03E-06 MAX = 1.11E-06

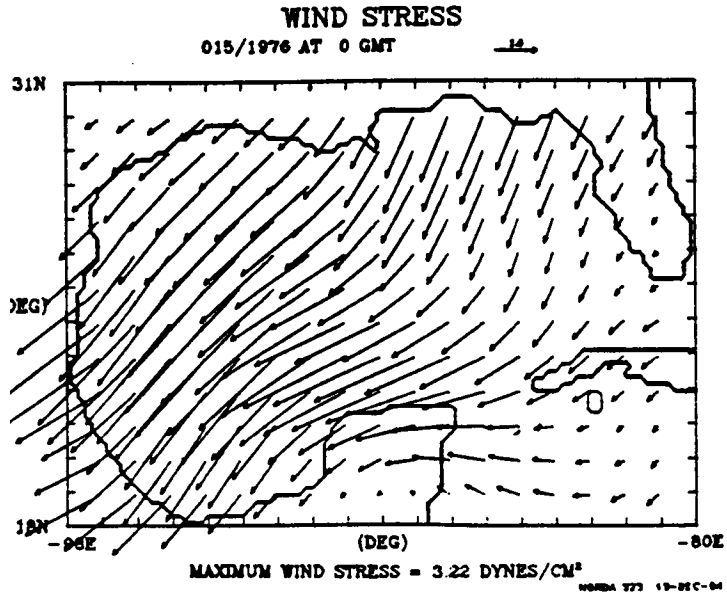
WIND STRESS
015/1976 AT 0 GMT
31N
)EG)
18N
-98E
(DEG)
-80E
MAXIMUM WIND STRESS = 3.22 DYNES/CM²

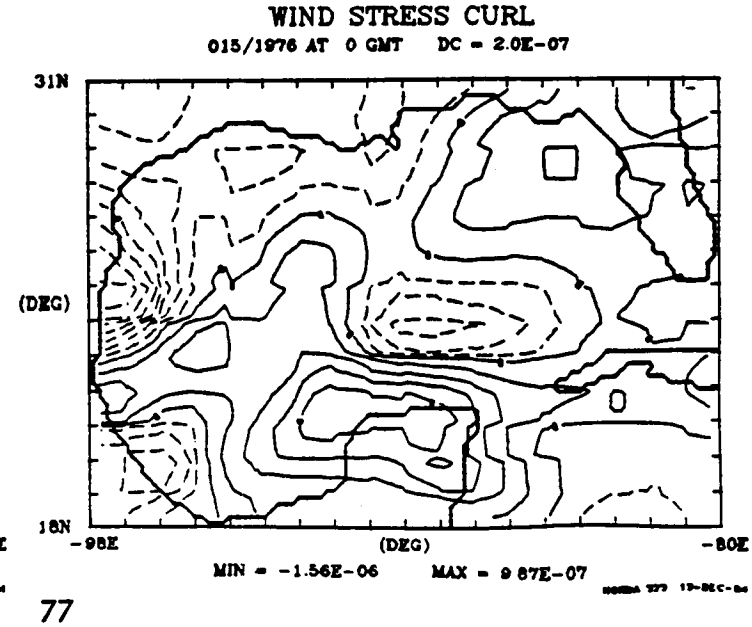
WIND STRESS CURL
015/1976 AT 0 GMT DC = 2.0E-07
31N
(DEG)
18N
-98E
(DEG)
-80E
MIN = -1.56E-06 MAX = 9.87E-07

FIGURE 28: Instantaneous wind stress and wind stress curl from the Navy Corrected Geostrophic Wind data set, for 0000 and 1200 GMT on 14 July and 0000 GMT on 15 July 1976.

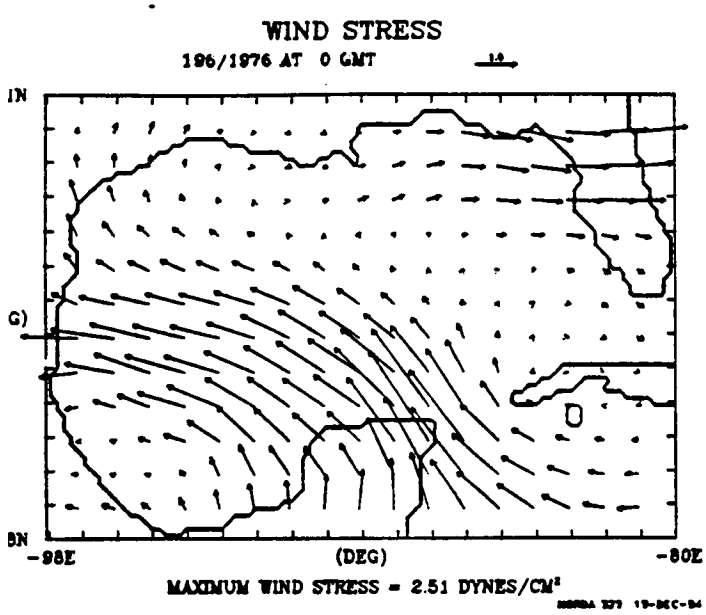
WIND STRESS
196/1976 AT 0 GMT
-98E
(DEG)
-80E
MAXIMUM WIND STRESS = 2.51 DYNES/CM²

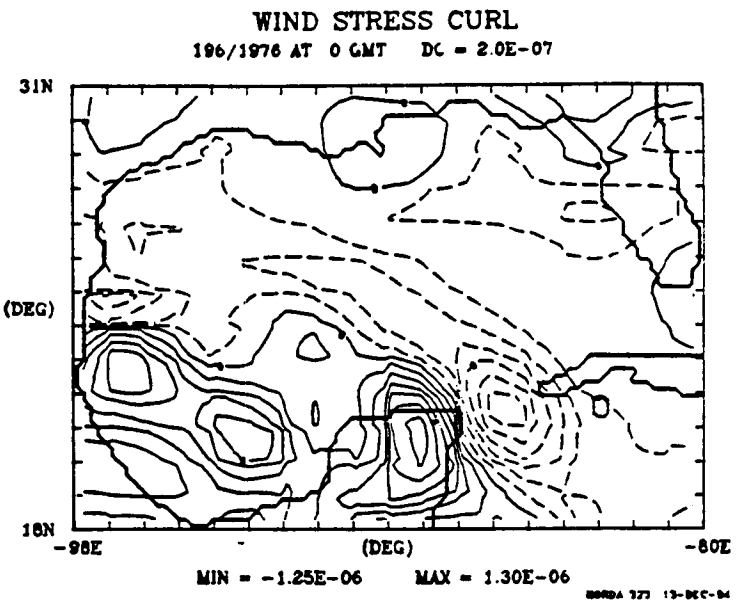
WIND STRESS CURL
196/1976 AT 0 GMT DC = 2.0E-07
31N
18N
(DEG)
-98E
-80E
MIN = -1.25E-06 MAX = 1.30E-06

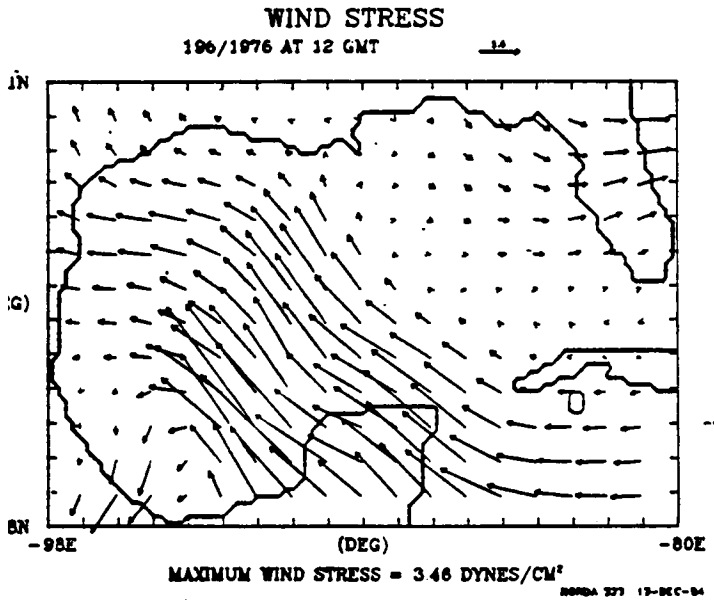
WIND STRESS
196/1976 AT 12 GMT
-98E
(DEG)
-80E
MAXIMUM WIND STRESS = 3.46 DYNES/CM²

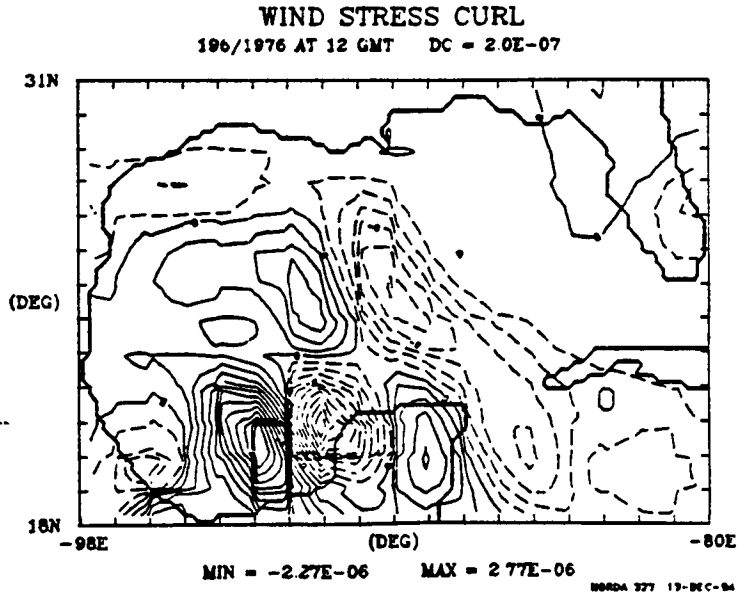
WIND STRESS CURL
196/1976 AT 12 GMT DC = 2.0E-07
31N
18N
(DEG)
-98E
-80E
MIN = -2.27E-06 MAX = 2.77E-06

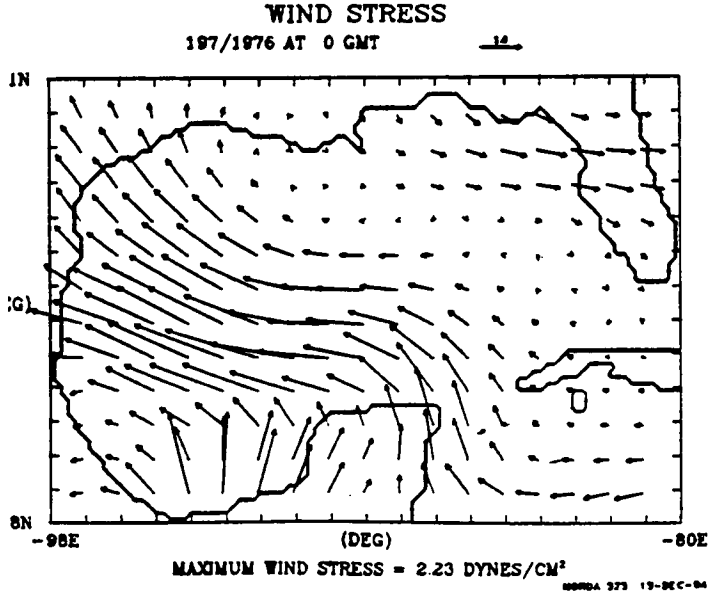
WIND STRESS
197/1976 AT 0 GMT
-98E
(DEG)
-80E
MAXIMUM WIND STRESS = 2.23 DYNES/CM²

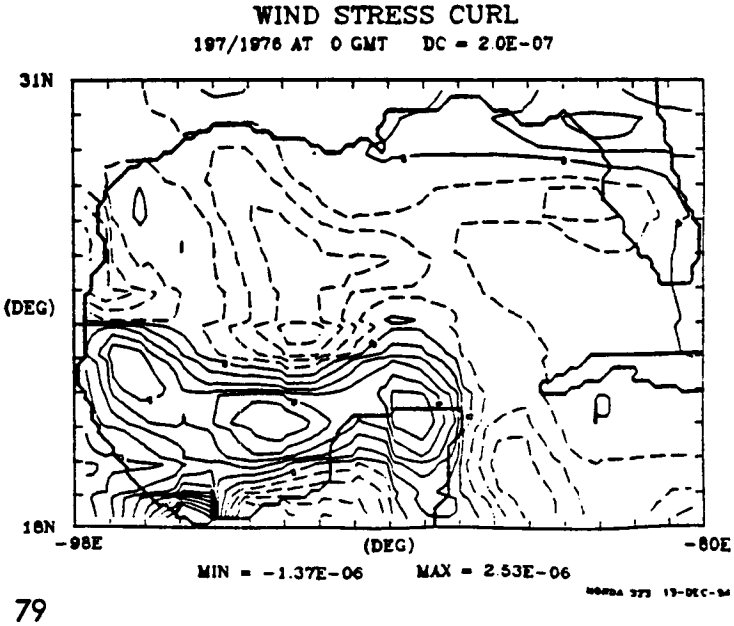
WIND STRESS CURL
197/1976 AT 0 GMT DC = 2.0E-07
31N
18N
(DEG)
-98E
-80E
MIN = -1.37E-06 MAX = 2.53E-06

FIGURE 29: Climatological (1967-1982) wind stress and wind stress curl from the Navy Corrected Geostrophic Wind data set, for winter (December, January, February).

WIND STRESS

WINTER 1967-1982

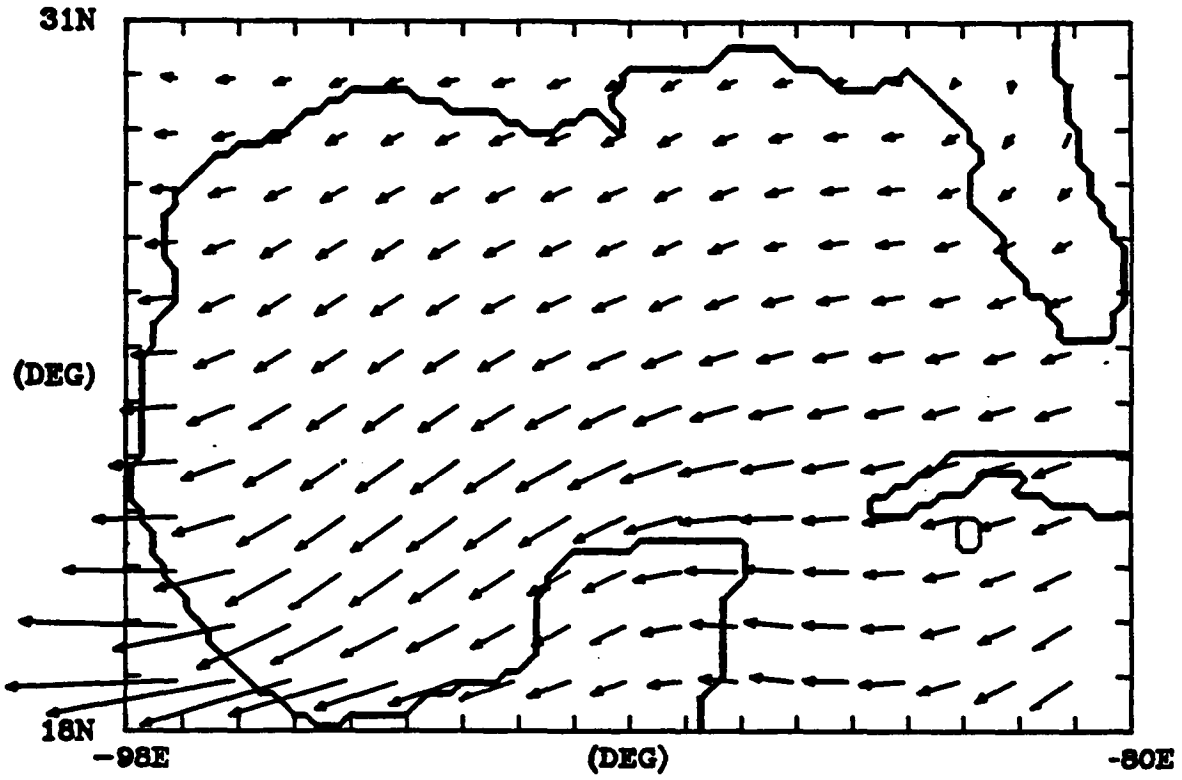

MAXIMUM WIND STRESS = 2.79 DYNES/CM^2

NORDA 223 12-DEC-84

WIND STRESS CURL

WINTER 1967-1982 DC = 1.0E-07 MKS

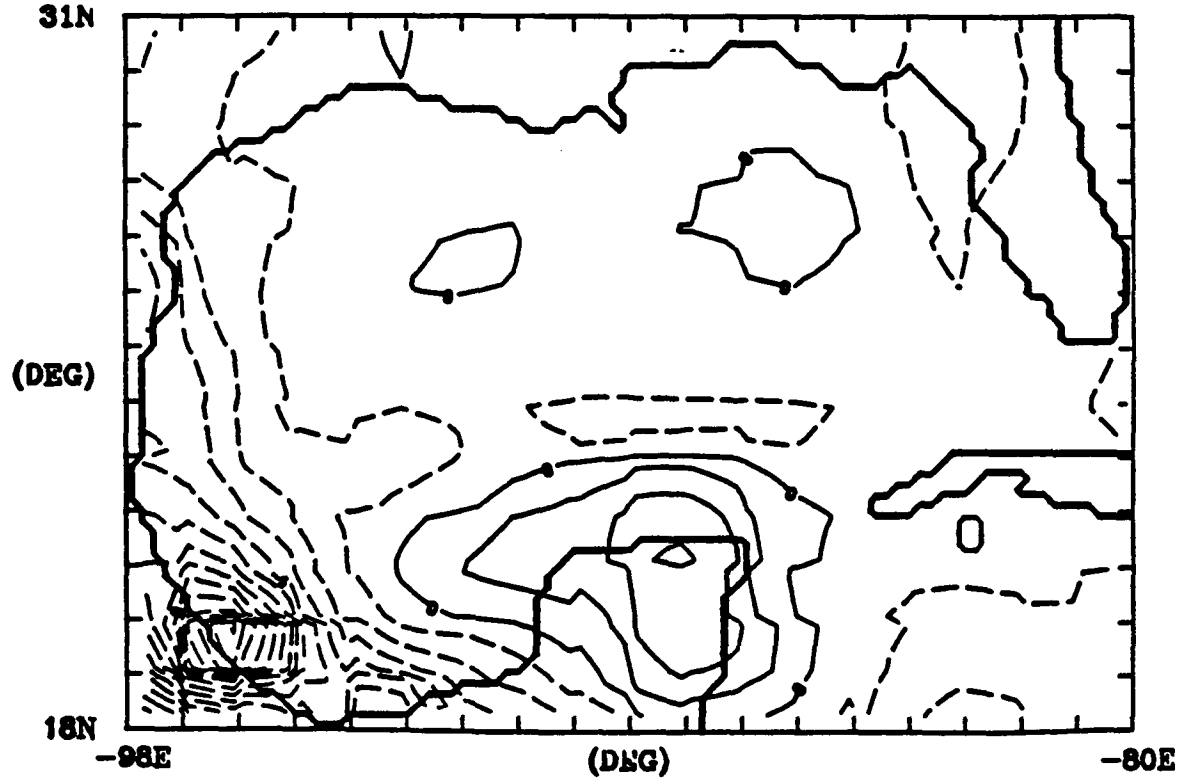

MIN = -1.42E-06 MAX = 3.15E-07

NORDA 223 12-DEC-84

FIGURE 30: Climatological (1967-1982) wind stress and wind stress curl from the Navy Corrected Geostrophic Wind data set, for spring (March, April, May).

WIND STRESS

SPRING 1967-1982

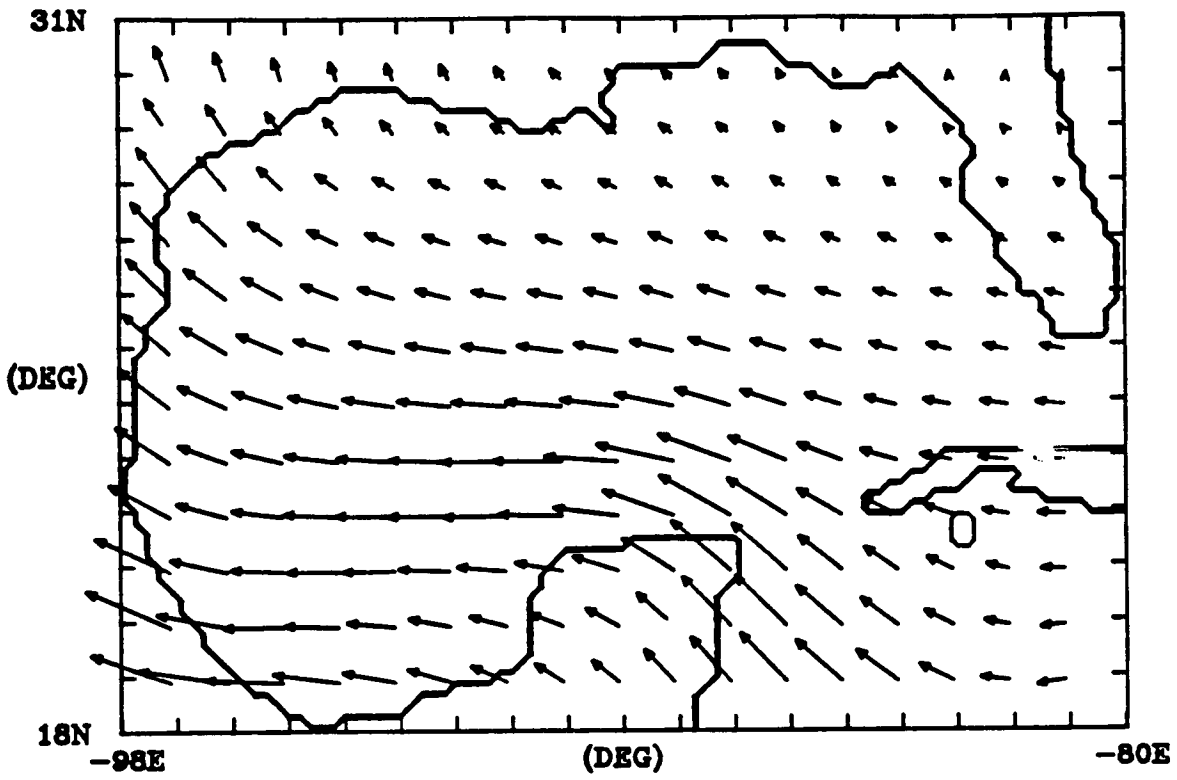

MAXIMUM WIND STRESS = 1.33 DYNES/CM^2

NORDA 323 12-DEC-84

WIND STRESS CURL

SPRING 1967-1982 DC = 1.0E-07 MKS

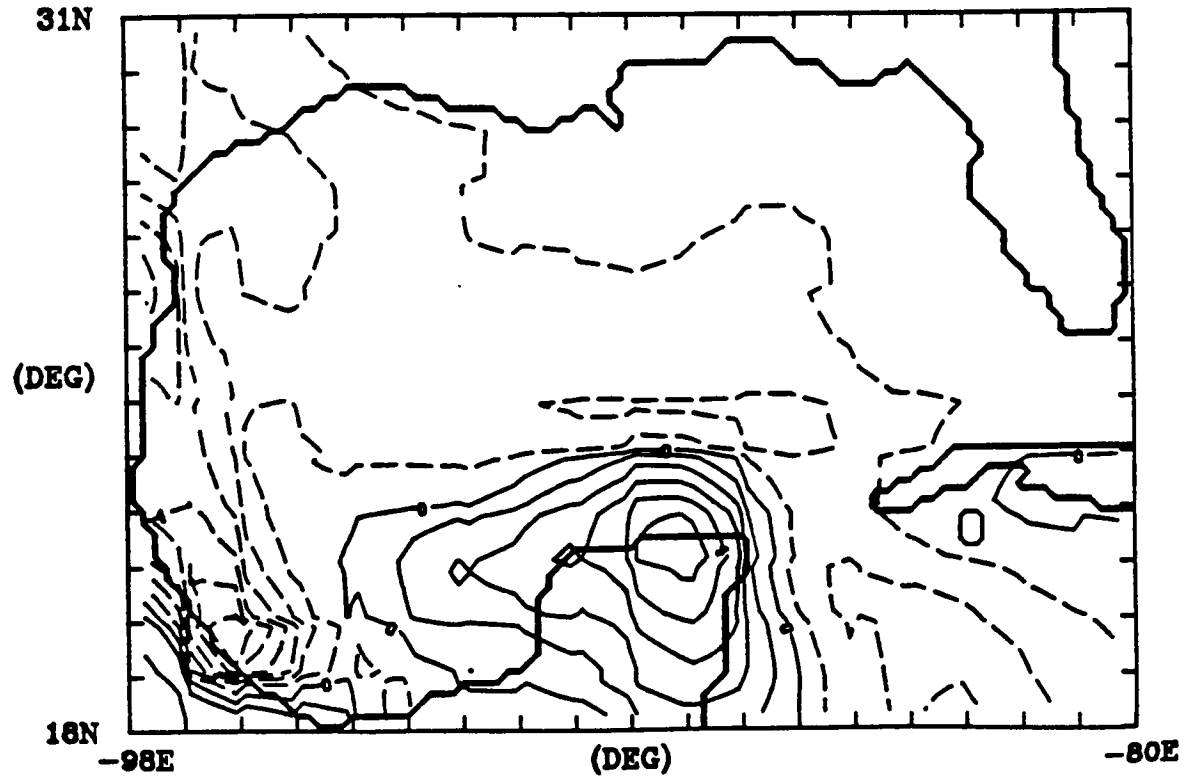

MIN = -7.86E-07 MAX = 5.85E-07

NORDA 323 12-DEC-84

FIGURE 31: Climatological (1967-1982) wind stress and wind stress curl from the Navy Corrected Geostrophic Wind data set, for summer (June, July, August).

WIND STRESS

SUMMER 1967-1982

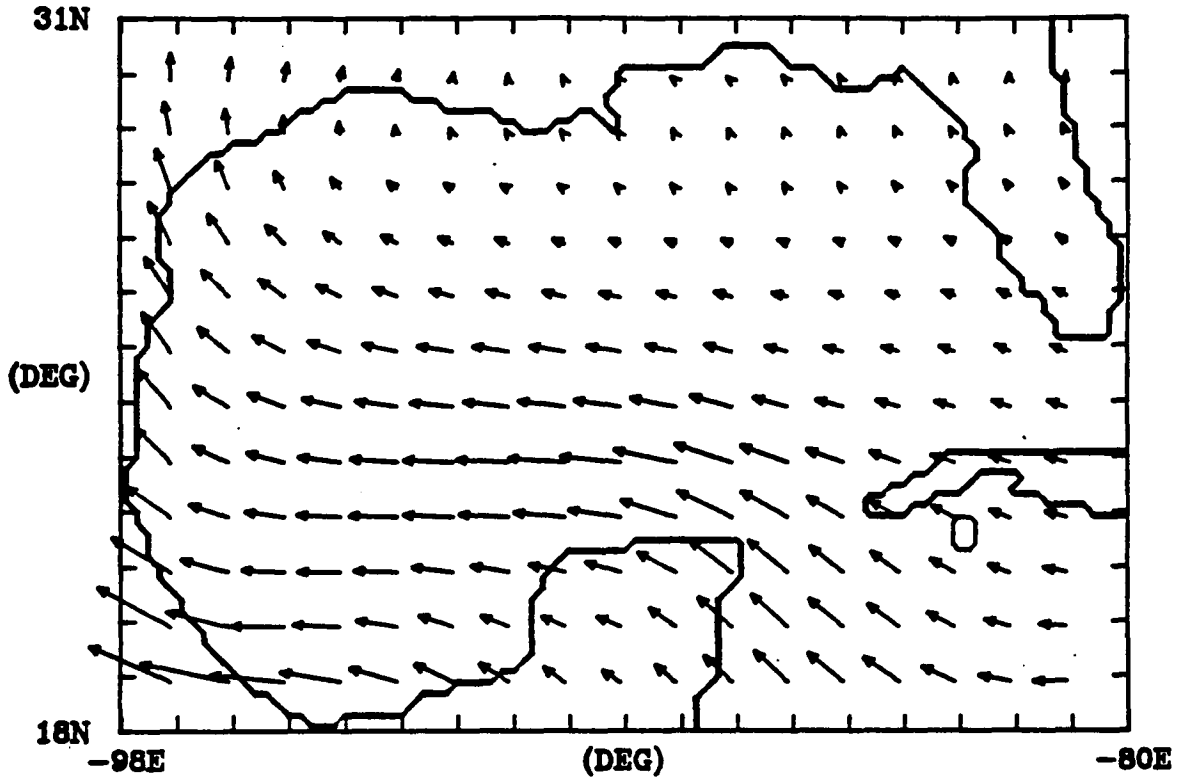

MAXIMUM WIND STRESS = 1.29 DYNES/CM^2

NORDA 329 12-DEC-84

WIND STRESS CURL

SUMMER 1967-1982 DC = 1.0E-07 MKS

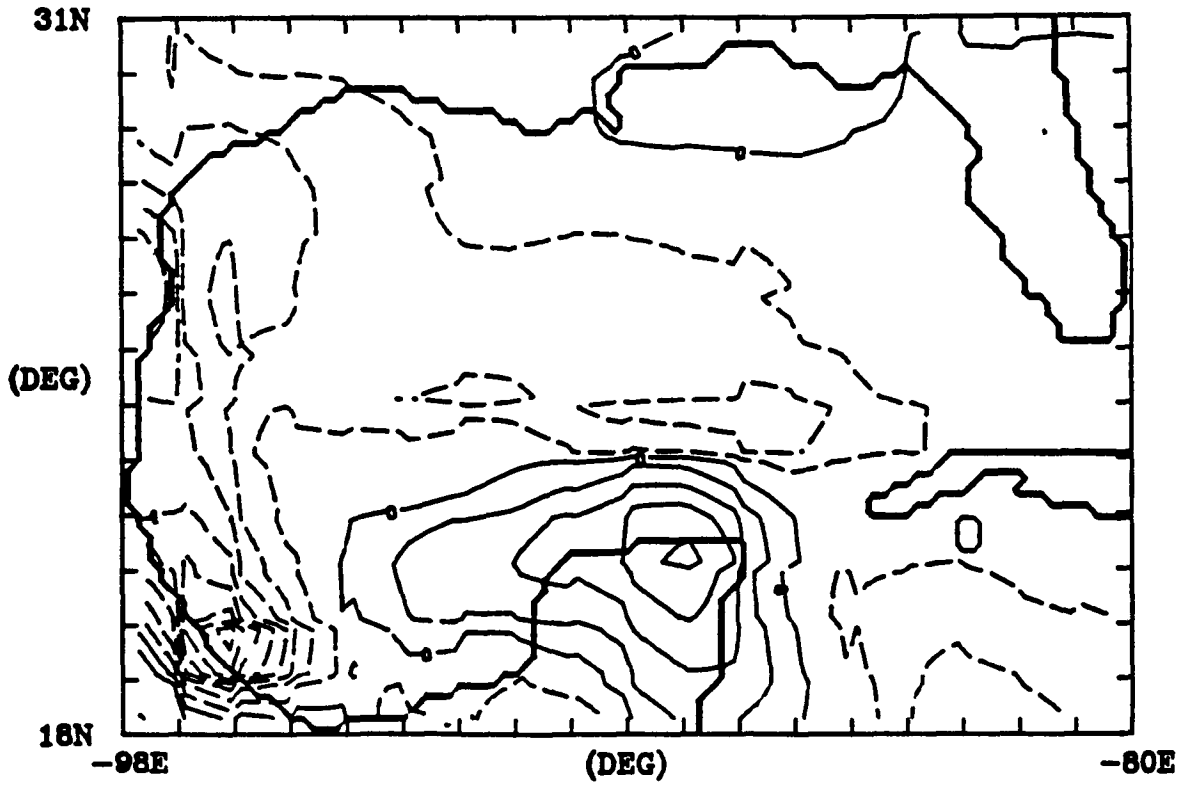

MIN = -8.64E-07 MAX = 4.31E-07

NORDA 329 12-DEC-84

FIGURE 32: Climatological (1967-1982) wind stress and wind stress curl from the Navy Corrected Geostrophic Wind data set, for fall (September, October, November).

WIND STRESS

FALL 1967-1982

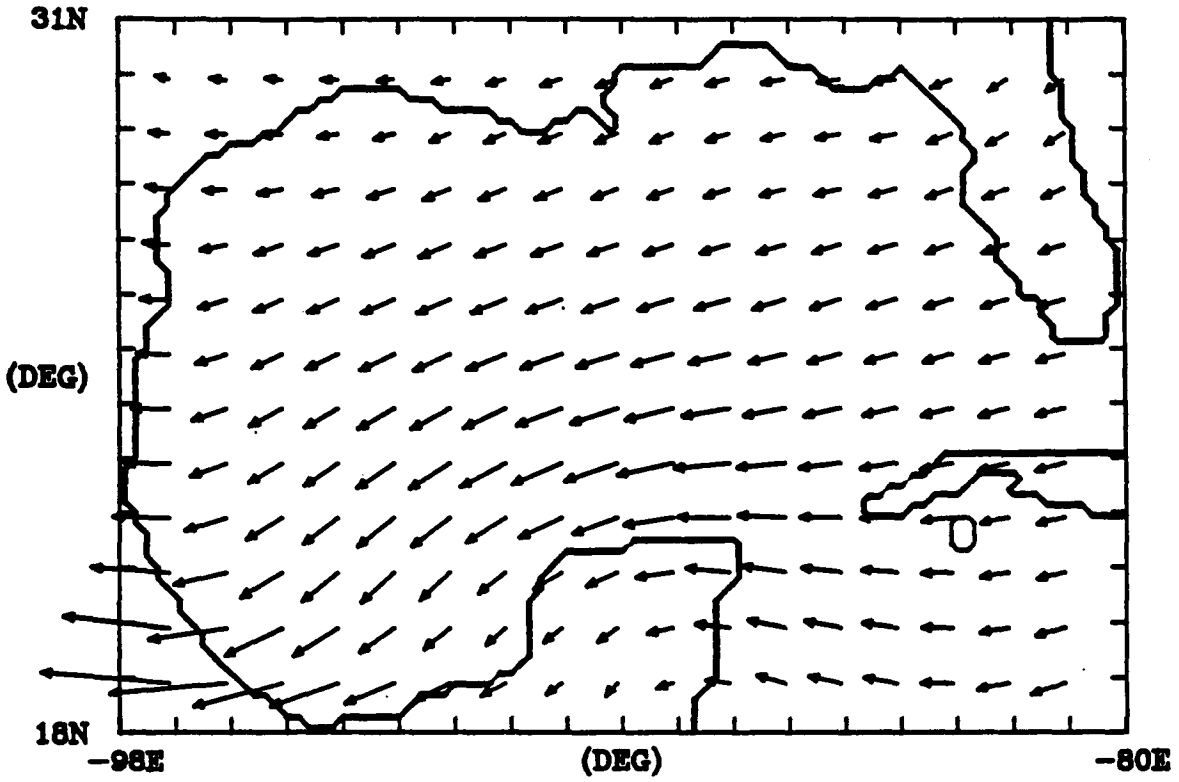

MAXIMUM WIND STRESS = 1.84 DYNES/CM^2

NORDA 329 12-DEC-84

WIND STRESS CURL

FALL 1967-1982 DC = 1.0E-07 MKS

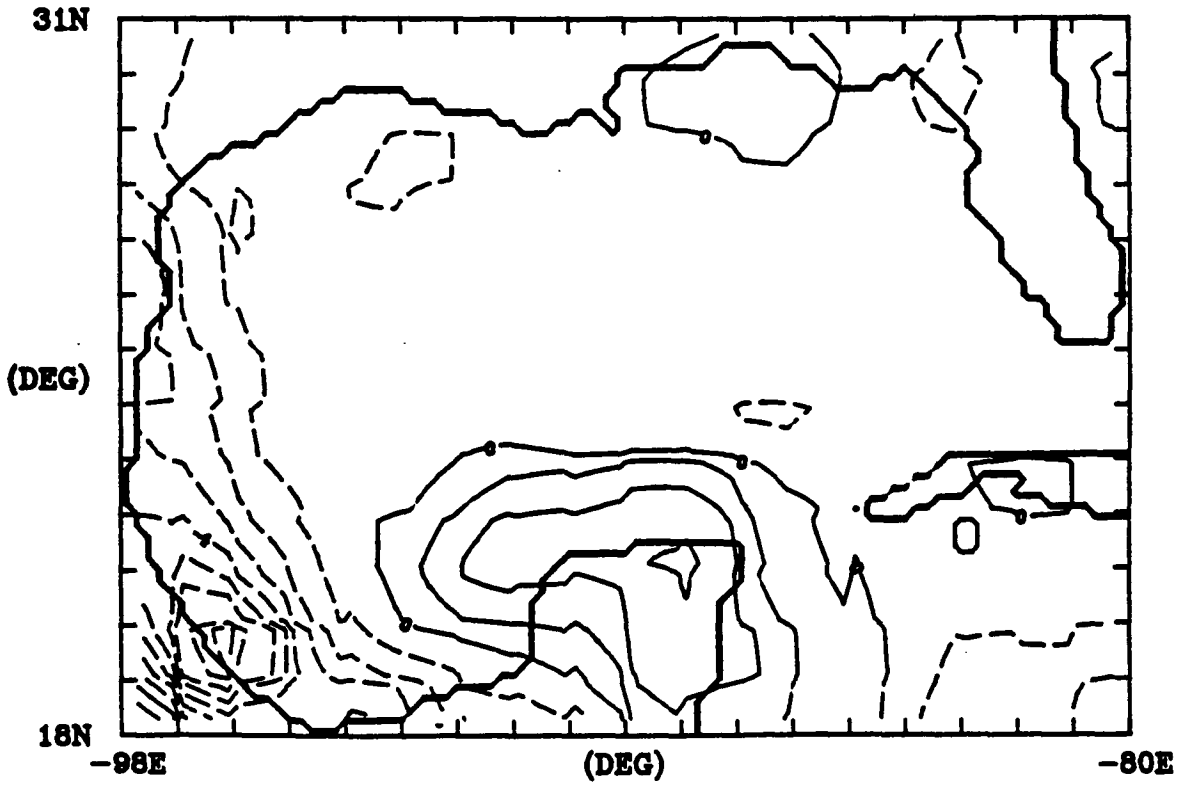

MIN = -9.53E-07 MAX = 3.22E-07

NORDA 329 12-DEC-84

FIGURE 33: Instantaneous view of upper layer averaged velocities from Experiment 68 on model day 3858. Vectors are only plotted at every second model grid point, i.e., every 0.4 degrees.

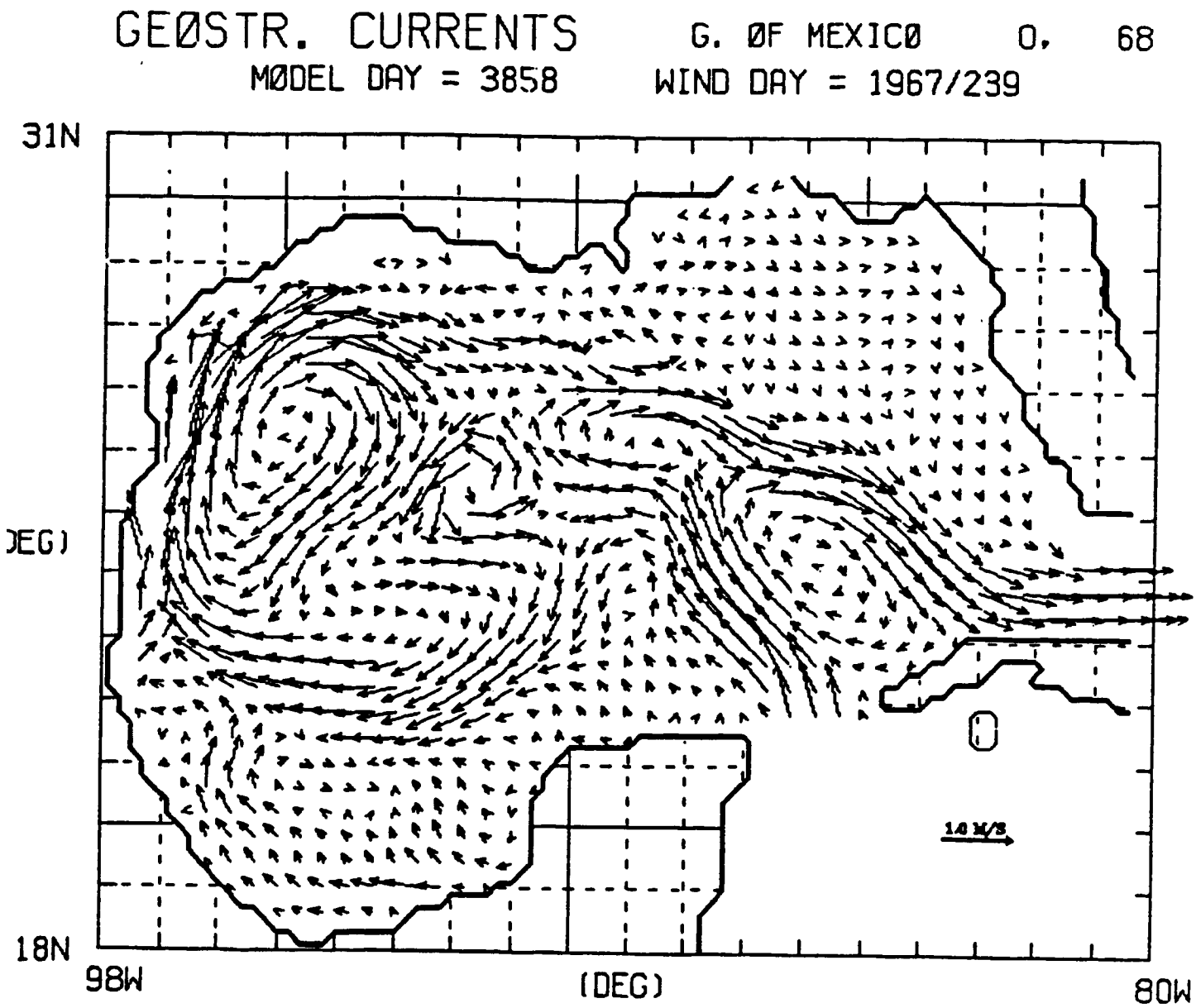

MAX PLØTED VECTØR = 1.46 (M/SEC)

FIGURE 34: Instantaneous view of upper layer averaged velocities from Experiment 68 on model day 3918. Vectors are only plotted at every second model grid point, i.e., every 0.4 degrees.

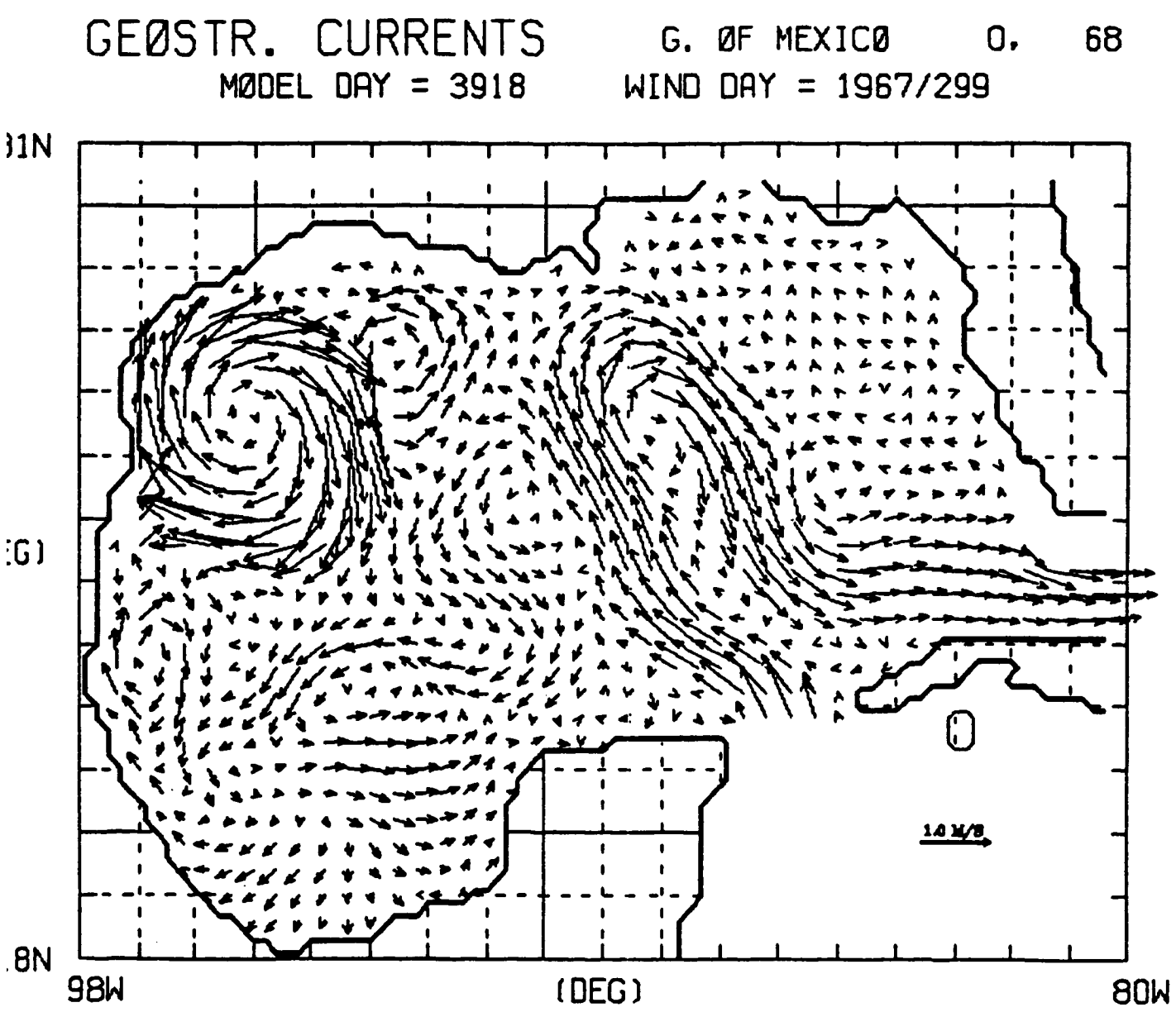

MAX PLØTED VECTØR = 1.29 (M/SEC)

FIGURE 35: Instantaneous view of upper layer averaged velocities from Experiment 68 on model day 3978. Vectors are only plotted at every second model grid point, i.e., every 0.4 degrees.

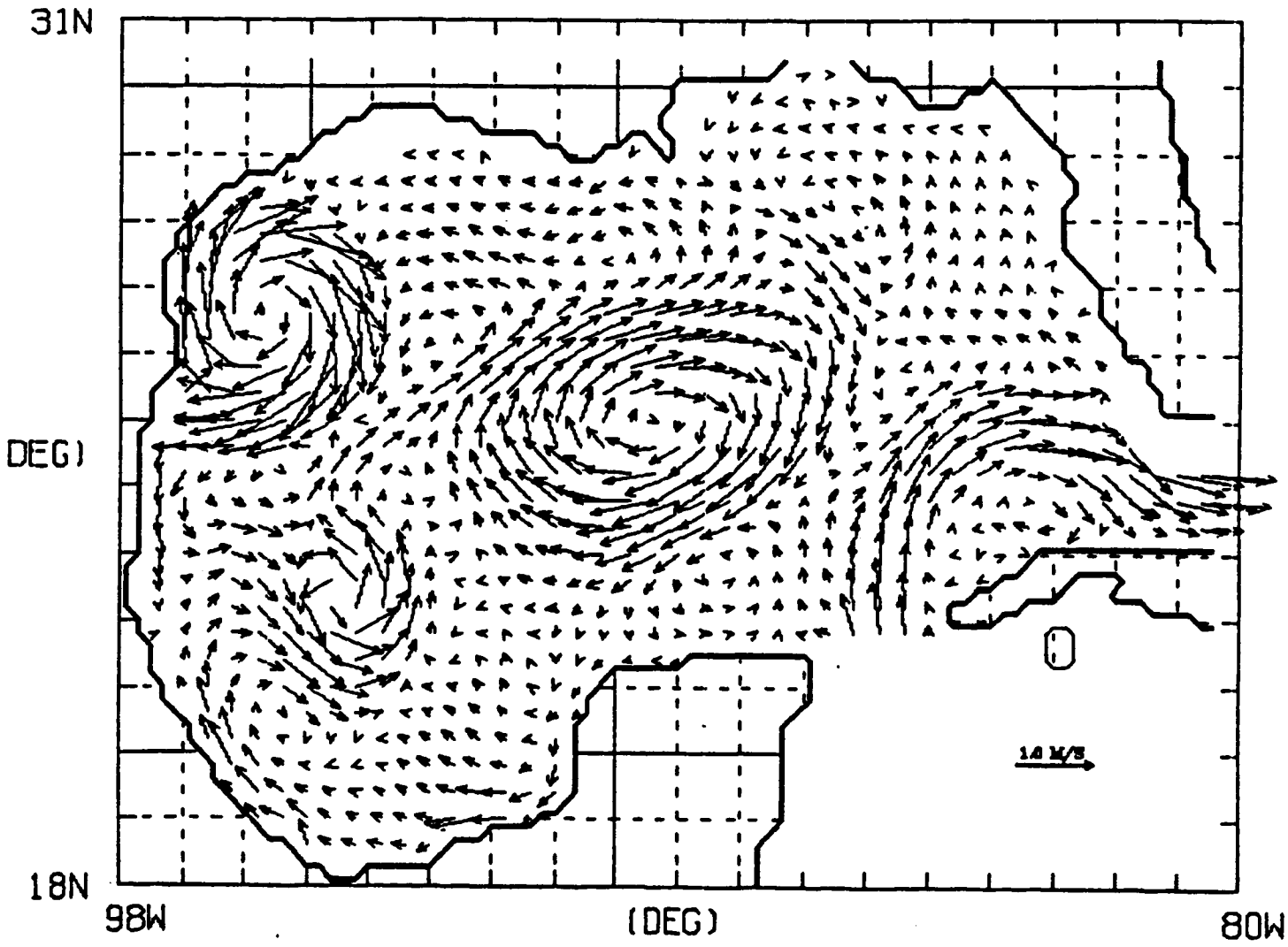

MAX PLØTED VECTØR = 1.39 (M/SEC)

FIGURE 36: Instantaneous view of upper layer averaged velocities from Experiment 68 on model day 4038. Vectors are only plotted at every second model grid point, i.e., every 0.4 degrees.

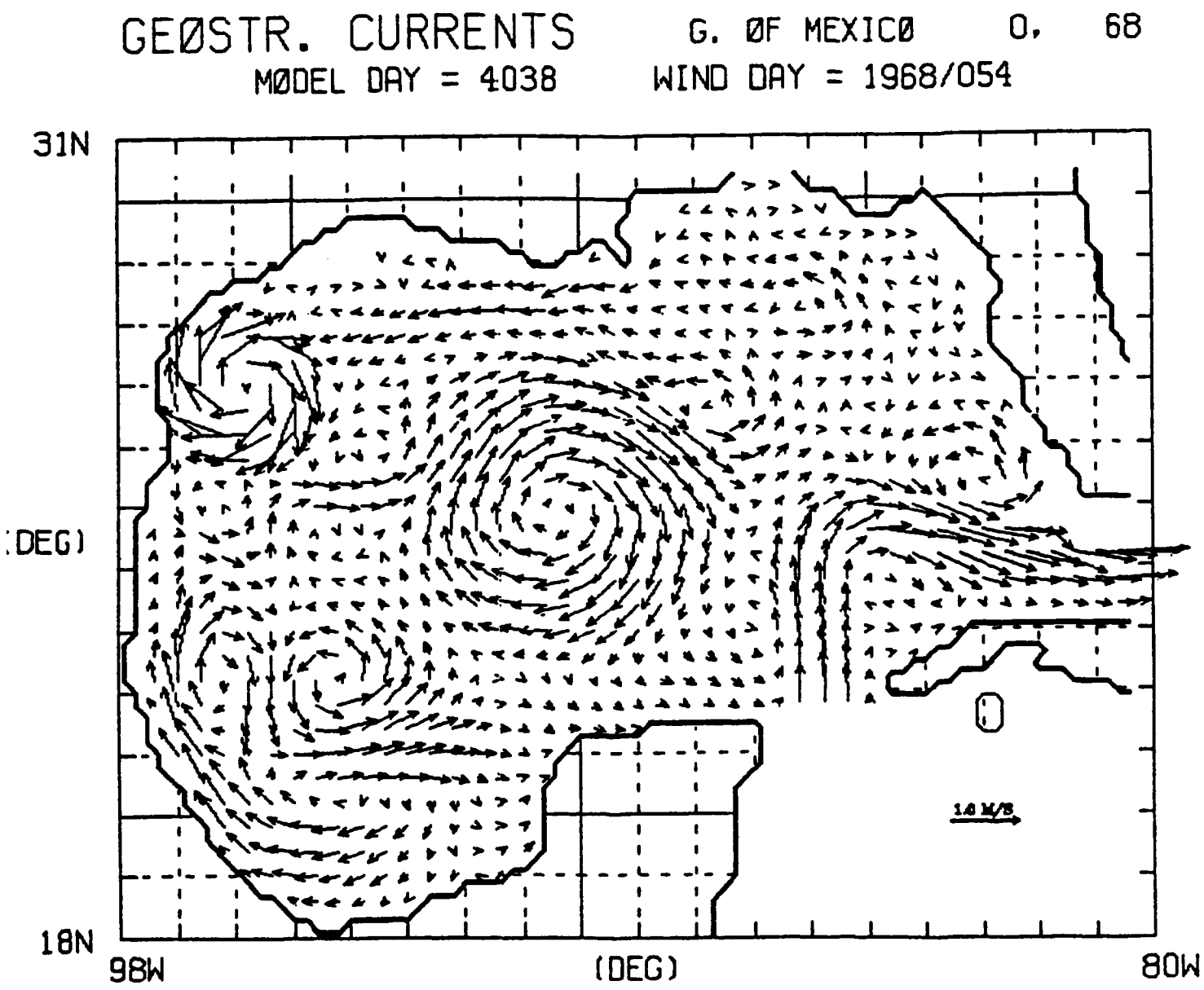
GEØSTR. CURRENTS
G. ØF MEXICØ
O. 68
MØDEL DAY = 4038
WIND DAY = 1968/054
31N
(DEG)
18N
98W
(DEG)
80W
1.0 M/S
MAX PLØTED VECTØR = 1.01 (M/SEC)

FIGURE 37: Instantaneous view of upper layer averaged velocities from Experiment 68 on model day 4098. Vectors are only plotted at every second model grid point, i.e., every 0.4 degrees.

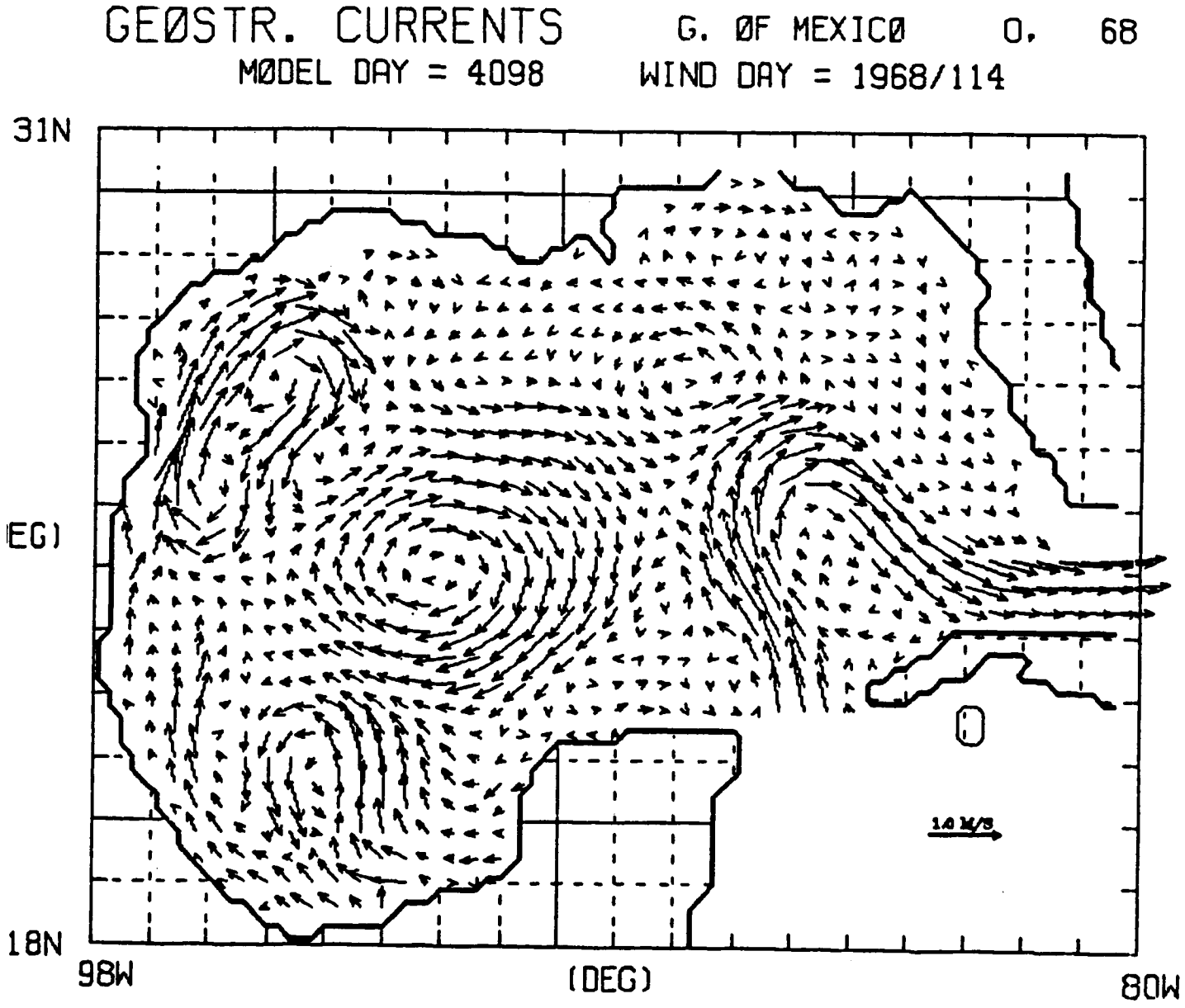

MAX PLØTED VECTØR = 1.04 (M/SEC)

FIGURE 38: Instantaneous view of upper layer averaged velocities from Experiment 68 on model day 4158. Vectors are only plotted at every second model grid point, i.e., every 0.4 degrees.

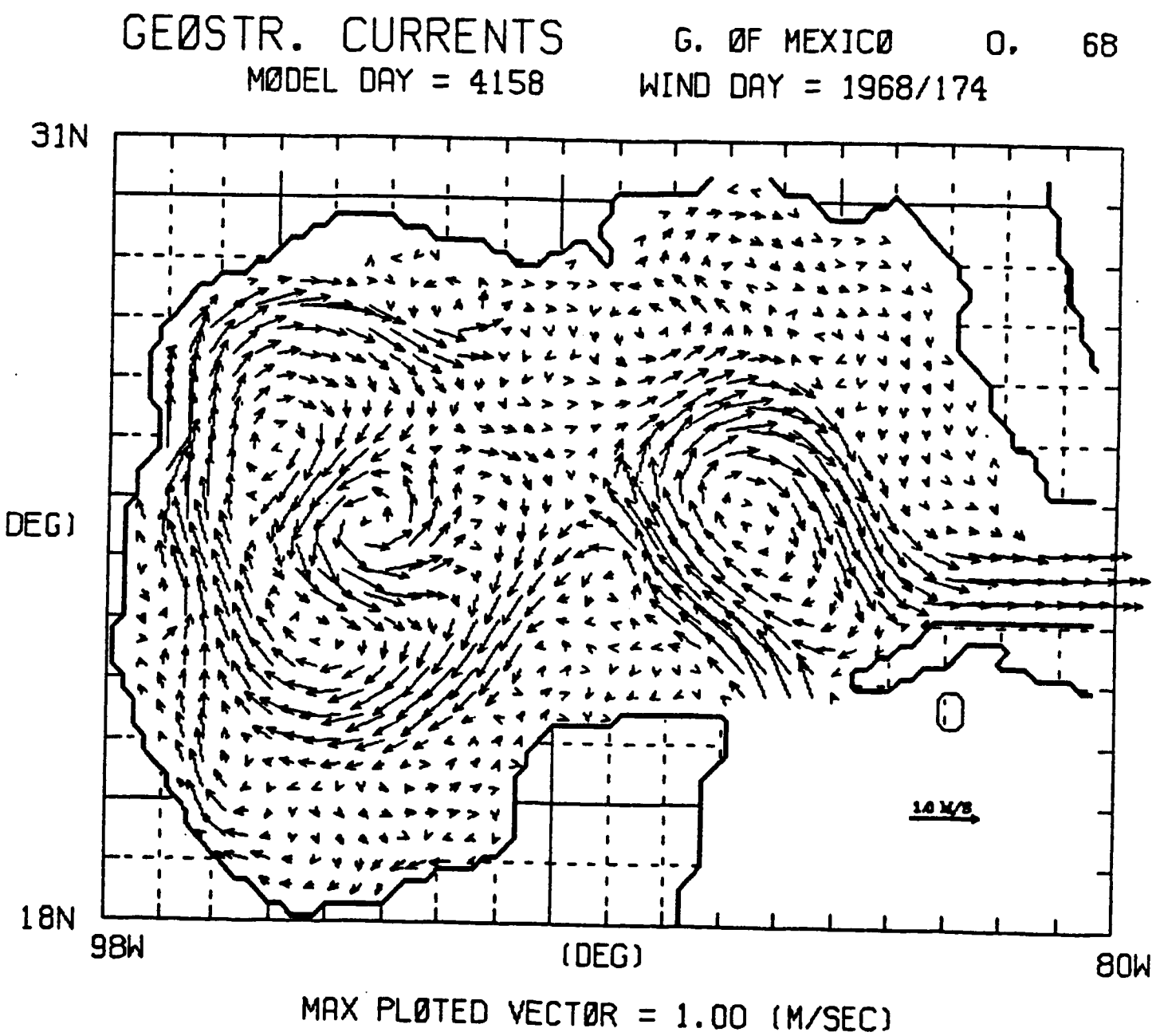
GEØSTR. CURRENTS
G. ØF MEXICØ
O. 68
MØDEL DAY = 4158
WIND DAY = 1968/174
31N
DEG)
18N
98W
(DEG)
80W
1.0 M/S
MAX PLØTED VECTØR = 1.00 (M/SEC)

FIGURE 39: Instantaneous view of upper layer averaged velocities from Experiment 68 on model day 4218. Vectors are only plotted at every second model grid point, i.e., every 0.4 degrees.

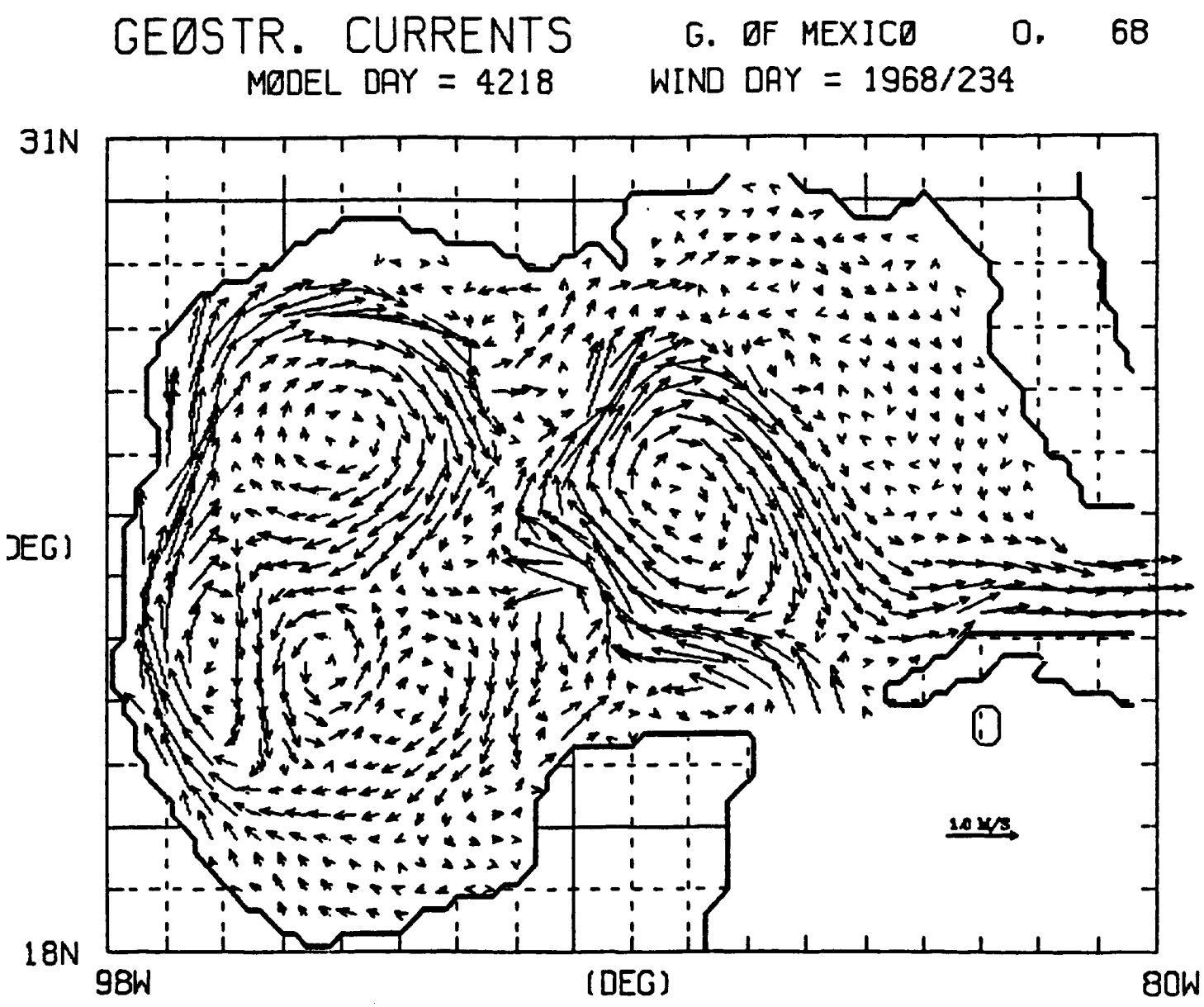
GEØSTR. CURRENTS
G. ØF MEXICØ
O. 68
MØDEL DAY = 4218
WIND DAY = 1968/234
31N
DEG)
18N
98W
(DEG)
80W
1.0 M/S
MAX PLØTED VECTØR = 1.84 (M/SEC)

REFERENCES:

Brooks, D.A. and Legeckis, R.V. 1982. A ship and satellite view of hydrographic features in the western Gulf of Mexico. J. Geophys. Res. 87: 4195-4206.

Elliott, B.A. 1979. Anticyclonic rings and the energetics of the circulation in the Gulf of Mexico. Ph.D. Dissertation, Texas A&M Univ., 188 pp.

Hurlburt, H.E. and Thompson, J.D. 1980. A numerical study of Loop Current intrusions and eddy shedding. J. Phys. Oceanogr. 10: 1611-1651.

JAYCOR 1983. A proposal for a Gulf of Mexico circulation modeling study. JAYCOR Proposal Number 8206-83.

Kirwan, A.D., Merrell W.J., Lewis, J.K. and Whitaker, R.E. 1984. Lagrangian observations of an aniticyclonic ring in the western Gulf of Mexico. J. Geophys. Res. 89: 3417-3424.

Kirwan, A.D., Merrell W.J., Lewis, J.K., Whitaker, R.E. and Legeckis, R. 1984. A model for the analysis of drifter data with an application to a warm core ring in the Gulf of Mexico. J. Geophys. Res. 89: 3425-3438.

Leipper, D.F. 1970. A sequence of current patterns in the Gulf of Mexico. J. Geosphys. Res. 75: 637-657.

Marsh J.G., Cheney R.E., McCarthy, J.J. and Martin T.V. 1984. Regional mean sea surfaces based on GEOS-3 and SEASAT altimeter data. Marine Geodesy 8: 385-402.

Maul, G.A. and Herman, A. 1984. Mean dynamic topography of the Gulf of Mexico with application to satellite altimetry. Marine Geodesy (to appear).

Merrell, W.J. and Morrison, J.M. 1981. On the circulation of the western Gulf of Mexico, with observations from April 1978. J. Geophys. Res. 86: 4181-4185.

Rhodes, R.C., Thompson, J.D. and Wallcraft A.J. 1984. The Navy Corrected Geostrophic Wind data set for the Gulf of Mexico. NORDA tech. rep. (to appear).

Vukovitch F.M. and Maul G.A. 1984. Cyclonic eddies in the eastern Gulf of Mexico. J. Phys. Oceanogr. (in press).

APPENDIX A

MODEL PARAMETERS

REFERENCE PARAMETERS (EXPERIMENT 40):

- upper layer inflow transport = 20 x 10^6 m^3 $sec^{\pm 1}$ (20 Sverdrup),
- lower layer inflow transport = 10 x 10^6 m^3 $sec^{\pm 1}$ (10 Sverdrup),
- wind stress = 0,
- horizontal eddy viscosity, A = 300 m^2/sec,
- grid spacing = 20 by 22 km (0.2 by 0.2 degrees),
- upper layer reference thickness, H1 = 200 m,
- lower layer reference thickness, H2 = 3300 m,
- minimum depth of bottom topography = 500 m,
- beta, df/dy = 2 x $10^{\pm 11}$ $m^{\pm 1}$ $sec^{\pm 1}$,
- Coriolis parameter at the southern boundary, f = 4.5 x $10^{\pm 5}$ $sec^{\pm 1}$,
- gravitational acceleration, g = 9.8 m/sec^2,
- reduced gravity, g' = .03 (H1 + H2)/H2 m/sec^2,
- interfacial stress = 0,
- coefficient of quadratic bottom stress = .003, and
- time step = 1.5 hours.

EXPERIMENT 9:

- upper layer inflow transport = 26 x 10^6 m^3 $sec^{\pm 1}$ (26 Sverdrup),
- lower layer inflow transport = 4 x 10^6 m^3 $sec^{\pm 1}$, (4 Sverdrup),
- grid spacing, 25 by 25 km,
- lower layer reference thickness, H2 = 3400 m,
- Coriolis parameter at the southern boundary, f = 5 x $10^{\pm 5}$ $sec^{\pm 1}$,
- coefficient of quadratic bottom stress = .002; and
- time step = 1 hour.
- All other parameters as in the reference experiment.

EXPERIMENT 28:

- upper layer inflow transport = 26 x 10^6 m^3 $sec^{\pm 1}$ (26 Sverdrup),
- lower layer inflow transport = 4 x 10^6 m^3 $sec^{\pm 1}$ (4 Sverdrup),
- wind stress = 0,
- coefficient of quadratic bottom stress = .002.
- All other parameters as in the reference experiment.

EXPERIMENT 31:

- upper layer inflow transport = 0,
- lower layer inflow transport = 0,
- wind stress from seasonal climatology based on ship observations,
- coefficient of quadratic bottom stress = .002.
- All other parameters as in the reference experiment.

EXPERIMENT 34:

- upper layer inflow transport = 26 x 10^6 m^3 sec^{-1} (26 Sverdrup),
- lower layer inflow transport = 4 x 10^6 m^3 sec^{-1} (4 Sverdrup),
- wind stress from seasonal climatology based on ship observations,
- coefficient of quadratic bottom stress = .002.
- All other parameters as in the reference experiment.

EXPERIMENT 40:

- All parameters as in the reference experiment.

EXPERIMENT 60:

- horizontal eddy viscosity, A = 100 m^2/sec,
- All other parameters as in the reference experiment.

EXPERIMENT 68:

- wind stress from 12 hourly Navy Corrected Geostrophic Wind set,
- All other parameters as in the reference experiment.

The Department of the Interior Mission

As the Nation's principal conservation agency, the Department of the Interior has responsibility for most of our nationally owned public lands and natural resources. This includes fostering sound use of our land and water resources; protecting our fish, wildlife, and biological diversity; preserving the environmental and cultural values of our national parks and historical places; and providing for the enjoyment of life through outdoor recreation. The Department assesses our energy and mineral resources and works to ensure that their development is in the best interests of all our people by encouraging stewardship and citizen participation in their care. The Department also has a major responsibility for American Indian reservation communities and for people who live in island territories under U.S. administration.

The Minerals Management Service Mission

As a bureau of the Department of the Interior, the Minerals Management Service's (MMS) primary responsibilities are to manage the mineral resources located on the Nation's Outer Continental Shelf (OCS), collect revenue from the Federal OCS and onshore Federal and Indian lands, and distribute those revenues.

Moreover, in working to meet its responsibilities, the **Offshore Minerals Management Program** administers the OCS competitive leasing program and oversees the safe and environmentally sound exploration and production of our Nation's offshore natural gas, oil and other mineral resources. The MMS **Minerals Revenue Management** meets its responsibilities by ensuring the efficient, timely and accurate collection and disbursement of revenue from mineral leasing and production due to Indian tribes and allottees, States and the U.S. Treasury.

The MMS strives to fulfill its responsibilities through the general guiding principles of: (1) being responsive to the public's concerns and interests by maintaining a dialogue with all potentially affected parties and (2) carrying out its programs with an emphasis on working to enhance the quality of life for all Americans by lending MMS assistance and expertise to economic development and environmental protection.